SUB | NIEDERSÄCHSISCHE STAATS- UND UNIVERSITÄTSBIBLIOTHEK GÖTTINGEN

Werk

Jahr: 1974
Kollektion: fid.geo
Signatur: 8 Z NAT 2148:40
Digitalisiert: Niedersächsische Staats- und Universitätsbibliothek Göttingen
Werk Id: PPN1015067948_0040
PURL: http://resolver.sub.uni-goettingen.de/purl?PPN1015067948_0040

LOG Id: LOG_0063
LOG Titel: Symposium on "Geomagnetic Anomalies, Rock Magnetism and Petrography"
LOG Typ: section

Übergeordnetes Werk

Werk Id: PPN1015067948
PURL: http://resolver.sub.uni-goettingen.de/purl?PPN1015067948
OPAC: http://opac.sub.uni-goettingen.de/DB=1/PPN?PPN=1015067948

Terms and Conditions

The Goettingen State and University Library provides access to digitized documents strictly for noncommercial educational, research and private purposes and makes no warranty with regard to their use for other purposes. Some of our collections are protected by copyright. Publication and/or broadcast in any form (including electronic) requires prior written permission from the Goettingen State- and University Library.
Each copy of any part of this document must contain there Terms and Conditions. With the usage of the library's online system to access or download a digitized document you accept the Terms and Conditions.
Reproductions of material on the web site may not be made for or donated to other repositories, nor may be further reproduced without written permission from the Goettingen State- and University Library.

For reproduction requests and permissions, please contact us. If citing materials, please give proper attribution of the source.

Contact

Niedersächsische Staats- und Universitätsbibliothek Göttingen
Georg-August-Universität Göttingen
Platz der Göttinger Sieben 1
37073 Göttingen
Germany
Email: gdz@sub.uni-goettingen.de

Symposium on "Geomagnetic Anomalies, Rock Magnetism and Petrography"

Preface

Geomagnetic anomalies produced by magnetic rocks in the earth's crust are observed almost everywhere. The petrographic composition of these rocks, however, is clearly known only in those cases where they are exposed at the surface or encountered in a drillhole. Consequently, for completely hidden magnetized bodies we can in many cases only state that they must contain minerals of the magnetite-maghemite spinel group or pyrrhotite. Much is lacking between this statement and a petrographic description of the rock. It was the aim of the "Symposium on Geomagnetic Anomalies, Rock Magnetism and Petrography" to reduce this gap. The symposium was held at the Second Scientific Assembly of the International Association of Geomagnetism and Aeronomy, Kyoto, September 1973. The program committee consisted of A. Hahn, (convener), C. M. Carmichael, T. N. Simonenko. Many of the papers from the symposium make up this volume.

According to the complexity of this interdisciplinary problem the papers cover a broad range. In this volume they are organized under the headings

1. Surveys and Survey Interpretations
2. Aspects of Rock Magnetism-General
3. Aspects of Rock Magnetism — Oceanic Material
4. Correlation with Petrography.

A. Hahn

J. Geophys. 40, 403–430, 1974

1. Surveys and Survey Interpretation

Long-Wavelength Aeromagnetic Anomalies and Deep Crustal Magnetization in Manitoba and Northwestern Ontario, Canada*

D. H. Hall

Geophysics Section, Department of Earth Sciences,
University of Manitoba, Winnipeg, Canada

Received March 12, 1974; Revised Version May 22, 1974

Abstract. A new type of aeromagnetic anomaly map (a long-wavelength anomaly map with anomaly widths in the range 60 km. $< \lambda <$ 4000 km) is presented for the area. It is believed that this group of anomalies represents a physically distinct field. This field shows considerable correlation with the broad features of deep crustal structure as derived from seismic sounding; linear relationships were found between the field and depths to the bottom of the crust and to the boundary between the upper and the lower crustal layers, as well as to the thickness of the lower crustal layer. A theoretical relationship connecting structure on magnetized layers to magnetic anomalies is given showing that the linear relationships are to be expected. It is shown that the lower crustal layer is the most likely source of the anomalies, with an intensity of magnetization of 5.3×10^{-3} emu/cc. It is also indicated that the upper crustal layer could also be the source, but that a shallow plate of magnetization could not explain the anomalies. Thus *deep crustal magnetization* must (on all interpretations made in the present paper), be responsible for the long-wavelength anomalies. Also, these anomalies are strongly related to major features in surface geology.

Key words: Long-Wavelength Aeromagnetic Anomalies — Deep Crustal Magnetization — Canadian Shield.

Note

In order to facilitate comparison with existing publications on magnetizations of rocks and with existing magnetic anomaly maps, e.m. units are used for magnetization, and gammas for field strengths.

(1 gamma = 1 nanotesla, and $I_{SIU} = 4\pi I_{emu}$)

---

* Paper presented at IAGA second scientific conference, Kyoto, September 1973.

Paper No. 3, Centre for Precambrian Studies, University of Manitoba.

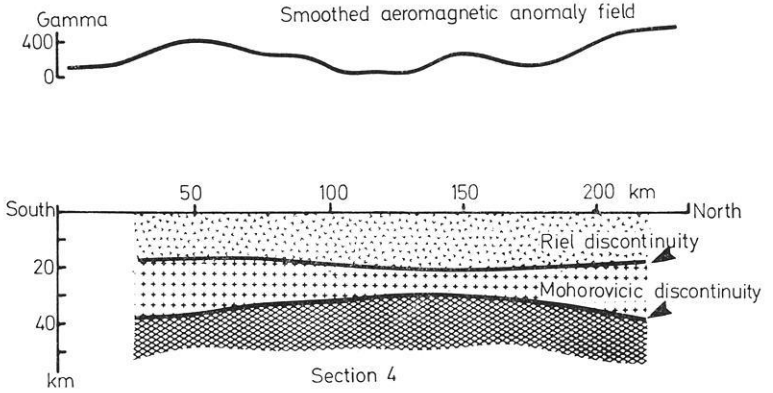

Fig. 1. Crustal section no. 4 (Fig. 3), with regional anomaly field along the corresponding line on Fig. 1 (1 gamma = 1 nanotesla)

Introduction

Regional Magnetic Anomalies

Compilation maps of aeromagnetic anomalies in the wavelength (anomaly width) band $\lambda > 20$ km. have proven to be of value in studies of magnetic units lying in the upper layer of the earth's crust, to depths of approximately 20 km. In northwestern Ontario and Manitoba, such maps have been constructed and interpreted by Bhattacharyya and Morley (1965), by Hall (1968a), by McGrath and Hall (1969), by Hall (1971), and by Coles (1973).

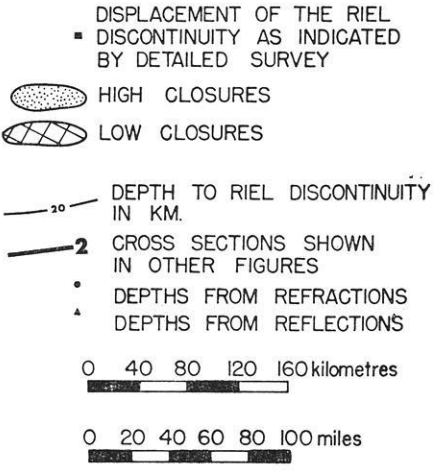

Fig. 2 Depth to Riel discontinuity (boundary between upper and lower crustal layers) (from Hall and Hajnal, 1973)

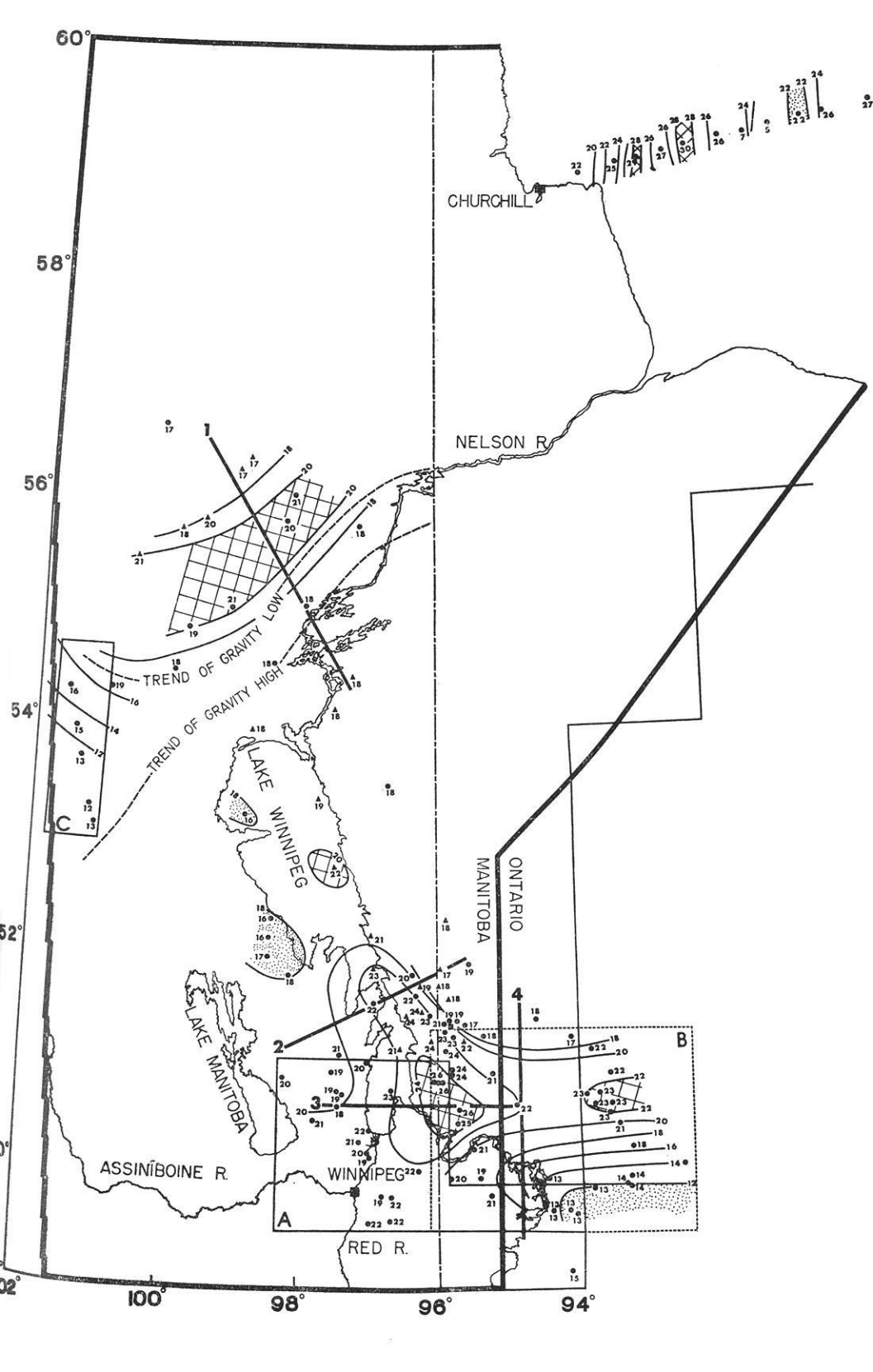
60°
58°
56°
54°
52°
100°
98°
96°
94°
CHURCHILL
NELSON R.
TREND OF GRAVITY LOW
TREND OF GRAVITY HIGH
LAKE WINNIPEG
LAKE MANITOBA
MANITOBA
ONTARIO
ASSINIBOINE R.
WINNIPEG
RED R.
A
B
C
1
2
3
4

A similar map has been prepared for the British Isles (Hall and Dagley, 1970). The first three of the references mentioned above represent successive stages in the preparation of a map of aeromagnetic anomalies in the band $\lambda > 20$ km. for the area. This map has recently been updated and is to be published by the Manitoba Mines Branch as a map (Hall, McGrath and Richards, 1974). This map, as indicated by its wavelength band, portrays a filtered (or smoothed) compilation of aeromagnetic maps with anomalies of width less than 20 km. removed by the filtering process. In the aforementioned publications, these maps are referred to as "regional anomaly maps".

The most prominent features seen on visual examination of the regional anomaly maps are anomalies and anomaly trends with widths measuring some tens of kilometers. In addition, however, somewhat larger areas with general levels of magnetic field differing one from the other can be seen on them. The Ontario-Manitoba maps quoted above are examples. The anomalies and anomaly trends group themselves into alternating belts of high and low field crossing the area. Wilson (1971) noted these groupings and attributed them to the effects of a system of crustal blocks, which differ in magnetic properties. The individual smaller wavelength anomalies determine the general character of the map while the grouping into belts is present as a more subtle effect. The question arises as to the possibility that the latter represents a physically distinct field of longer wavelength underlying the high-amplitude, narrow anomalies. Such underlying long-wavelength fields have been mapped in various parts of the world. Zietz *et al.* (1970) found that a field in the band 200 km $< \lambda >$ 2000 km lies over the United States. Regan (1974) has extended this work on a worldwide basis.

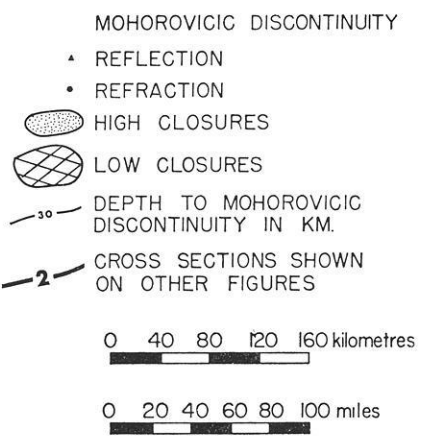

Fig. 3 Depth to Mohorovicic discontinuity (from Hall and Hajnal, 1973)

→

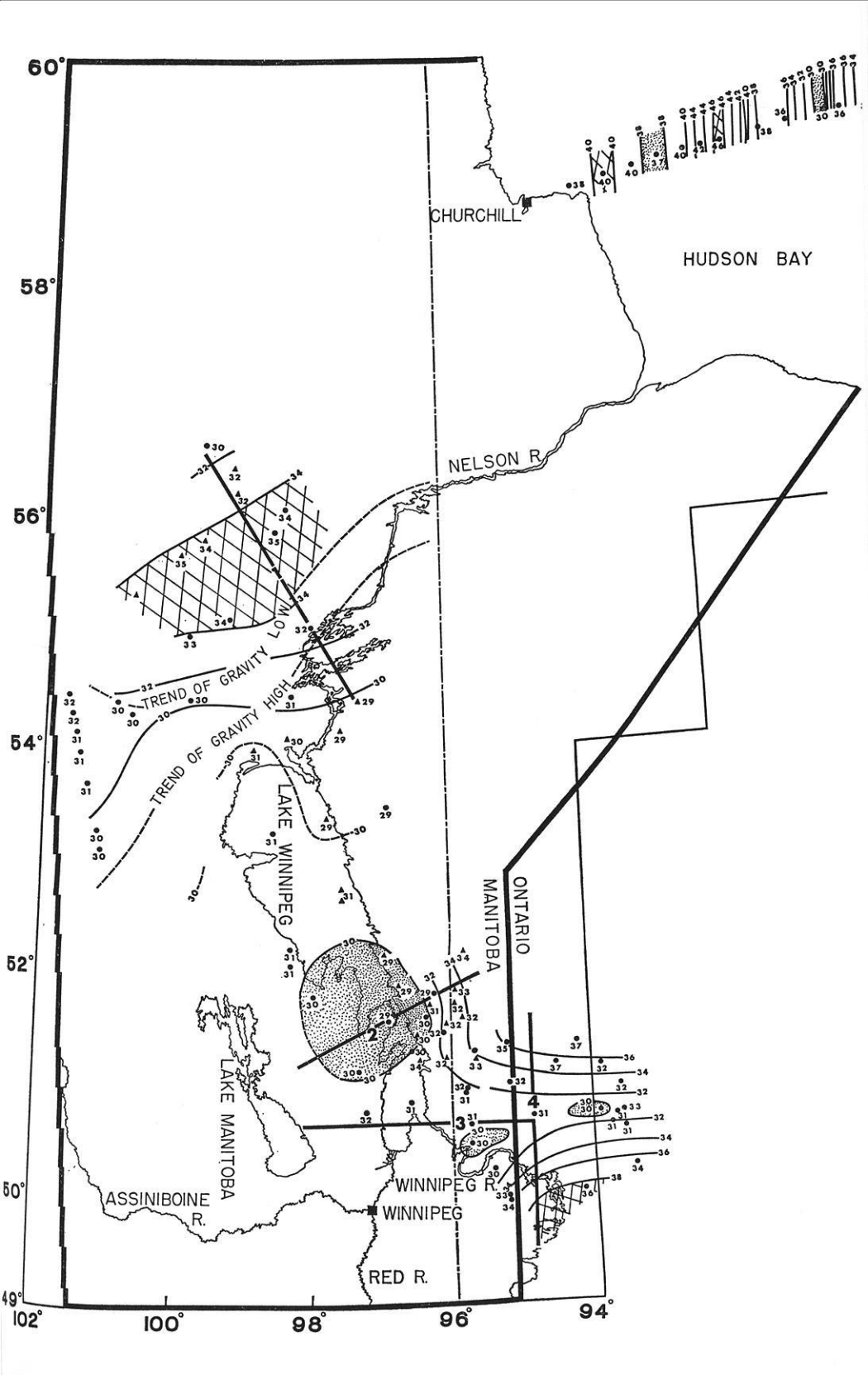
60°
58°
56°
54°
52°
50°
49°
102°
100°
98°
96°
94°
CHURCHILL
HUDSON BAY
NELSON R.
TREND OF GRAVITY LOW
TREND OF GRAVITY HIGH
LAKE WINNIPEG
LAKE MANITOBA
MANITOBA
ONTARIO
ASSINIBOINE R.
WINNIPEG
WINNIPEG R.
RED R.
1
2
3
4

Possible Long-Wave Length Components of Regional Anomaly Maps in Manitoba and Northwestern Ontario

Crustal seismic surveys have indicated a two-layer structure for the earth's crust in these areas. The upper layer bottoms at a seismic discontinuity which has been named locally "the Riel discontinuity". Maps of the Riel (R) and Mohorovicic (M) discontinuities have been published, covering a strip 1000 km long and 300 km wide in Manitoba and northwestern Ontario (Hall and Hajnal, 1973). These maps are reproduced in the present paper in Figs. 2 and 3. During comparison of these maps with other geophysical data certain long-wavelength components ($\lambda > 100$ km) were distinguished underlying the regional magnetic anomaly field. These components appeared to be correlated with structural features of the R and M discontinuities. It was suggested that the thicknesses of the crustal layers are somehow related to these long-wavelength anomalies (Hall and Hajnal, 1973, p. 903, and Fig. 1, this paper). Attempts were therefore made to extract the long-wavelength components from the regional anomaly maps and to follow up the suggestion that they might be somehow connected with crustal structure. The present paper gives the results of these studies.

The Long-Wavelength Anomaly Map

Choice of Cutoff Wavelength

The anomaly map in the present paper has a cutoff wavelength of 60 km. This value was chosen for two reasons. First, the shortest wavelength anomalies from the Riel and Mohorovicic discontinuities for a layered

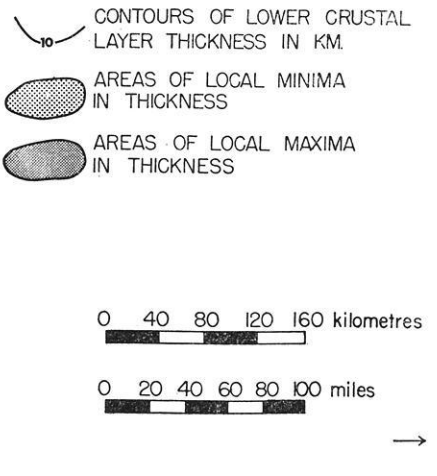

Fig. 4 Thickness of lower crustal layer

→

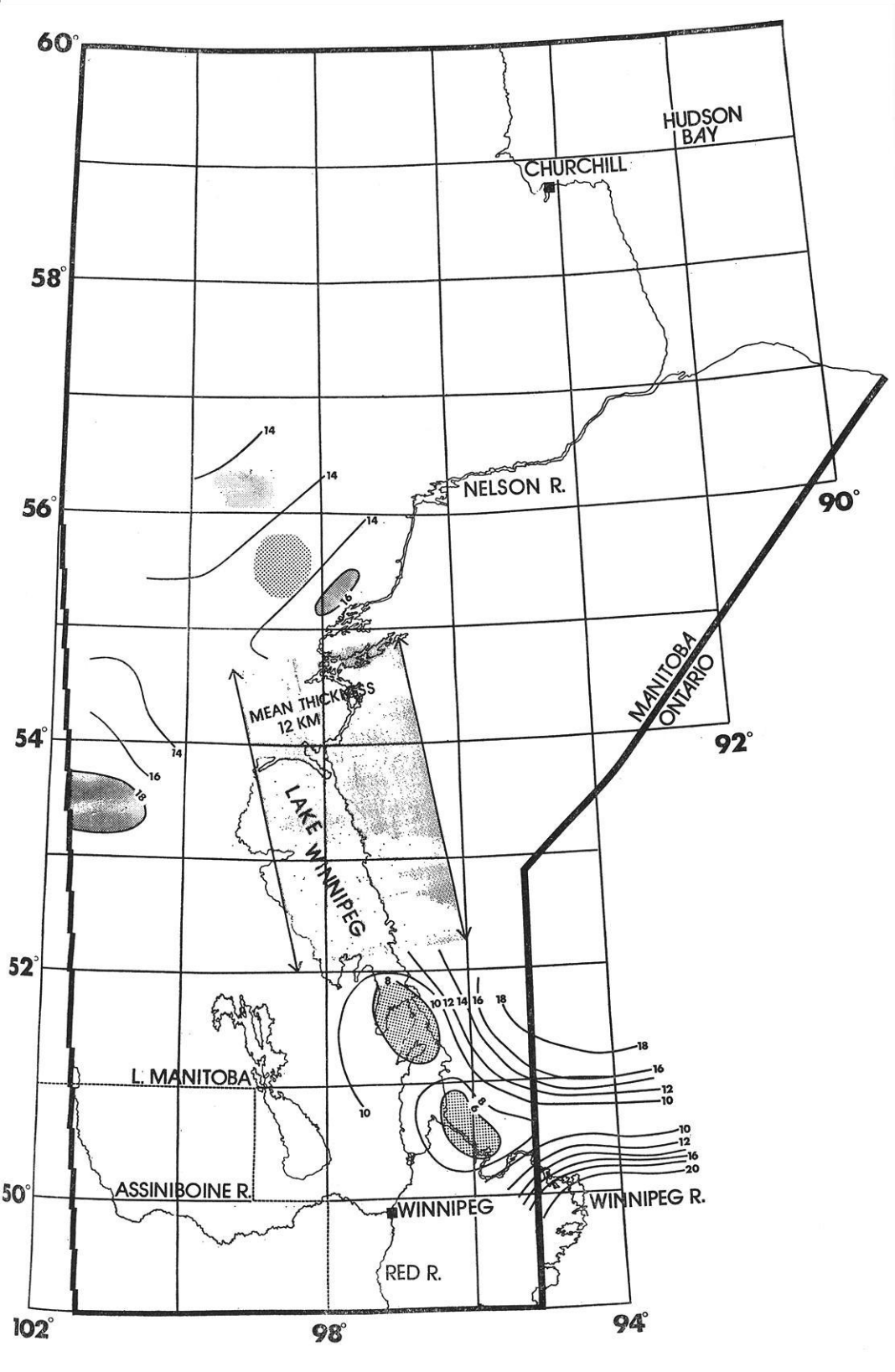
60°
58°
56°
54°
52°
50°
102°
98°
94°
92°
90°
HUDSON BAY
CHURCHILL
NELSON R.
MANITOBA
ONTARIO
MEAN THICKNESS 12 KM
LAKE WINNIPEG
L. MANITOBA
ASSINIBOINE R.
WINNIPEG
WINNIPEG R.
RED R.
14
16
18
8
10
12
20

magnetic model might reasonably be expected to be due to fault displacements. On calculation, such structures would yield wavelengths in the 50—60 km range. The map then represents a bandpass which would contain the physically distinct field due to layer-like crustal magnetization, if it exists. Secondly, existing data (at 3-km spacing) decimated to give a grid of data points with 9 km. spacing yields, on filtering with the operator developed by McGrath and Hall (1969), a cutoff wavelength of 60 km. This cutoff, then, is physically realistic and was computationally simple to obtain given the data and the computational methods available. Removal of the core-generated fields yields a bandpass of $60\text{ km} < \lambda < 4000$ km. The core-generated fields were approximated by fitting a second-order surface (over the area of Fig. 5) to the Dominion Observatories Branch (1965) map of total field, and subtracting this best-fit field from the smoothed data.

Interpretation of Long-Wavelength Anomalies

It is an observed fact (evident from visual comparison of Figs. 2, 3, 4 and 5) that the long-wavelength anomalies exhibit a close correlation with deep crustal structure as derived from seismic surveys. One possibility suggested by this fact is that the magnetic sources for this field lie deep within the crust, with their distribution controlled by broad crustal structure. Two extreme models for such deep magnetization can be constructed. The first consists of uniformly magnetized layers bounded by the *R* or the *M* discontinuity (or both). The second consists of lateral inhomogeneities in magnetization within either of the crustal layers, or below the

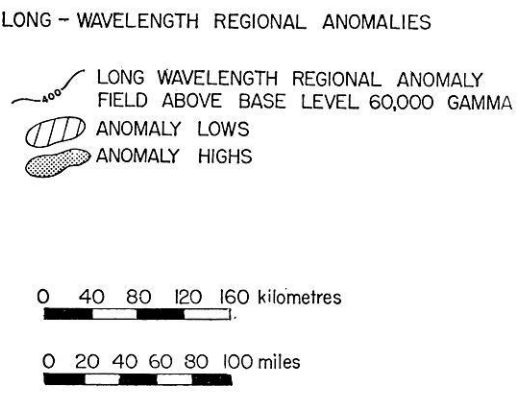

Fig. 5 Long-wavelength magnetic anomaly field ($60\text{ km} < \lambda < 4000$ km) in gammas above a best-fit second order surface to the core-generated field. (1 gamma = 1 nanotesla)

→

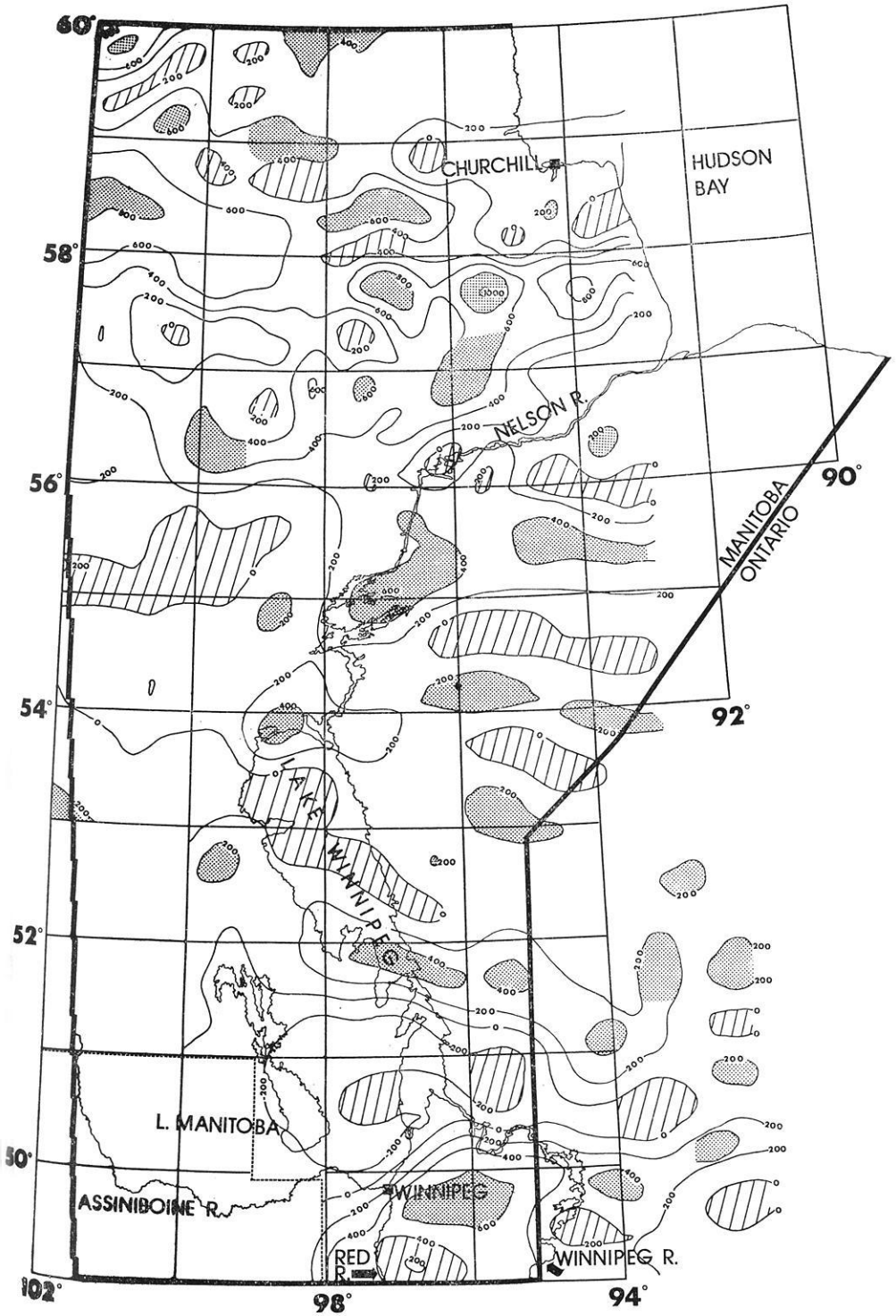
60°
58°
56°
54°
52°
50°
102°
98°
94°
90°
92°
CHURCHILL
HUDSON BAY
NELSON R.
MANITOBA
ONTARIO
LAKE WINNIPEG
L. MANITOBA
ASSINIBOINE R.
WINNIPEG
RED R.
WINNIPEG R.

crust. Such lateral inhomogeneities could also, in many cases, match the broad dimensions of crustal structure because of the following considerations.

As shown in Fig. 6, the long-wavelength anomaly map and the seismic interfaces can be divided into a number of zones. These zones, furthermore, mark out definite geological units as mapped at the surface. The deep crustal structure is clearly reflected in surface geology. This relationship is convincingly discussed by Wilson (1971), in proposing a block structure for the Superior province of the Canadian Shield. Thus even though the seismic boundaries of Figs. 2 and 3 are continuous over the whole area, the crustal layers bounded by them could have quite different compositions in different parts of the area, corresponding to the system of geological units mentioned above. If this is so, and if the various compositions affect magnetization markedly, then there would be lateral inhomogeneities in magnetization, with wavelengths comparable to those of crustal structures. These lateral inhomogeneities, even if the magneticunits corresponding to them extended to a uniform depth, could then cause anomalies having similar widths to those of structures on crustal interfaces. The corresponding anomalies would be very difficult to separate from those due to boundaries of uniformly magnetized layers. Further complications could occur if lateral inhomogeneities and undulating boundaries both acted to determine the anomalies.

Situations of this type are, of course, often met with in anomaly interpretation as part of the "ambiguity problem". The most an interpreter can do, in the absence of additional information, is to bear ambiguity in mind and begin exploring the implications of the various possible models.

There is one further implication of the connection between deep crustal structure and regional geology at the surface which should be mentioned. Thin plates of magnetization near the surface, controlled in width by deep

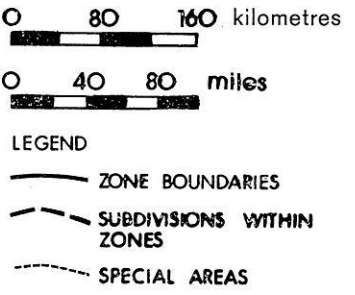

Fig. 6 Zones over which fields and depths to the crustal boundaries were averaged for Table 1

→

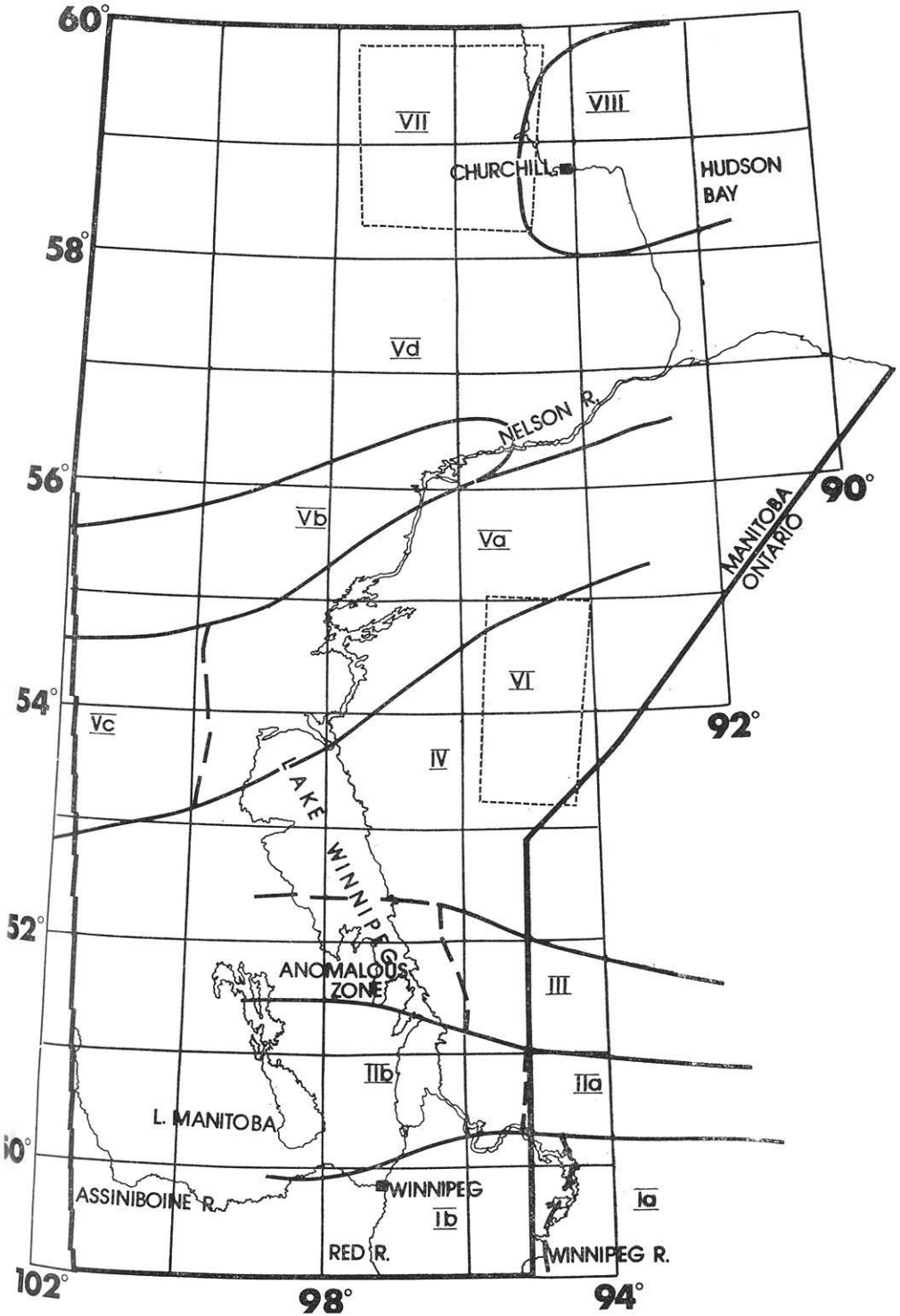
60°
58°
56°
54°
52°
50°
102°
98°
94°
92°
90°
VII
VIII
CHURCHILL
HUDSON BAY
Vd
NELSON R.
Vb
Va
MANITOBA
ONTARIO
VI
Vc
IV
LAKE WINNIPEG
ANOMALOUS ZONE
III
IIb
IIa
L. MANITOBA
ASSINIBOINE R.
WINNIPEG
Ia
Ib
RED R.
WINNIPEG R.

Table 1

Zone	$F(\gamma)$	M(km)	R(km)	LL(km)	t(km)	
I	425	38	13	25	18	Kenora Block[a]
IIa	0	32	21	11	1	English River Block[a]
IIb	−200	31	22	9	− 2	
III	250	34	18	16	7	Red Lake Block[a]
IV	125	30	18	12	3	Area of uniform crustal structure
Va	200	33	18	15	6	Structure in the vicinity
Vb	10	34	20	14	4	of the Nelson River
Vc	60	31	15	16	8	(Thompson) lineament
Vd	250	34	18	16	7	Area to north and west of the Nelson River (Thompson) lineament
VI	150	31	—	—	—	Special areas
VII	500	40	—	—	—	
VIII	200	43	27	16	3	West-central Hudson Bay

[a] Fault blocks of the western Superior Province as defined by Wilson (1971, p. 41). These are components of a proposed aulacogen structure (Hall and Hajnal, 1969, 1973). The "lower layer parameter" is given by $t = M - 1.5R$ for the area under study.

crustal structure, could conceivably cause long-wavelength anomalies, without requiring deep magnetization at all. Tests of this suggestion will be the subject of a later section.

Let us now begin to examine the suggested models. Leaving the suggestion of a near-surface plate of magnetization aside for the moment, let us compare the two extreme models of deep crustal magnetization: uniformly magnetized crustal layers, and lateral inhomogeneities. Both imply deep crustal magnetization, but the manner of its occurrence is very different in the two cases, with different implications in each for crustal evolution. Therefore, it is important to evaluate them both. Let us begin with the model suggesting uniformly magnetized crustal layers.

A Method of Comparing Crustal Structure and Long-Wavelength Anomalies

Comparison among Figs. 2, 3, 4, and 5 indicate 12 zones (shown on Fig. 6), in each of which crustal structure and magnetic field are relatively uniform, and significantly different from the corresponding quantities in

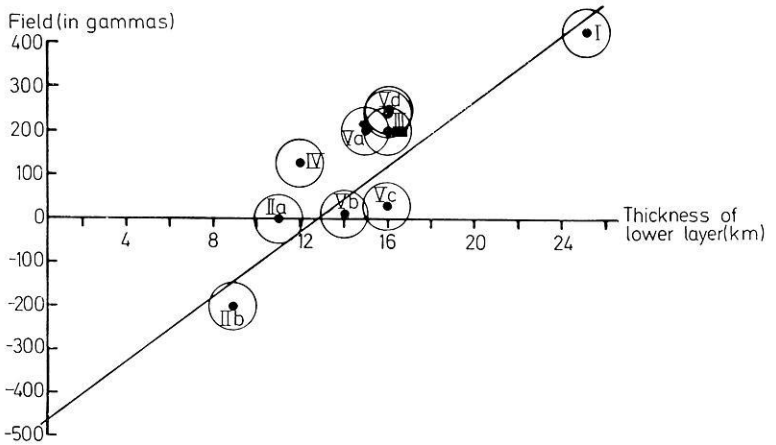

Fig. 7. Plot of field against thickness of lower layer, from values in Table 1 (1 gamma = 1 nanotesla)

neighbouring zones. In Table 1 the average values of field (F), total crustal thickness (M), upper-layer thickness (R), and lower-layer thickness (LL) for these zones are summarized. For the area covered by all of these data (comprising zones I to V) the values in Table 1 were obtained by simple averaging over the zones. Zones VI and VII are special areas, over which the long-wavelength anomaly data extend, but for which coverage with detailed crustal seismic surveys is not available. Data on crustal thickness are, however, available for these two zones from a line of data recorded by Mereu and Hunter (1969) (and compiled and compared with Figs. 2 and 3 by Hall (1971, p. 84)), and provide the values given in Table 1. Zone VIII covers a portion of west-central Hudson Bay. Magnetic data are taken from Fig. 5, as well as from the Aeromagnetic Map of Canada (Morley and MacLaren, 1967). Seismic information is taken from the papers of Hajnal (1968) and Hall (1968b). These zones for the most part represent geologically distinct features, the significance of which will be discussed in a later section.

Let us now examine these figures to see if they give any indications as to whether the model under examination in the present section (uniformly magnetized layers with intensity contrasts along or conformable with the crustal seismic discontinuities) applies in the area. An interesting relationship among F, LL, R and M emerges when plots of F against the others (as shown in Figs. 7, 8, 9 and 10) are made. The circles represent a reasonable estimate of uncertainty in the parameters plotted. Considering that a certain amount of scatter may be expected due to the influence of intensity inhomogeneities, which almost certainly exist within the crust, it is not unreasonable to suggest that linear relationships hold in these three figures. Regardless

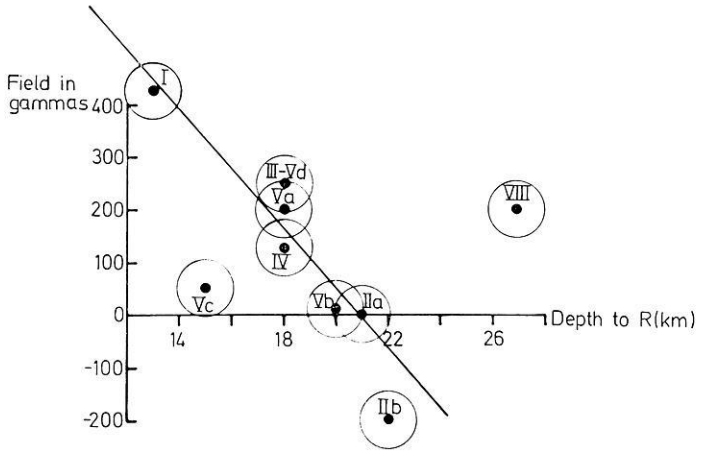

Fig. 8. Plot of field against thickness of upper crustal layer, from values in Table 1 (1 gamma = 1 nanotesla)

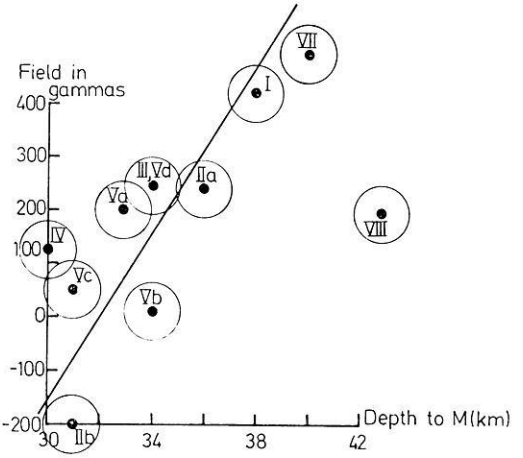

Fig. 9. Plot of field against thickness of crust, from values in Table 1 (1 gamma = 1 nanotesla)

of what interpretations we finally make of them, these linear relationships may be regarded as an observational fact. It is shown elsewhere (Hall, 1974) that such linear relationships are to be expected for the model under consideration.

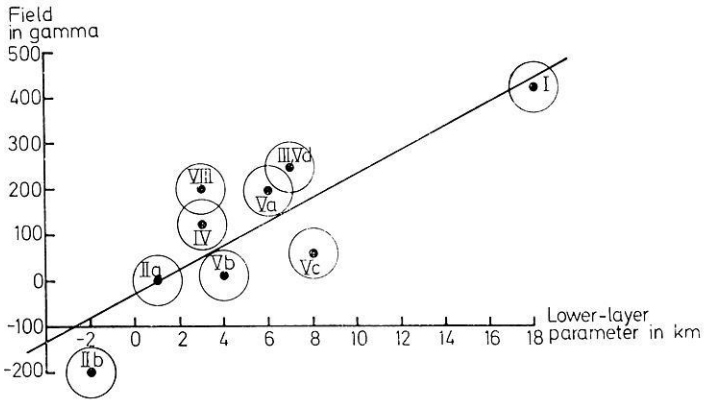

Fig. 10. Plot of field against lower-layer parameter $t = Z - 1.5z$, from values in Table 1 (1 gamma = 1 nanotesla)

Distributions of Magnetization Consistent with the Layered Model

If the R and M discontinuities are boundaries of magnetic zones, then a number of possible configurations might exist, as shown on Fig. 11. These may be summarized as follows.

(1) magnetization lying in the upper crustal layer between some horizon and the R-discontinuity, with magnetization absent (or relatively weak) in the lower crustal layer and upper mantle;

(2) magnetization extending downwards from the R-discontinuity, to a horizon at some level below (in the lower crust or the upper mantle), with magnetization absent (or relatively) weak in the upper crustal layers;

(3) magnetization extending downwards from a horizon at some level, to the M-discontinuity magnetization is absent (or relatively weak) below;

(4) magnetization extending from the M-discontinuity down to a horizon somewhere in the upper mantle. Magnetization is absent (or relatively weak) in the crust;

(5) magnetization extending through the lower crustal layer, and

(6) any of the above cases, but with boundaries of the magnetic zones conformable with the seismic discontinuities rather than coinciding with them.

Analysis of the Linear Plots

It may be shown (Hall, 1974) that for these configurations, F (the field strength) is proportional to either z (depth to Riel), Z (depth to Moho) or a quantity t if the field is caused by a uniformly magnetized lower layer.

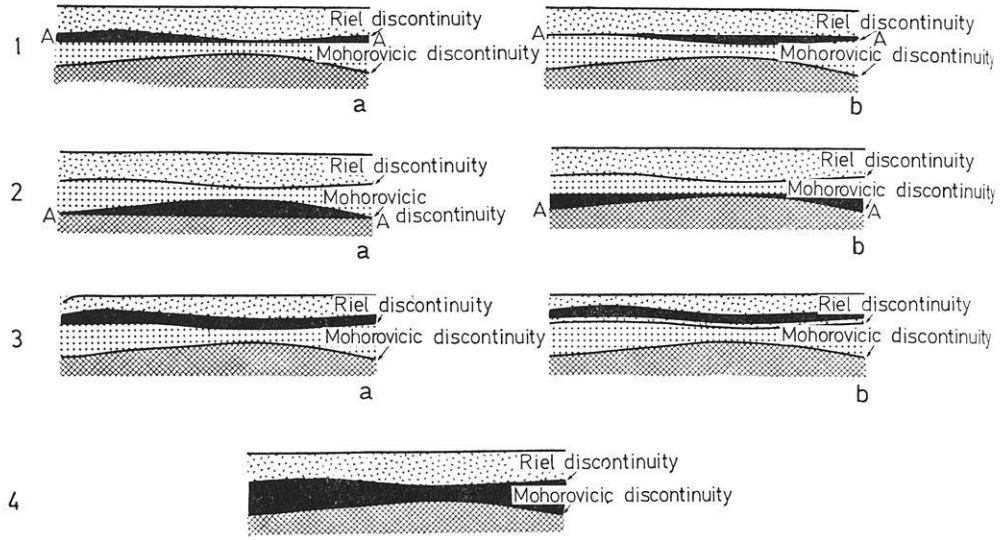

Fig. 11. Ways in which the R and the M discontinuities can control a magnetized zone (in black). Those marked AA have one horizontal surface; those marked "a" lie above. Case 1 is for the R and 2 for the M discontinuity; 3 is for a conformable magnetized zone; 4 is for a magnetic lower crustal layer

The quantity t is called "the lower layer parameter" and is given by $t = Z - 1.5z$ in the area under study. The slopes of the plots of F versus these quantities yield values of the corresponding intensities of magnetization.

Isostatic Case

A possible difficulty arises in using the plots of Figs. 8, 9 and 10 to distinguish the cases outlined in the previous section. If the depths to the R and M discontinuities are everywhere in the area under study related linearly (as would occur for areas related by any one isostatic system (Fig. 13) and if any one of the cases holds, involving control of magnetization by depth to the Riel, or to the Moho or by lower-layer thickness (leading to a linear plot of F versus the appropriate depth or thickness parameter), the plots for the other parameter would also be linear. This circumstance might make it difficult to use these plots to distinguish among the possible cases.

For hydrostatic equilibrium of crust in mantle, given any one isostatic system, we have:

$$z = -\left(\frac{\sigma_3 - \sigma_2}{\sigma_2 - \sigma_1}\right) Z + C \qquad (1)$$

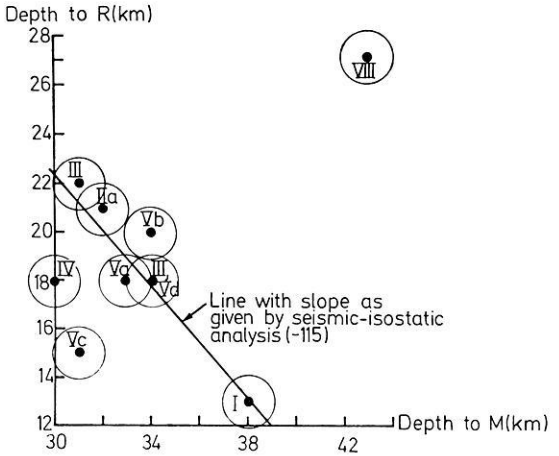

Fig. 12. Isostatic plot for crust in hydrostatic equilibrium with mantle, from values in Table 1

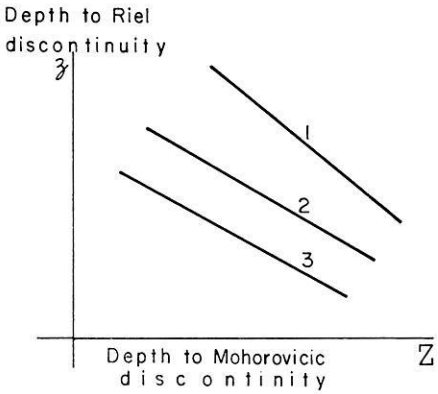

Fig. 13. Isostatic systems in plots such as Fig. 12

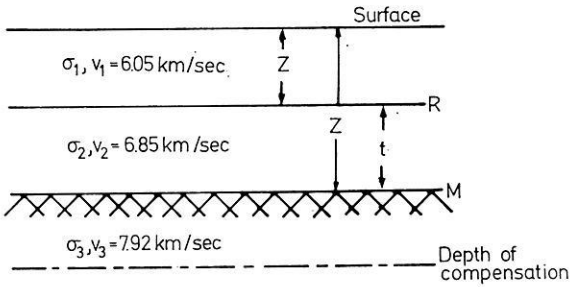

Fig. 14. Airy-Heiskanen model for isostatic plot

where z and Z are depth to Riel and Moho respectively, and C is a constant depending on the densities and the depth of compensation. This equation may be derived for a simple Airy-Heiskanen isostatic model (Fig. 14). Furthermore, in the case where $\sigma = AV + B$ (Birch, 1961, p. 302), with A and B constant over the area, $\sigma_n - \sigma_m = A(V_n - V_m)$. Hence seismic velocities can be used directly in Eq. (1) to determine the multipliers of Z, leading to what has been called the seismic-isostatic method in crustal studies (Hall, 1968b). The velocity values given by Hall and Hajnal (1969, 1973) (all with standard deviations of 0.05 km/sec) give:

$$z = (-1.35 \pm 0.30)\, Z + C \qquad (2)$$

Brown (1968) found these values applicable in detailed studies of isostasy, applying the seismic-isostatic method in conjunction with studies of gravity anomalies over the three southern-most blocks of Fig. 6.

Over an area where the density model down to the level at which compensation takes place, and the depth of compensation, remain constant, a plot of z versus Z forms a single straight line. If any of these conditions differ in an adjacent area, a different line will relate z to Z for that area. Thus these two depths are related in general by families of lines, as shown in Fig. 13. Each line will be referred to as related to a particular "isostatic system".

It is evident that in any isostatic system, z and Z will be proportional. Then if F is related to any one of z, Z, or t by a linear relationship, a plot of F against any other of these quantities will also be linear. Thus plots of F against these depth or thickness parameters would not distinguish one case from another, given a single isostatic system.

Isostatic Systems in the Area

Let us examine isostasy in the area to see if these problems might be encountered in our analysis. In Fig. 12, Riel depth is plotted against Moho depth. It is evident that a single isostatic system holds, by and large, in the area. At first sight this fact would indicate that it will be impossible to use the linear plots to distinguish among the various models considered (Fig. 11). However, Fig. 12 shows some interesting deviations from the system which is obviously dominant over much of the area. These anomalous cases are of importance in evaluating possible magnetic models.

Possible Discrimination between Magnetic Models

Regions IV, Vc and VIII are with the main group of points in Fig. 12 Thus for these three points, the equivalence of the models in Fig. 11 does not hold. If their points in any of Figs. 8, 9, or 10 lies closer to the main

line than in the remaining two plots, then this circumstance can be taken as evidence for favouring the type of magnetization represented by that particular plot. Before we proceed to the selection of our preferred model, let us examine the intensities of magnetization within the crust implied by the various cases represented on Fig. 11. These values are 7.7×10^{-3} emu/cm^3 (case 1), 16.6×10^{-3} emu/cm^3 (case 2), and 5.4×10^{-3} emu/cm^3 (case 4), as derived from the slopes of the plots in Figs. 8, 9, and 10. We should note that the values of these slopes conform within the limits of error given, to the interrelationships given in Eqs. (1) and (2). Thus, as would be expected from Fig. 12, the field versus depth plots are, in their slopes at least, isostatically interrelated.

Selection of Model

Interpretation of Derived Intensities of Magnetization

The method of interpretation used does not require that magnetization be continuously distributed laterally in the layers considered. Linear field versus depth plots would still be possible, as long as a significant portion of each zone of Fig. 6 was underlain by magnetization in the layer under consideration. The linear plot would imply that the intensities of magnetization are roughly the same in all the magnetized portions of the layer and the value of the intensity derived from the slope of the line would be an average of the intensities of these magnetizations.

The derived intensities are 7.7×10^{-3}, 16.6×10^{-3} and 5.4×10^{-3} emu/cm^3, depending on whether the M discontinuity, the R discontinuity or the lower-layer thickness are taken as controlling the long-wavelength anomaly field. If we exclude any special conditions at depth acting to enhance the intensity (such as the Hopkinson effect) and consider intensities of magnetization measured for surface samples as a reliable guide, the figures quoted above leave only the last of the three of them as an acceptable possibility. This conclusion follows from what is known about the intensities of magnetization of igneous rocks (of which the crustal layers are most likely largely composed). From intensities as measured on samples, it appears that (excluding very young volcanic rocks) the largest value of J (the sum of induced and remanent intensity) for rocks common enough to be spread over large areas is for basalts. Typical values of J for ocean-floor basalts are in the range $3—5 \times 10^{-3}$ emu/cc. Granitic rocks average one order of magnitude less. Nagata (1961, p. 313) cites values for J for the "granitic" and "basaltic" crustal layers for a locality in Japan as 1×10^{-3} and 5×10^{-3} emu/cm^3 respectively as determined from magnetic anomalies.

Recent volcanoes and flows provide interesting results. Averages of J over a whole volcano or system of flows are found up to 50×10^{-3} emu/cm^3 (Malahoff, 1969, p. 446). However, the bulk of this magnetization is due to remanence (TRM). This type of magnetization decays with time. If the relaxation time and law of decay suggested by Nagata (1961, p. 155) holds, assuming a Q of 10 (a reasonable value for young volcanic rocks), J would be reduced to below 5×10^{-3} emu/cm^3 after 10^9 years. Thus, even if the precambrian crust had originally been built up to a large extent by volcanic processes, incorporating in it rocks with J's typical of today's young volcanoes and flows, we would expect these intensities to have dropped to the lower values typical of (say) ocean floor basalts.

Discussion of the Particular Models

a) Riel Discontinuity Alone Controlling the Anomalies. If the magnetization were to be above the discontinuity, it would have to be reverse magnetization. The required value (7.7×10^{-3} emu/cm^3) would be possible in precambrian rocks only under exceptional circumstances. Reverse magnetization would require a remanent intensity higher than J. The largest values of J reported for magnetic units at depth in the upper crust in the area are about 4×10^{-3} emu/cm^3 (Hall, 1968a, p. 1286); also, this magnetization lies in concentrations of limited extent (for example, 30 km wide and 5 km deep, as beneath the Aulneau dome). Surface sampling in the area similarly indicates that values as high as 7.7×10^{-3} emu/cm^3 are not encountered over wide areas (Hall, 1968a; Coles, 1973). As regards direction of magnetization, predominantly normal magnetization is suggested for the upper crust (Hall, 1968a) from the interpretation of regional magnetic anomalies, as well as from measurements of remanent magnetization of surface samples (Coles, 1973). Magnetization below the discontinuity would be normal in direction, and remanent and induced intensity of magnetization could be as low as 3.35×10^{-3} emu/cm^3 (for $Q = 1$). The value 7.7×10^{-3} emu/cm^3 for J is still somewhat higher than values encountered previously in the interpretation of regional magnetic anomalies.

b) Mohorovicic Discontinuity Alone Controlling the Anomalies. This case appears to be rules out on all reasonable grounds, because of the large intensity (16.6×10^{-3} emu/cm^3) required.

c) Magnetized Lower Layer. This case suggests reasonable intensity values; also, it is pointed to as a possible case by a number of other circumstances. First of all, the three points for regions IV, Vc and VIII (which lie off the main Manitoba isostatic model in Fig. 12, and therefore are possible discriminating points in the selection of models) lie closer to the best-fit

line in Fig. 10 than they do in Figs. 8 or 9. This circumstance points to the lower-layer model as the best of the three discussed in the present section. Consequently this model was tested further as described in the section below.

Further Tests of the Lower-Layer Model

Coles (1973) has developed a computer programme (Block) to calculate the field over a system of magnetized blocks, each of which can be assigned values for intensity and direction of magnetization. This programme was used as a further test of our model. The lower crustal layer over the area under study was divided into 70 blocks, each extending vertically through the layer, using depths as given by Figs. 2 and 3. Intensity of magnetization was taken as 5×10^{-3} emu/cm^3 and direction of magnetization as parallel to the geomagnetic field. This choice of direction was based on the fact that in earlier deep crustal interpretations (Hall, 1968a, p. 1286 and 1292), near-normal directions of magnetization were found. Subsequently published results of measurements of remanent magnetization of surface rocks in the area (Coles, 1973) support this choice. Contours of the field calculated using Block are shown in Fig. 15. In comparison with Fig. 5 (the long wavelength anomaly map) it can be seen that in general there is good agreement. Some difference in detail is to be expected as the result of lateral inhomogeneities at all levels in the crust. The most serious disagreement occurs at the Bloodvein anomaly, marked as an "anomalous zone" on Fig. 6. The nature of this zone merits a separate discussion.

The Bloodvein Anomaly

This anomaly raises two problems. Either it represents a trend in crustal structure which is not correctly represented by the seismic surveys, or it represents a major inhomogeneity above or below the interface between the crustal layers. Application of Hall's (1968c) method of fitting a sloping step to anomaly curves strongly favours a distribution of magnetization ying in the upper crustal layer, for the Bloodvein anomaly. This interpretation would suggest that the long-wavelength anomaly field is not inconsistent with the seismic discontinuities in this locality.

Apart from the reasonable exception of the Bloodvein anomaly, the block-modelling of the lower crust shows the lower-layer interpretation to be an adequate representation of the observed field.

Interpretation in the Frequency Domain

Interpretations of power spectrum versus frequency (Coles, 1973) also show that crustal sources are consistent with the observed data.

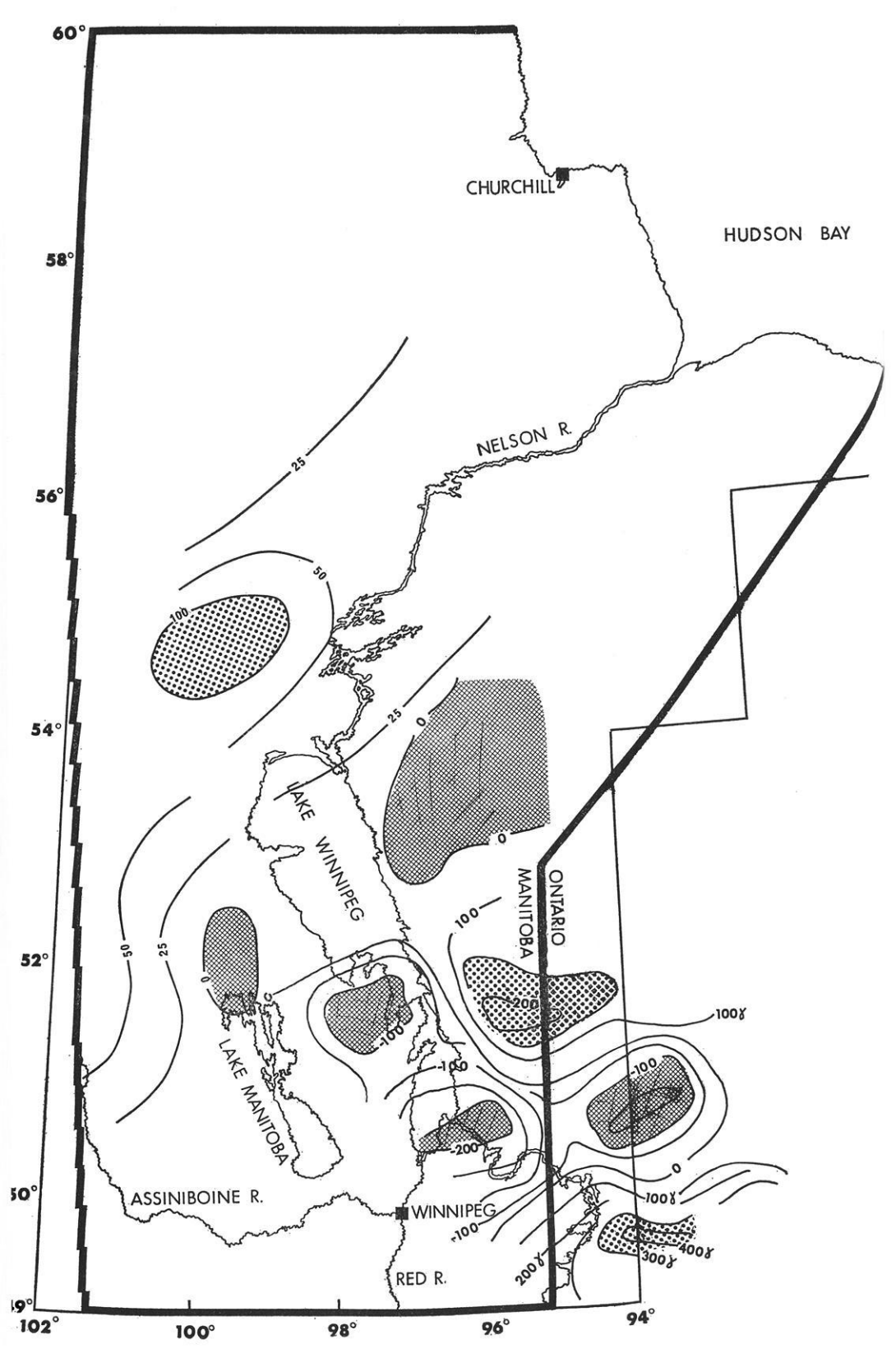
60°
58°
56°
54°
52°
50°
49°
102°
100°
98°
96°
94°
CHURCHILL
HUDSON BAY
NELSON R.
LAKE WINNIPEG
LAKE MANITOBA
MANITOBA
ONTARIO
ASSINIBOINE R.
WINNIPEG
RED R.
25
50
100
0
-100
-200
100γ
200γ
300γ
400γ

Extension beyond the Area of Mapped Riel and Moho

The set of depth-field plots allows extension of our interpretations to several areas beyond that covered by our maps of the R and M discontinuities. A line of recordings of explosions in Lake Superior (during project Early Rise) was run to the north and east of the area by Mereu and Hunter (1969), who interpreted depths to the M-discontinuity from them. These results were compiled with the Manitoba results and with the results of crustal seismic surveys in Hudson Bay by Hall (1971).

Area VI (Table 1 and Fig. 6) lies over Mereu and Hunter's (1969) traverse. Average field and depth to M are known for the area, and are plotted on Fig. 9. Area VI, as can be seen, fits the plot reasonably well. If the layered model can be extended to this area, with the main conclusion of our analysis that magnetization in the lower crustal layer is most likely if the model holds, then we can draw the following conclusion. (1) The area is part of the main Manitoba isostatic system (otherwise, given lower-layer magnetization, there would be no agreement with Fig. 9); (2) The R-discontinuity is present, and its depth is in the 17—19 km range (as is seen by comparing the average field (150 γ) for the area with Fig. 8). If the above calculations and conclusions prove to be correct, we have the basis of a *magnetic-isostatic method* of studying crustal structure.

Area Vd is one of particular interest since it lies almost certainly in the Churchill province of the Canadian Shield. Its position can be viewed as being north of a broad and complex zone separating the Superior and Churchill provinces. Mereu and Hunter's (1969) traverse crosses this area, indicating beneath the traverse a section of considerable thickness (40 km). The area is marked by having field values ranging up to 800 γ (no other area has values in excess of 400 γ). The values of F and depth to M from Table 1 for Area Vd, fit Fig. 9 acceptably. Like Area VI, this area must be part of the main Manitoba isostatic system, and the R-discontinuity must be present. In this case, its depth would be in the 10—12 km range. We might conclude further that the whole of area Vd is underlain by a relatively thick crust.

Another area of interest is the portion of Fig. 5 north of 59° latitude (marked as Area VII on Fig. 6), where the field drops to a relatively low average value, 200 γ. It was indicated in earlier crustal studies of the region (Hall, 1968b, p. 358), that the crustal model of region VIII (the

←

Fig. 15. Component of magnetic field parallel to the geomagnetic field, calculated by programme Block modelling lower crustal layer, assuming uniform magnetization of 5×10^{-3} emu/cm^3, parallel to earth's field. Field values are in gammas (1 gamma = 1 nanotesla; $I_{SI} = 4\pi I_{EMU}$)

western portion of Hudson Bay) extends into the area. The field value of 200 γ, agreeing as it does with that for area VIII, is consistent with this hypothesis. This area lies over an important structural element of the Churchill geological province, the Wollaston Lake fold belt (see e.g. Davidson, 1972, p. 388). Our geophysical analysis indicates this structure as being characterized by a relatively thick crust, a relatively thin lower layer and a moderate to low long-wavelength magnetic anomaly field.

These additional cases add strength to the hypothesis of lower-layer magnetization, since they exhibit markedly different conditions all conforming with one aspect or another of the layered model.

Lateral Inhomogeneities

The alternative remains that some or even all of the features on Fig. 5 could be explained by lateral concentrations of magnetization. These could be relatively thin near-surface plates, or concentrations at greater depths within the crust. Let us examine some possible cases.

Deep Distributions

It is of considerable importance to examine lateral concentrations of magnetization as possible explanations of the field difference between Areas Ib and IIb. This point is critical because the points for Areas I and IIb are key ones in establishing the linearity of the plots in Figs. 7—10.

All indications point to near-normal magnetization in the crust in the area. This case was, therefore, investigated by examining the effect of a block of magnetization lying beneath the large anomaly with 600 γ peak (Fig. 5), in Area Ib, contrasted with no magnetization anywhere beneath Area IIb. The amplitude of the anomaly could be reproduced by a block extending vertically through the upper crust, with intensity of magnetization equal to 3×10^{-3} emu/cm^3. Or, it could be reproduced by a block extending downwards through the lower crust, with an intensity of 5×10^{-3} emu/cm^3. On the basis of the required intensity values, both possibilities are reasonable. However, the block in the lower crust reproduces the anomaly shape better than does the one for the upper crust. It is in fact the best-fit block. Thus a deep crustal distribution is a reasonable one as an explanation of the anomaly, with the result pointing towards a lower-crustal source. This latter model (lower-crustal block) would in fact fit the long-wavelength anomaly field reasonably well. Thus, if lower-crustal magnetization is present, it could be either continuously or discontinuously distributed laterally in the layer. An argument in favour of an upper-crustal source might be the fact that a lower intensity is required, although the required intensity in the lower layer is not unreasonable for basalt.

Thin Near Surface Plate

If a relatively thin near-surface block is considered as the source of the anomaly in zone Ib, it is found that an intensity of 6×10^{-3} emu/cm^3 is required for a thickness of 5 km. Thus an exclusively near-surface source of the anomaly appears to be unlikely because of the high values of intensity required. A similar argument applies to zone Vb.

Final Choice of Magnetic Model

It would appear that there is a good case for the hypothesis that over the area treated, there is widespread deep crustal magnetization giving rise to the long-wavelength anomaly field. The most likely location of this magnetization is in the lower crustal layer, although the interpretations made to date leave also the upper crust as a possible location for it. The inferred intensity of magnetization lies within common ranges found for basalts, other than the very youngest. There is a rather interesting connection between these results, deduced from the long-wavelength anomalies, and previous results (Hall, 1968a) from intermediate-wavelength anomalies. In the latter case, zones of magnetization, some tens of kilometers across, and of vertical dimensions extending from an average of 7 km below the surface to an average of 17 km depth were found. These zones appear to lie beneath granitic plutons, common in the area. The magnetic zones at depth beneath these granitic areas have an intensity of magnetization averaging 3×10^{-3} emu/cc. These zones may represent lower-layer material rising behind the granite plutons during their emplacement (or the residue in a differentiation process), or simply a physical zoning, where upwelling heat favoured the generation of magnetic minerals. Thus these zones in the upper crustal layer would appear to be in some way connected with the lower layer. These relationships are sketched in Fig. 16.

In an earlier interpretation Hall (1968a) examined the evidence offered by the data then available on the presence or absence of lower-layer magnetization. He suggested that, although a definite conclusions was not yet possible, that it appeared that lower-layer magnetization was absent. It is now clear, after considerable extension of the coverage, that the initial area was not suited to revealing the deeper magnetization, and that the subsequent coverage suggests this deeper component.

Conclusions

In the present paper, a new type of magnetic anomaly map for Manitoba and northwestern Ontario (filtered aeromagnetic anomalies in the range of anomaly width 60 km $< \lambda <$ 4000 km) is presented. This map

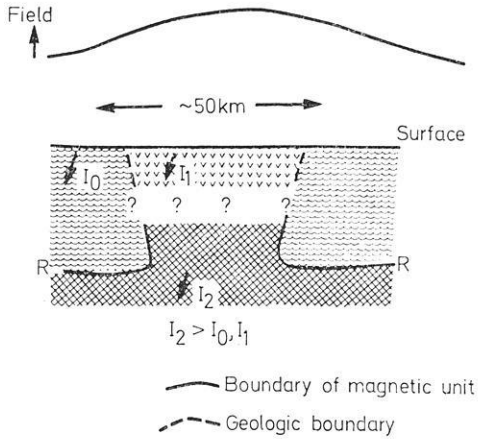

Fig. 16. Suggested distribution of magnetization below granitic areas where regional anomaly highs occur, combining magnetic units treated by Hall (1968a) and results of the present paper

shows close correlation with deep crustal structure as mapped by seismic sounding. This correlation takes the form of straight-line relationships between the field and the following quantities: depth to boundary between upper and lower crustal layers: total thickness of crust, and thickness of lower crustal layers. The plausibility of lateral inhomogeneities being the cause of the anomalies was also investigated, using block models. In addition, the effect of isostatic compensation on results derived from crustal layering was considered. The following conclusions emerged.

(1) Most of the areas within the region fall within a single isostatic system. Three regions do not. If all regions fall within one system, it is impossible to discriminate among the three possibilities for layered models mentioned above. If some regions do not, discrimination is possible.

(2) There are anomalous regions, however, and these point to the lower crustal layer as the most probable seat of the origin of the long-wavelength anomaly field. The required intensity of magnetization in this layer would be 5.3×10^{-3} emu/cm^3; this value is close to the average value for measured samples of basalt.

(3) The upper crustal layer is also a possible seat for magnetization related to the long-wavelength anomaly field, although the lower layer is more probable on the basis of the data analyzed in the present paper.

(4) Shallow plates of magnetization appear to be very unlikely as the origin of the anomalies. Thus we are led to look for *deep crustal magnetization* whether it lies in the upper or the lower crustal layer.

Acknowledgements. This research was done with support by the National Research Council of Canada, and the University of Manitoba Northern Studies Commitee. This support is gratefully acknowledged.

The author wishes to thank Dr. Richard Coles for providing his programme Block for use prior to its publication. The help of Mr. David Richards in computer processing throughout the investigation is acknowledged. Mr. Charles Hasselfield carried out computer processing and programming during the testing of the block models.

References

Bhattacharyya, B.K., Morley, L.W.: The delineation of deep crustal magnetic bodies from total field aeromagnetic anomalies. J. Geomagnet. Geoelectr. *17*, 237–252, 1965

Birch, F.: Composition of the Earth's Mantle: in The Earth Today; Royal Astronomical Society. 295–311, 1961

Brown, R.J.: Isostasy and crustal structure in the English River gneissic belt: Unpublished M. Sc. Thesis. University of Manitoba, 1968

Coles, R.L.: Relationships between measured rock magnetizations and interpretations of longer wavelength anomalies in the Superior province of the Canadian Shield. Unpublished Ph. D. thesis, University of Manitoba, 215 p., 1973

Davidson, A.: The Churchill Province: in Variations in Tectonic Styles in Canada, 382–388, 1972

Dominion Observatories Branch: F-isodynamic chart, Canada, 1965

Hajnal, Z.: A two-layer model for the earth's crust under Hudson Bay; In Earth Science Symposium on Hudson Bay, P. J. Hood (ed.) Geological Survey of Canada paper 326–336, 1969

Hall, D.H., Dagley, P.: Regional magnetic anomalies; An analysis of the Smoothed Aeromagnetic Map of Great Britain and Northern Ireland. Institute of Geological Sciences, Report 70/10, 1970

Hall, D.H.: Regional magnetic anomalies, magnetic units, and crustal structure in the Kenora District of Ontario. Can. J. Earth Sci. *5*, 1277–1298, 1968a

Hall, D.H.: A seismic-isostatic analysis of crustal data from Hudson Bay, in Earth Science Symposium on Hudson Bay, P. J. Hood, Ed. Geological Survey of Canada Paper 68–53, 337–364, 1968b

Hall, D.H.: A magnetic interpretation method for calculating body parameters for buried sloping steps and thick sheets. Geoexploration. *6*, 187–206, 1968c

Hall, D.H.: Geophysical determination of deep crustal structure in Manitoba. The Geological Association of Canada, Special Paper No. *9*, 83–88, 1971

Hall, D.H.: In preparation 1974

Hall, D.H., Hajnal, Z.: Crustal Structure of northwestern Ontario. Refraction seismology. Can. J. Earth Sci. *6*, 81–99, 1969

Hall, D.H., Hajnal, Z.: Deep seismic crustal studies in Manitoba. Bulletin of the Seismological Society of America *63*, 885–910, 1973

Hall, D.H., McGrath, P.H., Richards, D.J.: Regional Magnetic anomalies in Manitoba. Manitoba Mines Branch (in press), 1974

Malahoff, A.: Magnetic Studies over Volcanoes. Hawaii Institute of Geophysics Contribution *198*, 436–446, 1969

McGrath, P.H., Hall, D.H.: Crustal structures in northwestern Ontario: Regional magnetic anomalies. Can. J. Earth Sci. *6*, 101–107, 1969

Mereu, R.F., Hunter, J.A.: Crustal and upper mantle structure under the Canadian Shield from Project Early Rise. Bull. Seism. Soc. Am. *59*, 147–165, 1969

Morley, L.W., MacLaren, A.: Magnetic anomaly map of Canada. Map number 1255A, 1967

Nagata, T.: Rock Magnetism, Revised Edition, 350 pp., Tokyo: Maruzen Co., 1961

Regan, R.D.: World Wide Magnetic Anomalies from Pogo and Cosmos Data, IAGA Second General Scientific Assembly, 1974

Wilson, H.D.B.: The Superior Province in the Precambrian of Manitoba. The Geological Association of Canada, Special Paper, No. *9*, 41–49, 1971

Zietz, I., Andreasen, G.E., Cain, J.C.: Magnetic anomalies from satellite magnetometer. J. Geophys. Res. *75*, 4007–4017, 1970

D. H. Hall
Geophysics Section
Department of Earth Sciences
University of Manitoba
Winnipeg, Canada

J. Geophys. 40, 431–433, 1974

Local Magnetic Anomalies of the Area of the Upper Kolyma River (North-East of the USSR)

L. I. Izmailov

North-East Complex Research Institute, Magadan

Received March 12, 1974

Abstract. Most of the local magnetic anomalies in the area of the Upper Kolyma River are linear while a subordinate number are arcuate. The anomalies follow fracture zones and the arcuate anomalies usually mark the outer zones of granitic intrusions. The bodies producing the anomalies are situated between the surface and 300 m deep. In most cases these bodies were identified as zones of pyrrotine mineralization within the sediments, in a few cases as dokes. Other magmatic rocks were practically nonmagnetic. In a few bodies investigated, small amounts of magnetite and hematite con tribute up to 15% of the total magnetization.

In the Upper Kolyma region the pyrrotine mineralization correlates well with the presence of gold.

Key words: Magnetic Anomalies – Rock Magnetism – Mineralization.

The territory of the Upper Kolyma River is characterized by original distribution of magnetic field character. There are mostly linear and less arc-type magnetic anomalies. As to the tectonics the above territory applies to Injali-Debin synclinore and Bujundin-Balychagansky anticlinore (its Northern part). It is composed of sedimentary rocks of Verkhoyansk complex, represented by thick rather monotonous series of alevralites, clay slates and sandstones of Permian, Triassic and Jurassic age. The faults of different depth, age and orientation were widely spread in the region. The most part of the fracture zones is connected with the final stages of the geosyncline development and has concordant striking with the synclynore and anticlinore. The depth fracture zone forsaw the structural and rather often metallogenic plan of the territory in question. They are traced by the anomalies of magnetic and gravitational field, they are well observed in the relief. The other part of the breaches is less streched but much more numerous. Usually they are fixed by the zones of high cracking, shearing, milonitizing etc. In the local magnetic field they are expressed by positive anomalies, which have linear and arc-type forms in the plan. As a rule, linear anomalies are situated aside the intrusive bodies.

Their lenght is different: in the West it reaches 50 kms in average, in the South 6–10 kms. The width of linear anomalies varies from 3 till 7 kms.

The anomalies reflect the magnetization objects, corresponding by their form to steep layers with different stretching in depth.

Arc-like anomalies usually join big granite intrusive bodies, being situated in different distances from them — from hundreds meters to the first kilometers and partly repeating their entering contour. The anomalies length is in average 2—5 kms and the width 1—2 kms.

The depth of upper selvages of the most magnetic objects varies in the limit of 0—300 m.

During several years the geological nature of the anomalous objects has been studied in complex. Quantitative calculation have shown that mainly these objects are bared by the day, especially taking into account rather dismembered relief of the region. The placing of the dawn selvage varies in wide limits very often exceeding magnetic bodies in dozen times. If these objects are in day we must observe them. Streched bodies, differing by their litologic composition from sediments are only the dikes of quartz porphyres, porphyrites, lamprophyres, dacites and others, most of them being intensive propylizated. However spacely magnetic field anomalies and the dikes do not coincide, often they do not cross in their stretching. In order to see the undiscovered bodies the chinks were passed.

Ferromagnetic properties of rocks including the core were studied. It proved to be that the sediments and in a small quantity the dikes are magnetoactive. Their magnetization varies in large limits and is averaging 700—1000 cgs units.

Magmatic formation of the region excluding some dike rocks are practically nonmagnetic.

The investigation of mineralogical content of rocks sediments, intrusives and their magnetization has shown that the local magnetic anomalies are due to the zones of pyrotine mineralization.

The pyrotine is represented by two modifications — paramagnetic hexogonal and ferrimagnetic monoclinal, what was fixed by roentgenostructural analysis and powder pattern.

The temperature of pyrrotine forming according to thermodemagnetization varies in large limits — from 100° till 270°C and seldom exceeds this mineral's Curie point. The temperature values are confirmed with the help of decrepitation, by thermomagnetization and by studying Koenigsberger coefficients as well. Though in most cases the magnetization is explained by the presence of ferromagnetic pyrrotine, but sometimes there takes place (till 10—15% of the whole magnetization) the contribution of minerals having higher Curie points. Magnetization vector of these minerals differs to the angle of 30—110°. These minerals proved to be magnetite and hematite. In sediments they are of rolled form, what says of their sedimentary origin. Thus, the moment of sediments forming is caught in the magnetic characteristic and much later discovered pyrrotinization.

It was shown during the investigations that the heating of monoclinic pyrrotine till 400° at the atmosphere does not cause any unreversal structural changes.

Pyrrotine mineralization is very much connected with the golden one; the pyrrotine mineralization being earlier than the golden stage of a common metamorphic — hydrothermal process.

Similar zones of pyrrotine mineralization are widely spread not only in North-east of the USSR, but in some other regions of the USSR (Eastern Siberia, Enisei mountain-ridge etc.) and also in Canada, Tanzania etc.

Dr. L. I. Izmailov
Dzerdginskyi Street 10
Flat 12, Magadan
USSR

J. Geophys. 40, 435–438, 1974

Investigations of Secular Variation Anomalies in the Middle Ural Region

V. A. Shapiro and N. A. Ivanov

Institute of Geoph. Ural Sci. Centre of USSR Academy of Science

Received March 12, 1974

Abstract. In a 120000 km^2 area of the Middle Ural Region a network of stations was repeatedly observed during several years. The aim was to determine local differences in the secular variation of the total intensity of the geomagnetic field. Out of a number of anomalies of this type two examples are considered in detail. They are situated 140 km west and 180 km east of Sverdlovsk respectively and show differences of more than 10 γ/year over distances in the order of 10 km. One of these anomalies was clearly observed between 1968 and 1970 and decreased between 1970 and 1971.

The exact geological cause of these anomalies is not yet known. However, active faults appear to extend through the crust in this area.

Key words: Secular Variation — Anomalous Zone — Geomagnetic Field — Proton Magnetometer — Active Faults.

A total field magnetic survey is being carried out in Urals with partial occupation of the Zauralie and Preduralie regions, following profiles located along the roads, with distances between profiles up to 50 km and distances between the points of the survey up to 5 km. In the Institute of Geophysics of the Ural Scientific Centre USSR Academy of Science, this survey has been performed every year since 1968 in order to find and study the geomagnetic secular variation anomalies in the Urals. The survey is performed according to the method of synchronous observations with two proton magnetometers. One temporary magnetic observatory is situated at the point of reference, and a portable instrument is placed in succession at points of the survey network. Besides the proton magnetometer, the four component magnetic variational station H, D, Z, T with scale value Z, T, 0,3 and H, D, 1,0 gamma/mm and with the recording rate 90 mm per hour, works at the point of reference. The proton magnetometers with sensitivity $\pm$0,1 gamma were developed and made in the laboratory. The survey is repeated periodically every 1 or 2 years. Observations on the discovered anomalies are performed several times each year. The separation of ordinary points of survey from the temporary observatories does not exceed 100—150 km. Simultaneous base station measurements permit elimination of the influence of geomagnetic field variations, induced by ionospheric

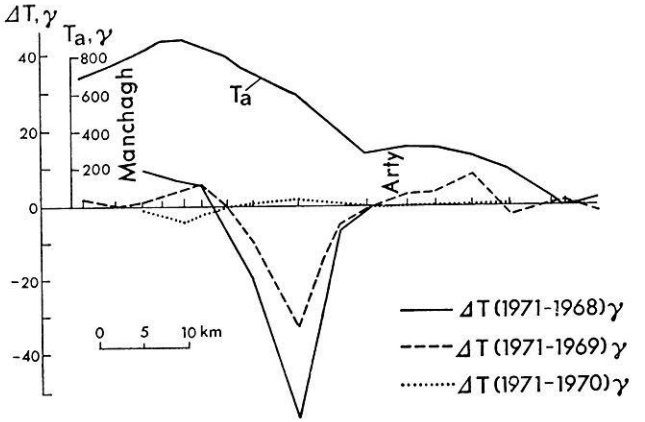

Fig. 1. Constant magnetic anomaly T_a and local secular variation anomaly ΔT in the Manchagh-Arty area

sources. Hence, the error of the mean difference ΔT between the measurements at observatories and at the ordinary point isn't more than $\pm 0{,}6 - \pm 1{,}4$ gamma. At the present time, a considerable part of Middle Urals territory in the region of Sverdlovsk and Kurgan is under this total field survey. The survey area is 250 km along the meridian and 550 km along the latitude. During repeated observations taken each 1 or 2 years, considerable variations of ΔT are observed, and also in some regions smaller local anomalies are discovered.

In 1969 a secular variation anomaly was discovered between the Arty and Manchagh settlements, 140 km west from Sverdlovsk. The width of this anomaly is 15 km (Fig. 1). During 1968—1970, a maximum change of ΔT with amplitude 55 gamma was observed. In 1970—1972 the intensity of ΔT change decreased greatly and the anomaly had reversed its sign. Sedimentary sandy-carbon rocks of Permian, Carboniferous and Devonian ages occur down to depths about 7 km from the earth's surface in the anomaly region. The crystalline basement consists of strongly metamorphosed gneisses, slates and amphibolites. Gneisses are interrupted by magnetic rocks in some places including basic and ultrabasic rocks. According to seismic data the depth to the ultrabasic layer is 19 km, the depth to the Mohorovičič discontinuity is 38 km. The magnetic rock in the crystalline basement produces a constant magnetic anomaly Ta with intensity 900 gamma in the epicentre and 400—600 gamma at the secular variation anomaly area (Fig. 1). It appears that the changing of tectonic stresses influences the magnetic properties of the crystalline basement. We think that stress changes in time cause our secular variation anomalies. To judge by the half-

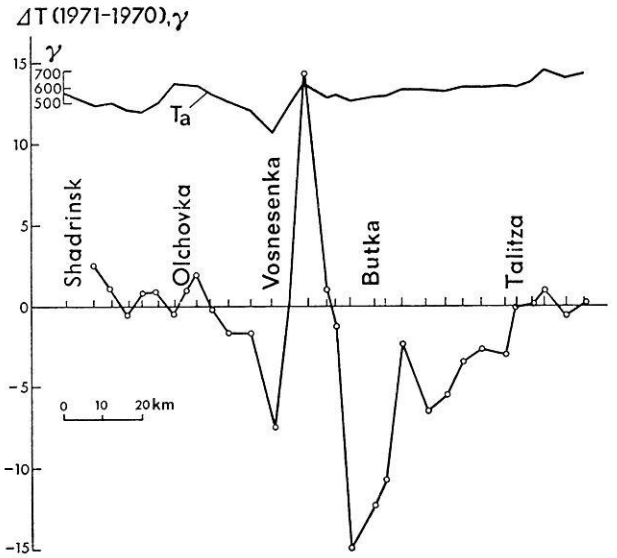

Fig. 2. Constant magnetic anomaly T_a and local secular variation anomaly ΔT in the Shadrinsk-Talitza area

width of our anomaly, the depth to magnetic basement is approximately 8 km. The rate of decrease and reversal of sign testify to rapid tectonic force change in this region. The survey and the anomaly investigations are continuing in more detail.

A second local secular variation anomaly was discovered in 1971 on the Eastern slope of the Urals near Butka settlement, 180 km East from Sverdlovsk (Fig. 2). Anomaly length is 60 km according to the survey profile. The Butka anomaly is characterized by positive and negative peaks with intensity of ΔT up to 15 gamma in a one year period. At the present time, the anomaly has been investigated along one profile. In 1972 this anomaly had been surveyed twice, and in 1973 it was surveyed several times. In 1973 four-component magnetic variational stations were placed both in the normal field at the point of reference, and also in the anomalous region, in order to explore not only total field changes, but also the field components. We also examined several profiles perpendicular to the original one. The results of repeated observations of the anomaly showed that it has complicated forms and long time durations.

Geological conditions in the anomaly region are characterized by sharp changes in crystalline base depth, from 8 km depth in the west to only 2 km in the east. The depth to the Conrad discontinuity is 23 km, and to the Mohorovičič—39 km. Moreover, west of the anomaly the depth to

Mohorovičič discontinuity is 45 km, and to the east the depth is 43 km. The presence of these ruptures of the Conrad surface and of the basalt layer points to the complicated geological conditions in this region.

The latitude profiles of a helium survey and magnitotelluric soundings in the described region have also revealed considerable anomalies at the points of intersection with our own Butka anomalous zone.

It seems likely that our own observations, and also the helium and magnetotelluric surveys, are revealing the existence of active faults extending right through the crust.

In the surveyed territory, besides the two described anomalies, some other places were found with changes of ΔT deflections higher than the errors of the measurement. But these other anomalies are not discussed in this work because they were not observed in detail.

Vsevolod A. Shapiro
Institute of Geophysics
Ural Sci. Centre
USSR Academy of Science
USSR 620169, Sverdlovsk, K-66
Pervomaiskaya 91

J. Geophys. 40, 439–451, 1974

2. *Aspects of Rock Magnetism — General*

Thermal Enhancement of Magnetic Susceptibility

D. J. Dunlop

Geophysics Laboratory, Department of Physics and Erindale College, University of Toronto, Toronto, Canada

Received March 12, 1974

Abstract. The interpretation of geomagnetic anomalies with deep-seated sources sometimes requires postulating magnetic susceptibilities larger than those measured for common rock types at the earth's surface. A possible explanation is that rocks buried at depths approaching the Curie point isotherm exhibit enhanced susceptibility due to the Hopkinson effect. In measurements on a sample of single-domain magnetite (0.04 μm particles), the susceptibility increased by a factor 2 between 20 and 500 °C and by a factor 3 at 550 °C. The Hopkinson peak was less pronounced in multidomain magnetites: the relative increase in susceptibility at 550 °C was by a factor 2 in 0.1 μm particles and a factor 1.5 in 0.25 μm particles. Single-domain hematite (0.1–1 μm) gave a spectacular Hopkinson peak, with relative susceptibility enhancement by a factor 5 at 530 °C and a factor 20 at 640 °C. However, rocks containing fine-grained maghemite and magnetite showed an enhancement of 50–70 % at most. The reasons for this variability in the height of the Hopkinson peak are not understood, but the width and shape of the peak are clearly related to the blocking temperature spectrum. Distributed blocking temperatures are associated with a broad peak, while discrete blocking temperatures are accompanied by a sharp susceptibility peak within 50–100 °C of the Curie point. A corollary is that remanent magnetization decreases roughly in inverse proportion to increase in susceptibility, so that the Koenigsberger Q_n ratio decreases sharply at high temperature. For this reason, deep-seated anomalies can almost certainly be interpreted in terms of induced magnetization only. Finally, somewhat shallower bodies (temperatures of 200–400 °C) may exhibit thermally enhanced magnetization for two reasons: first, titanomagnetites have widely varying Curie points depending on titanium content, and second, observed anomalies are the result of a geomagnetic field applied over 10^6 years and viscous magnetization is also known to be enhanced at high temperature.

Key words: Magnetic Anomalies — Susceptibility — Induced Magnetization — Remanent Magnetization — Hopkinson Effect — Curie Point Isotherm.

Introduction

Relatively intense regional magnetic anomalies whose sources are apparently 10–30 km deep in the crust are widespread in the Precambrian Shields of the world. The effective magnetizations of the sources as deduced by Bhattacharya and Morley (1965), Hall (1968), McGrath and Hall (1969) and Krutikhovskaya *et al.* (1973), among others, correspond to suscep-

tibilities of 10^{-3} — 10^{-2} emu/cm^3. Since the susceptibilities of the surface rocks in shield areas are commonly 10^{-4} — 10^{-3} emu/cm^3, one is forced to conclude that either remanent magnetization is responsible for most regional anomalies or else that susceptibility is somehow enhanced at depth in the crust. The latter possibility is explored in this paper.

Susceptibility and Domain Structure

The magnetization induced by a given field H depends on whether the domain structure must be rotated, as in single-domain (SD) grains, or whether domain wall displacements are also possible, as in multidomain (MD) grains. The theoretical initial susceptibility χ_0 of unaxial, randomly oriented SD grains is (Stoner and Wohlfarth, 1948; Dunlop, 1969)

$$\chi_0 = 0.349 \frac{M_S}{H_R} \tag{1}$$

where the remanent coercive force H_R (the reverse field required to reduce to zero the remanence following saturation in the forward direction) essentially measures the resistance of anisotropy forces to rotation of the spontaneous magnetization M_S. The intrinsic susceptibility χ_i of MD grains is likewise inversely proportional to coercive force (in this case, the resistance to wall motion) but the self-demagnetizing field reduces the observed susceptibility to (Neel, 1955; Nagata, 1961; Stacey, 1963)

$$\chi_0 = \frac{\chi_i}{1+N\chi_i} \approx \frac{1}{N} \tag{2}$$

where N is the demagnetizing factor, determined by the shape of the grain. Both Nagata (1961) and Stacey and Banerjee (1974) suggest an average value $N=3.8$—3.9 for titanomagnetite grains in igneous rocks, very little different from the value $4\pi/3$ appropriate to equidimensional grains.

Fig. 1 compares measured values of χ_0 for single-domain and two-domain grains of magnetite and other strongly magnetic minerals with Eqs. (1) and (2). It is interesting that while some of the SD samples have extreme M_S/H_R values seldom, if ever, encountered in nature, the resulting range of χ_0 is only 0.1—0.6 emu/cm^3. χ_0 for SD magnetite is thus comparable to χ_0 for MD magnetite. The great contrast between the Koenigsberger ratios of SD and MD magnetite reflects the more intense TRM (thermoremanent magnetization) of SD grains, not a susceptibility contrast.

Although two-domain grains display some SD-like features (Dunlop, 1974), Fig. 1 shows that their susceptibilities are greatly reduced by self-demagnetization. Grains with higher domain multiplicities have χ_0 essentially independent of H_R, as predicted by Eq. (2).

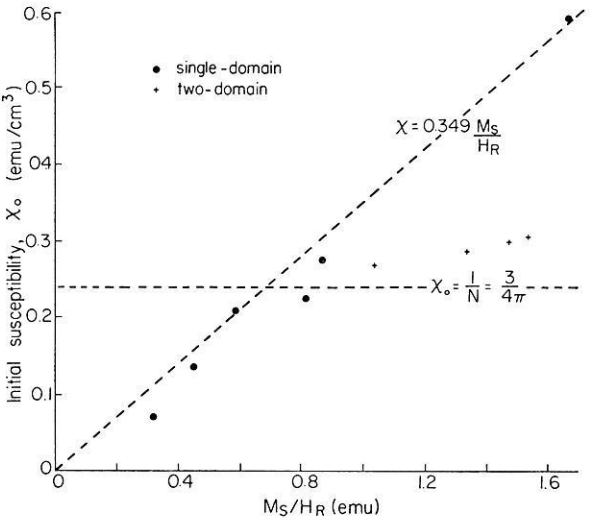

Fig. 1. Initial susceptibilities of some natural and synthetic samples of magnetite and maghemite, as a function of the ratio M_S/H_R. The theoretically expected dependences for SD and MD materials (Eqs. 1 and 2) are shown as dashed lines. SD materials agree well with theory, while two-domain materials are intermediate between SD and MD behaviour. (After Dunlop, 1974)

Above a critical blocking temperature T_B, both SD and MD grains become superparamagnetic (SPM): that is, barriers to domain rotation or wall motion are overcome by thermal energy and very large susceptibilities can result. For SD grains (Bean and Livingston, 1959),

$$\chi_0 = \frac{M_S}{H} L\left(\frac{vM_SH}{kT}\right) \tag{3}$$

where v is grain volume, k is Boltzmann's constant and T is temperature. The Langevin function $L(\alpha)$ equals α for $\alpha \lesssim 0.2$ and equals 1 for large α.

Since the blocking temperature for MD grains is invariably close to the Curie point, M_S is rather small throughout the blocking region and SPM enhancement of χ_0 is not as significant as in the SD case.

Susceptibility of Crustal Rocks

Table 1 lists measured values of χ_0 for a variety of crustal igneous and metamorphic rocks ranging in age from Archean to Tertiary. The rocks were originally measured because of their paleomagnetic interest and by no means comprise a representative sampling of the continental crust.

Table 1. Susceptibilities of some crustal rocks. Both the observed susceptibility and the calculated value corresponding to 100% magnetite are tabulated. The numbers (I through VI) accompanying the Steens and Iceland samples refer to the oxidation index (Wilson and Watkins, 1967) of these basalts

Rock type	Volume % Fe_3O_4, p	χ_0 as observed (10^{-4}emu/cm^3)	χ_0 for $p = 100\%$ (emu/cm^3)
Tertiary basalts			
1) Cobb seamount[a]	0.41	8.55	0.210
2) Cape Dyer basalts[b]	<0.01	0.18	0.295
	0.02	0.44	0.184
	0.03	0.86	0.324
	0.11	1.96	0.179
3) Steens basalts I[c]	0.18	6.02	0.344
II	0.18	5.27	0.291
III	0.17	6.39	0.377
IV	0.23	4.85	0.211
V	0.18	3.88	0.221
4) Iceland basalts I[d]	0.22	10.0	0.455
II	0.27	11.8	0.436
III	0.26	5.97	0.234
IV	0.29	5.98	0.204
V	0.23	4.69	0.201
VI	0.23	4.95	0.214
Archean metabasalts			
1) Kirkland Lake	<0.01	0.14	0.185
greenstones[e]	0.01	0.26	0.202
	0.08	2.86	0.344
Diabases			
1) Matachewan dike[e]	0.01	0.23	0.216
2) Logan sills[f]	0.03	0.68	0.237
3) Glamorgan dike[g]	0.02	0.56	0.276
4) Coronation sills[h]	0.27	6.83	0.258
	0.44	9.45	0.214
5) Tasmanian dolerite[i]	0.11	2.55	0.244
6) Lambertville diabase[j]	0.12	3.44	0.287
Gabbros, anorthosites			
1) Modipe gabbro[k]	0.02	0.41	0.255
2) Sudbury norite[l]	0.02	0.39	0.204
3) Michikamau anorthosite[m]	0.25	9.78	0.387
4) Michael gabbro[n]	0.44	14.7	0.332
5) Glamorgan gabbro[g, o]	0.01	0.18	0.206
	0.06	2.13	0.335
Diorites, granites			
1) Kirkland Lake diorite[e]	0.02	0.30	0.189
2) Dudmon diorite[g, o]	0.79	33.8	0.428
3) Bark Lake granodiorite[g, o]	0.24	10.3	0.428
4) Spavinaw granite[p]	0.33	8.50	0.259

Nevertheless several significant trends appear in the data. First of all, since the volume percent of magnetic material was known from saturation magnetization measurements, it was possible to find the value of χ_0 corresponding to 100% magnetite for each rock. Despite the variety of rock types, these all lay between 0.18 and 0.46 emu/cm^3, a range entirely consistent with the theory of the previous section and the data of Fig. 1.

A second point is that all the rock types examined, even those generally considered to be very magnetic (eg. Tertiary continental and submarine basalts), contained less than 1% by volume magnetite. As a result, the observed susceptibilities (with one or two exceptions) were 10^{-3} emu/cm^3 or less. It is interesting that the Spavinaw granite and the Bark Lake granodiorite (both of Precambrian age) each contain about 0.3% magnetite and are as strongly magnetic as most of the more mafic rocks. Although these two rocks are probably atypical, they do demonstrate that felsic rocks cannot be dismissed as possible sources of regional anomalies.

Finally, Table 1 shows that despite great variability in observed susceptibilities, χ_0 tends to be lower for older, more metamorphosed rocks. For example, the Kirkland Lake greenstones contain about one-tenth the magnetic material found in Tertiary volcanic equivalents. Precambrian diabases like the Matachewan and Glamorgan dikes and the Logan sills are 5—10 times less magnetic than the Phanerozoic Tasmanian dolerite and Lambertville diabase. Bearing this trend in mind, we have even more difficulty in reconciling the effective magnetizations of deep magnetic anomaly sources in Precambrian terrain with the susceptibilities typical of surface rocks in these areas.

Remanent and Induced Magnetization

There are two ways of resolving the paradox that typical crustal rocks seem to have susceptibilities that are insufficient to account for regional magnetic anomalies. One way is to appeal instead to the TRM of rocks contaning SD or small MD grains of titanomagnetite. These rocks can readily supply the requisite magnetization, the "enhancement factor" being the Koenigsberger ratio Q_t between TRM and induced magnetization produced by the earth's field. Stacey (1967) has shown that Q_t is much

←

[a] Merrill and Burns, 1972; [b] Deutsch, Kristjansson and May, 1971; [c] Watkins, 1969; [d] Watkins and Haggerty, 1968; [e] Pesonen, 1973; [f] Robertson and Fahrig, 1971; [g] Dunlop, Hanes and Buchan, 1973; [h] Fahrig, Irving and Jackson, 1971; [i] Stott and Stacey, 1960; [j] Hargraves and Young, 1969; [k] Evans and McElhinny, 1966; [l] Hood, 1961; [m] Murthy, Evans and Gough, 1971; [n] Fahrig and Larochelle, 1972; [o] Buchan and Dunlop, 1973; [p] Spall and Noltimier, 1973.

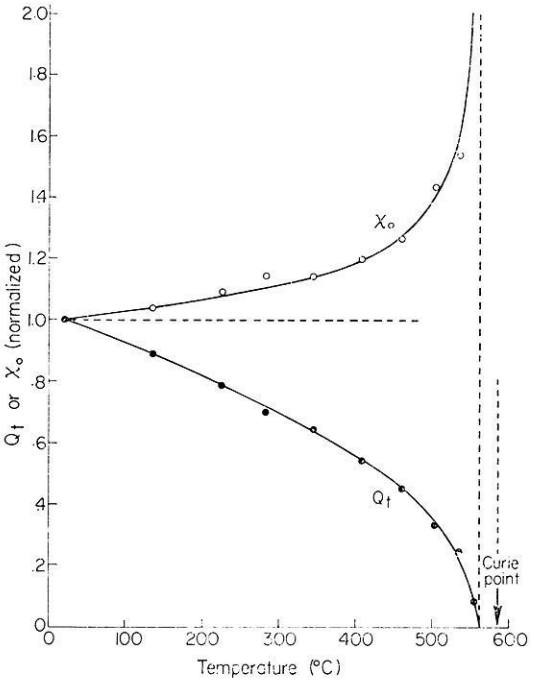

Fig. 2. The normalized temperature dependence of initial susceptibility χ_0 and Koenigsberger ratio Q_t for a typical submicron magnetite. Between the Curie point and the blocking temperature (the dashed line about 30 °C below the Curie point), Q_t is zero but χ_0 is considerably enhanced

greater than 1 for magnetite grains smaller than a few microns but less than 1 for larger grains.

Appealing to TRM as the source of anomalies has of course the unfortunate consequence that the magnetization direction is unrelated to that of the present field, complicating the interpretation process. The alternative is to suppose that induced magnetization is enhanced deep in the crust. Susceptibility changes significantly with hydrostatic pressure (Nagata, 1961, Girdler, 1963) but the increase of susceptibility with temperature (the Hopkinson (1889) effect) is a more important effect if the rocks are buried close to the depth of the Curie point isotherm. Fig. 2 illustrates the effect. The enhancement is generally significant only within 100 °C or so of the Curie temperature.

There is at present no evidence so compelling that we can choose one explanation over the other. However it is worth noting that since regional anomalies are very widespread in Precambrian Shields, it is only natural to favour as sources rock types that are similarly widespread. Obvious

candidates would be the deep equivalents of the granitic rocks which are ubiquitous at the surface. Some authors (e.g. Krutikhovskaya *et al.*, 1973) favour very large basic intrusives as sources. In either case, the rocks are coarse-grained and would be expected to exhibit generally low Q_t values. Furthermore, as Fig. 2 illustrates, Q_t decreases steadily as the temperature increases and is zero throughout the region between the blocking temperature and the Curie point. This is of course the same region in which susceptibility is maximum because of superparamagnetism. Thus even SD grains behave like low-Q_t materials at high temperature.

On the other hand, it is not clear that susceptibility enhancement by the Hopkinson effect is sufficient or occurs over a sufficiently wide range of temperature to significantly enhance the magnetization of deeply buried rocks. We shall examine these questions and the physical factors controlling the Hopkinson effect in the next section.

The Hopkinson Effect in Rocks and Minerals

In SD grains and small MD grains with pseudo-SD magnetic moments (Dunlop, 1973a), the susceptibility increases with temperature for two reasons. Below the blocking temperature T_B of a particular grain, Eq. (1) predicts that χ_0 is proportional to M_S/H_R. Above T_B, χ_0 jumps to the value given by (3), eventually falling to zero with M_S at the Curie point. The grains in a rock have a spectrum of sizes and hence of T_B, with the result that both effects contribute to χ_0 of the rock in the blocking region.

The height of the Hopkinson peak, which determines the maximum enhancement of susceptibility, is controlled both by H_R at room temperature, T_0, and by the minimum blocking temperature. The larger $H_R(T_0)$ and the higher $(T_B)_{\min}$, the larger the enhancement factor $H_R(T_0)/H_R(T_B)$. On the other hand, if $(T_B)_{\min}$ is too high, M_S is small and so is the SPM susceptibility. The width of the Hopkinson peak, which determines over what range of temperatures (and by extension, over what range of crustal depths) there is significant enhancement of χ_0, is controlled almost entirely by the width of the blocking temperature spectrum.

Large MD grains invariably have a narrow T_B spectrum just below the Curie point, and according to Eq. (2), there is no susceptibility increase below $(T_B)_{\min}$. We can expect therefore a rather narrow and not particularly high Hopkinson peak in MD materials.

Figs. 3, 4 and 5 illustrate these principles. Fig. 3 compares χ_0 and M_S/H_R data and the blocking temperature spectrum (determined from stepwise thermal demagnetization of a 1-oersted TRM) for two submicron magnetites described by Dunlop (1973a, b). The small MD grains (mean size about 0.1 μm) have a narrow range of T_B just below the Curie temperature of 583 °C, and except in this range, χ_0 and M_S/H_R have identical

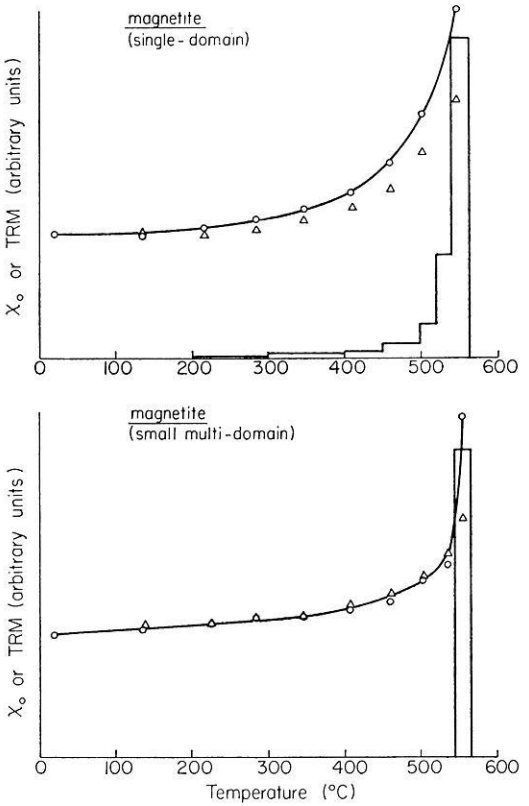

Fig. 3. A comparison of the temperature dependences of χ_0 (circles) and M_S/H_R (triangles) and the distribution of blocking temperatures (the derivative spectrum of TRM) for two fine-grained magnetites. The samples are numbers 2 and 4 of Dunlop, 1973a, b. χ_0 and M_S/H_R have similar temperature variations, as expected theoretically, and deviations between the two functions are closely correlated with the blocking-temperature spectrum

temperature dependences. The Hopkinson peak is narrow but relatively high (enhancement factor about 3). The SD grains (mean size about 0.04 μm) have a broad range of T_B and a correspondingly broader Hopkinson peak. The enhancement factor is again about 3. Throughout the blocking range, χ_0 is distinctly higher than M_S/H_R, the difference being clearly correlated with the spectrum of blocking temperatures.

Fig. 4 makes a similar comparison of data except that here (and in Fig. 5) there is no continuous record of the T_B spectrum. Instead the form of the spectrum is indicated by a series of partial TRM's. Because it contains relatively large needle-like grains (0.2—0.3 μm long), the SD magnetite has a T_B spectrum reminiscent of MD grains. The Hopkinson peak is narrow

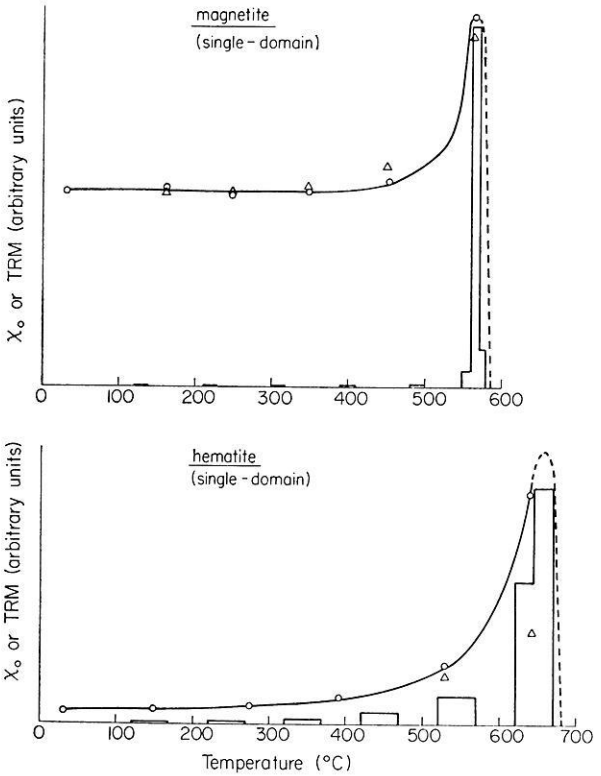

Fig. 4. Hopkinson effect data for SD magnetite and hematite (samples 3 and 6 of Dunlop and West, 1969). Symbols are as in Fig. 3. Only a partial indication of the blocking temperature distribution is given, a series of partial TRMs being plotted. Note the spectacular Hopkinson enhancement factor of the hematite.

and there is an enhancement in χ_0 of less than a factor 2, apparently confined to the blocking region. The SD hematite (grain size 0.1—1 μm) has a broader T_B spectrum and Hopkinson peak, with spectacular enhancement of χ_0 — by a factor 5 at 530 °C and a factor 20 at 640 °C. The enhancement reflects the fact that the room-temperature value of χ_0 is very low (because of the large coercive force of hematite at T_0) compared to the SPM susceptibility. Unfortunately hematite is not of interest in the context of crustal anomalies, being at least two orders of magnitude less magnetic than magnetite, but it does provide a spectacular illustration of the principles involved.

Fig. 5 shows susceptibility data for two rocks with fairly broad T_B spectra and correspondingly broad Hopkinson peaks. Rhadhakrishnamurty and Likhite (1970) show a number of similar examples, which they classify

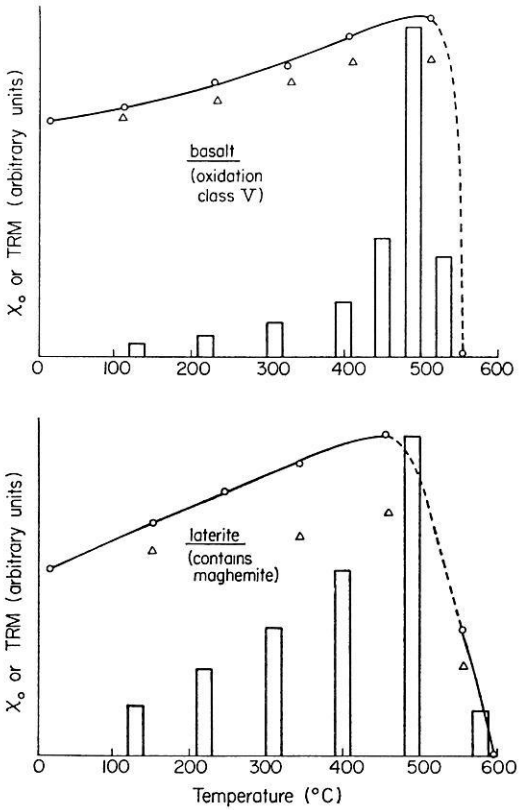

Fig. 5. Hopkinson effect data for two rocks (samples 1 and 2 of Dunlop and West, 1969). Symbols, etc. as in Fig. 4. The broad Hopkinson peaks reflect the broad blocking temperature distributions

as being of SD-type. (However, since we have seen in Figs. 3 and 4 that SD magnetites can have quite narrow T_B spectra and Hopkinson peaks, this classification is a little misleading). The susceptibilities of the rocks in Fig. 5 are only enhanced by 50—70%, but both Radhakrishnamurty and Likhite (1970) and Nagata (1961, pp. 98, 143, 163) show examples of basalts with enhancement factors of 1.5—2.5.

The Source of Deep-Seated Anomalies

The Hopkinson effect data presently available is scanty and refers specifically to basalts and fine-grained magnetites. It clearly needs to be supplemented by data on MD magnetites and coarse-grained rocks. Nevertheless a modest enhancement, by a factor 2 or so, of the susceptibility

of deeply buried crustal rocks seems to be entirely possible. Larger enhancements appear unlikely. Since the range of significant susceptibility increase is typically no more than 100 °C and often more like 50 °C, the depth extent of crustal bodies whose effective magnetization is enhanced by this mechanism can scarcely be more than a few km.

The actual depth in the crust at which enhancement occurs is less certain. The surface geothermal gradient in shield areas is about 30 °C/km but a lower figure is appropriate for the whole crust, perhaps as low as 10 °C/km. The Curie point (580 °C) isotherm for magnetite could then be as deep as 50 km, although thermal evolution models (e.g. MacDonald, 1963) and phase equilibrium considerations (Turner and Verhoogen, 1951) favour a depth in the range 25 to 40 km.

Of course, somewhat shallower bodies (temperatures of 200–400 °C) may exhibit enhanced magnetization if they contain titanomagnetites with a high titanium content and correspondingly lower Curie temperature. This is particularly likely to be true of deep intrusions in which the titanomagnetites have retained their primitive compositions.

A final point to note is that observed anomalies reflect the magnetization produced by the geomagnetic field acting over the past 10^6 years. Viscous (time-dependent) magnetization is known to be enhanced, sometimes spectacularly, at high temperature (e.g. Shashkanov and Metallova, 1970) and could well result in an effective susceptibility appreciably higher than that measured in short-term experiments.

Acknowledgments. My interest in the possible role of the Hopkinson effect in explaining regional anomalies was first aroused in a discussion with Dr. E. Irving. This research was supported by the National Research Council of Canada.

References

Bean, C.P., Livingston, J.D.: Superparamagnetism. J. Appl. Phys. *30*, 120S–129S, 1959

Bhattacharya, B.K., Morley, L.M.: The delineation of deep crustal magnetic bodies from total field aeromagnetic anomalies. J. Geomagn. Geoelectr. *17*, 237–252, 1965

Buchan, K.L., Dunlop, D.J.: Magnetisation episodes and tectonics of the Grenville Province. Nature Phys. Sci. *246*, 28–30, 1973

Deutsch, E.R., Kristjansson, L.G., May, B.T.: Remanent magnetism of Lower Tertiary lavas on Baffin Island. Can. J. Earth Sci. *8*, 1542–1552, 1971

Dunlop, D.J.: Hysteretic properties of synthetic and natural monodomain grains. Phil. Mag. *19*, 329–338, 1969

Dunlop, D.J.: Thermoremanent magnetization of submicroscopic magnetite. J. Geophys. Res. *78*, 7602–7613, 1973a

Dunlop, D.J.: Superparamagnetic and single-domain threshold sizes in magnetite. J. Geophys. Res. *78*, 1780–1793, 1973b

Dunlop, D. J.: Hysteresis of single-domain and two-domain iron oxides. In preparation, 1974

Dunlop, D. J., Hanes, J. A., Buchan, K. L.: Indices of multidomain magnetic behaviour: alternating-field demagnetization, hysteresis, and oxide petrology. J. Geophys. Res. *78*, 1387–1393, 1973

Dunlop, D. J., West, G. F.: An experimental evaluation of single-domain theories. Rev. Geophys. Space Phys. *7*, 709–757, 1969

Evans, M. E., McElhinny, M. W.: The paleomagnetism of the Modipe gabbro. J. Geophys. Res. *71*, 6053–6063, 1966

Fahrig, W. F., Irving, E., Jackson, G. D.: Paleomagnetism of the Franklin diabases. Can. J. Earth Sci. *8*, 455–467, 1971

Fahrig, W. F., Larochelle, A.: Paleomagnetism of the Michael gabbro and possible evidence of the rotation of Makkovik Subprovince. Can. J. Earth Sci. *9*, 1287–1296, 1972

Girdler, R. W.: The effects of hydrostatic pressures on thermal remanent magnetizations. Ann. Géophys. *19*, 118–122, 1963

Hall, D. H.: Regional magnetic anomalies, magnetic units, and crustal structure in the Kenora District of Ontario. Can. J. Earth Sci. *5*, 1277–1296, 1968

Hargraves, R. B. Young, W. M.: Source of the stable remanent magnetization in Lambertville diabase. Am. J. Sci. *267*, 1161–1177, 1969

Hood, P. J.: Paleomagnetic study of the Sudbury Basin. J. Geophys. Res. *66*, 1235–1241, 1961

Hopkinson, J.: Magnetic and other physical properties of iron at a high temperature. Phil. Trans. Roy. Soc. London Ser. A *180*, 443, 1889

Krutikhovskaya, Z. A., Pashkevich, I. K., Simonenko, T. N.: Magnetic anomalies of Precambrian Shields and some problems of their geological interpretation. Can. J. Earth Sci. *10*, 629–636, 1973

MacDonald, G. J. F.: The deep structure of continents. Rev. Geophys. Space Phys. *1*, 587–665, 1963

McGrath, P. H., Hall, D. H.: Crustal structure in northwestern Ontario: regional magnetic anomalies. Can. J. Earth Sci. *6*, 101–107, 1969

Merrill, R. T., Burns, R. E.: A detailed magnetic study of Cobb Seamount. Earth Planet. Sci. Lett. *14*, 413–418, 1972

Murthy, G. S., Evans, M. E., Gough, D. I.: Evidence of single-domain magnetite in the Michikamau anorthosite. Can. J. Earth Sci. *8*, 361–370, 1971

Nagata, T.: Rock Magnetism, Tokyo: Maruzen, 1961

Neel, L.: Some theoretical aspects of rock magnetism. Advan. Phys. *4*, 191–242, 1955

Pesonen, L.: On the magnetic properties and paleomagnetism of some Archean volcanic rocks from the Kirkland Lake area. M.Sc. thesis, Univ. of Toronto, Nov. 1973

Radhakrishnamurty, C., Likhite, S. D.: Hopkinson effect, blocking temperature and Curie point in basalts. Earth Planet. Sci. Lett. *7*, 389–396, 1970

Robertson, W. A., Fahrig, W. F.: The great Logan Loop – the polar wandering path from Canadian Shield rocks during the Neohelikian era. Can. J. Earth Sci. *8*, 1355–1372, 1971

Shashkanov, V. A., Metallova, V. V.: Temperature dependence of the magnetic viscosity coefficient. Akad. Nauk SSSR, Izv., Fiz. Zemli, no. 7, 88–91, 1970

Spall, H., Noltimier, H. C.: Some curious magnetic results from a Precambrian granite. Geophys. J. *28*, 237–248, 1972

Stacey, F. D.: The physical theory of rock magnetism. Advan. Phys. *12*, 45–133, 1963

Stacey, F. D.: The Koenigsberger ratio and the nature of thermoremanence in igneous rocks. Earth Planet. Sci. Lett. *2*, 67–68, 1967
Stacey, F. D., Banerjee, S. K.: The Physical Principles of Rock Magnetism. Amsterdam: Elsevier 1974
Stoner, E. C., Wohlfarth, E. P.: A mechanism of magnetic hysteresis in heterogeneous alloys. Phil. Trans. Roy. Soc. London Ser. A *240*, 599–642, 1948
Stott, P. M., Stacey, F. D.: Magnetostriction and paleomagnetism of igneous rocks. J. Geophys. Res. *65*, 2419–2424, 1960
Turner, F. J., Verhoogen, J.: Igneous and Metamorphic Petrology. New York: McGraw-Hill, 1951
Watkins, N. D.: Non-dipole behaviour during an Upper Miocene geomagnetic polarity transition in Oregon. Geophys. J. *17*, 121–149, 1969
Watkins, N. D., Haggerty, S. E.: Oxidation and magnetic polarity in single Icelandic lavas and dykes. Geophys. J. *15*, 305–315, 1968
Wilson, R. L., Watkins, N. D.: Correlation of petrology and natural remanent polarity in Columbia Plateau basalts. Geophys. J. *12*, 405–424, 1967

D. J. Dunlop
Geophysics Laboratory
Department of Physics
and Erindale College
University of Toronto
Toronto, Canada

J. Geophys. 40, 453–465, 1974

Magnetic Techniques for Ascertaining the Nature of Iron Oxide Grains in Basalts

C. Radhakrishnamurty

Tata Institute of Fundamental Research, Bombay

E. R. Deutsch

Department of Physics, Memorial University of Newfoundland, St. John's

Received March 12, 1974

Abstract. Qualitative techniques are described by which the domain nature and magnetite-maghemite oxidation state of the iron oxides in basalts may be rapidly identified through measurements of hysteresis and susceptibility over a wide temperature range. Detailed studies made on different suites of basalts have revealed that their magnetic properties in most cases can be explained only on the basis of single-domain behaviour. Also it has been found that the observed variations in these properties between basalts are usually best explained by differences in the position the iron oxide minerals in the different samples occupy along the magnetite-maghemite oxidation chain. These observations suggest that the role of titanium usually found in association with iron oxides in basalts is to subdivide the grains physically rather than to form solid solutions of titanomagnetites or titanomaghemites. Some implications of these results to basalt formation and the magnetic anomalies such rocks could cause are discussed.

Key words: Magnetic — Techniques — Basalt — Susceptibility — Hysteresis — Oxidation — Magnetite — Titanium — Domains — Superparamagnetic.

1. Introduction

The few percent of iron oxide minerals present in basalts are responsible for the bulk magnetic properties of these rocks. Microscopic observations on thin sections or polished surfaces of the basalts reveal that the usual size of the iron oxide grains is in the range of 1 to 100 microns. Such large magnetic grains are expected to behave like multidomains and in fact Néel (1955) expressed this view although the magnetic properties of basalts could not be adequately explained in terms of multidomain behaviour.

Chemical analysis of the iron oxide minerals separated from basalts usually indicates the presence of some titanium. Chevallier, Bolfa and Mathieu (1955), Uyeda (1958) and others concluded from investigations on synthetic specimens that solid solutions can occur over a wide compositional range between the spinel end members Fe_3O_4 and Fe_2TiO_4, with a

corresponding variation in magnetic properties such as Curie point (T_c). This has led to the widespread adoption by workers in rock magnetism of titanomagnetite and titanomaghemite series, whereby the observed magnetic properties of the rock are interpreted in terms of the place of the iron oxide minerals within either series. However, in actual rocks T_c as estimated from the chemical composition of the grains seldom agrees with that deduced from magnetic measurements. Moreover, the observed Curie points are not well defined, especially for basalts presumed to show values less than 400 °C on the basis of their Ti content. Further difficulties in determining T_c arise from changes the magnetic grains undergo during the laboratory heating itself, resulting in the irreversibility of heating and cooling cycles.

Oxidation of magnetite has engaged the attention of both geologists and chemists for the past fifty years, but still some aspects of this process need further study for a better understanding. Lepp (1957) first pointed out that the product of oxidation depends only on the grain size of the magnetite used and the rate of reaction. Later Feitknecht and Gallagher (1970) showed that grains of magnetite smaller than 3000 A in diameter tend to become oxidized to maghemite, whereas larger ones turn into hematite or they form disproportionately both magnetite and hematite through several intermediate cation deficient phases. The magnetic properties of synthesized cation deficient magnetites with different Ti contents have been studied as a function of degree of oxidation (Readman and O'Reilly, 1972). However, the manner in which the oxidation process itself depends on the grain size of the titanomagnetites is difficult to visualize in the absence of studies similar to those reported on sized grains of pure magnetite.

In a critical study (Radhakrishnamurty, Raja, Likhite and Sahasrabudhe, 1972) of the magnetic behaviour of several hundred basalts, not a single case was found which could be unambiguously attributed to the presence of large titanomagnetite grains with low T_c. All the ten cases encountered in the study which indicated low T_c turned out to be ambiguous due to grain size effects of the magnetic minerals in them. Thus, the occurrence in continental basalts of titanomagnetites of the synthetic type itself is perhaps not as soundly established a fact as has been generally assumed. For these reasons, consideration of the role of titanium in determining magnetic properties along the magnetite-maghemite chain has been omitted as an open question for the sake of the present analysis.

The above features of the iron oxide minerals could certainly cause many complexities in the way of understanding the magnetic properties of basalts. Fortunately, magnetite and maghemite have distinct magnetic properties and hence can be identified by simple magnetic tests. Recently, it was shown (Radhakrishnamurty, Likhite, Raja and Sahasrabudhe, 1971) that such tests can be unambiguously extended to cation deficient (CD) phases of magnetite, as these have specific magnetic properties by which

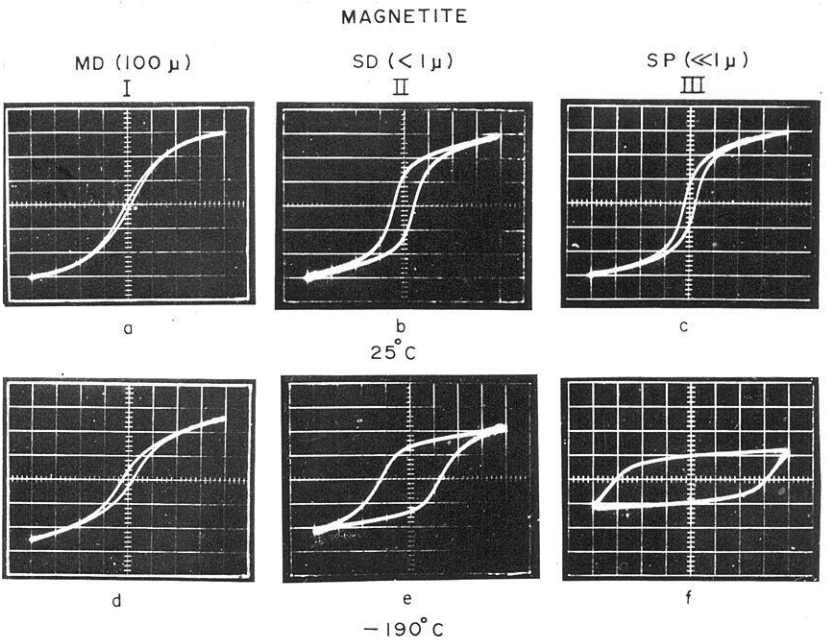

Fig. 1. Typical hysteresis loops for one synthetic and two basalt samples. MD — multidomain, SD — single-domain and SP — superparamagnetic grains. a, b, c, at 25 °C; d, e, f, at −190 °C for the same samples. Scale: X-axis (magnetic field) 1 small division = 125 Oe for a and d; and 62.5 Oe for the rest. Y-axis (magnetic moment) 1 s.d. = 0.9 emu for all

they can be distinguished from pure magnetite and maghemite. However, the first step for an understanding of the magnetic properties of basalts is to ascertain the domain nature of the iron oxide grains in such rocks.

2. *Hysteresis of Iron Oxide Grains*

The magnetic hysteresis phenomenon depends on the domain structure of the grains in a material. At any particular temperature, there is a narrow range of sizes in which the grains of a magnetic material show maximum coercive force (H_c) and retentivity (J_r) and such grains are termed optimum single-domains (SD); smaller grains exhibit superparamagnetism (SP) due to thermal agitation and much larger grains become multidomains (MD). From simple theory, both SP and MD grains are presumed (Bean, 1955) to show vanishingly small H_c and J_r. However, experimentally, some finite values of H_c and J_r may be observed for clusters of SP particles due to dipole interaction (Evdokimov, 1963; E. Kneller, private communication,

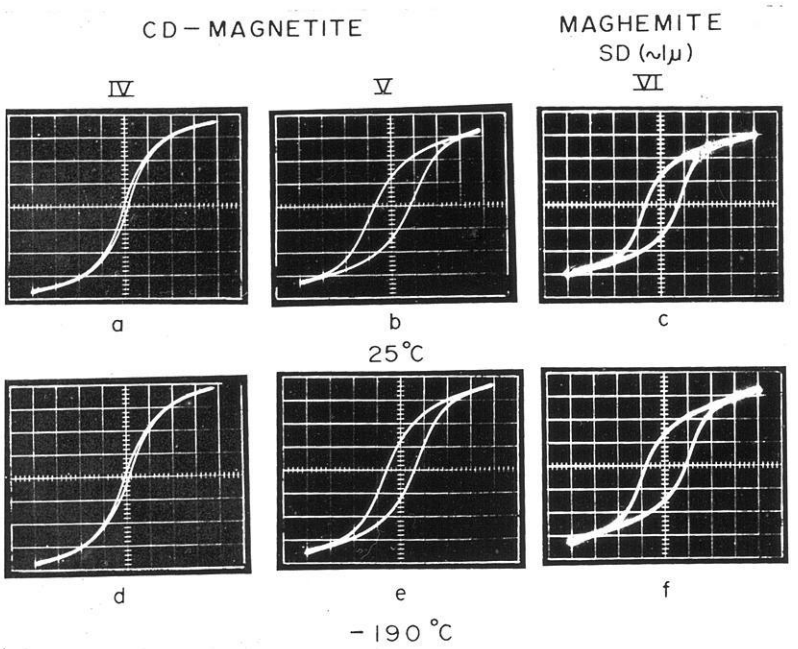

Fig. 2. Hysteresis loops for two basalts containing cation deficient magnetite and a synthetic sample of maghemite. Scale: X-axis 1 s.d. = 75 Oe; Y-axis 1 s.d. = 2.0 emu

1972) amongst them and for MD grains due to crystal defects in them.

Since the terms MD, SD, CD and SP comprise both domain states and composition, it may be explained that in this paper use of "SD" is reserved for "pure" magnetite, whereas "CD" refers to cation deficient grains that may be either SD or MD, though usually the former. "SP" and "MD" terms are applied to grains of any composition.

Magnetite undergoes a phase transition at -150 °C, below which its magnetocrystalline anisotropy constant K increases tenfold compared to that at room temperature (T_r). Morrish and Watt (1958) showed from studies on magnetite micropowders that for SD particles, H_c is several times greater at -196 °C than at T_r and that for MD grains the corresponding increase is by about a factor of two. These observations are consistent with the known positive correlation between H_c and K. Morrish and Watt also found that maghemite shows a small increase in H_c at low temperatures.

In Fig. 1 are shown the typical hysteresis loops for three samples; a, b, c were obtained at 25 °C and d, e, f are corresponding loops for the same samples at -190 °C. The loop in Fig. 1a is for a sample prepared by dispersing a small quantity of 100 micron size grains of magnetite in plaster

of Paris and the peak field used was 2500 Oe. This sample shows the expected increase in H_c at -190 °C (Fig. 1d) corresponding to MD grains of magnetite. The loops shown in Fig. 1b, c and 1e, f are for basalts obtained in a peak field of 1250 Oe. It should be mentioned here that a small field has been chosen for these two basalt samples to show the change in H_c clearly, though this change has the same trend even in much higher fields. The large increase in H_c at -190 °C (Fig. 1e) compared to that at 25 °C (Fig. 1b) strongly suggests that the magnetic grains in sample II are SD magnetite. The similar behaviour shown by sample III (Fig. 1c and 1f) is again consistent with SD magnetite at low temperature. However, at T_r, this sample is in a metastable magnetic state and shows a Rayleigh loop (hysteresis in 10 Oe) which indicates that a significant fraction of the particles in it are superparamagnetic (Radhakrishnamurty and Sastry, 1970; Néel, 1970); the estimated particle size is about 100 A.

Fig. 2 shows the hysteresis loops for two basalt samples (IV and V) and one synthetic sample (VI) prepared by dispersing commercial maghemite in plaster of Paris. Surprisingly sample IV shows little or no change in its hysteresis with temperature (Fig. 2a and 2d), while sample V shows a distinct decrease in H_c at -190 °C (Fig. 2e) compared to that at 25 °C (Fig. 2b). This character is just opposite to that of magnetite. Such samples have been shown to contain CD magnetite phases (Radhakrishnamurty, Likhite, Raja and Sahasrabudhe, 1971). The hysteresis behaviour of maghemite sample VI, shown in Fig. 2c and 2f conforms to the expectation, namely there is a small increase in H_c at -190 °C compared to that at 25 °C.

Thus, basalts containing the above six kinds of minerals and grain sizes have been identified from their characteristic hysteresis behaviour at different temperatures. Of course, composite mixed behaviour might be, and often is, encountered in basalts and is in principle also detectable by experiment. However, it should be emphasised that the magnetic analysis of such composite rocks is still at best semi-quantitative.

As was pointed out previously (Radhakrishnamurty and Likhite, 1970b), the presence of SP particles in a basalt can be revealed by the low field (10 Oe) hysteresis loop and that of optimum SD grains by their characteristically large relative remanence (ratio of remanent to maximum intensities) in medium fields (100—500 Oe). The presence of MD and CD magnetite can be established by hysteresis studies in high fields (1000—5000 Oe). However, it should be mentioned in this context that the sensitivities of the three different instruments used (Likhite, Radhakrishnamurty and Sahasrabudhe, 1965; Likhite and Radhakrishnamurty, 1966), for hysteresis studies in low, medium and high fields decrease somewhat with increasing magnetic fields due to increase in noise levels of the instruments. Hence, it may not be possible to observe distortionless loops for all kinds of basalts in all the different ranges of fields. Typically a sample should develop

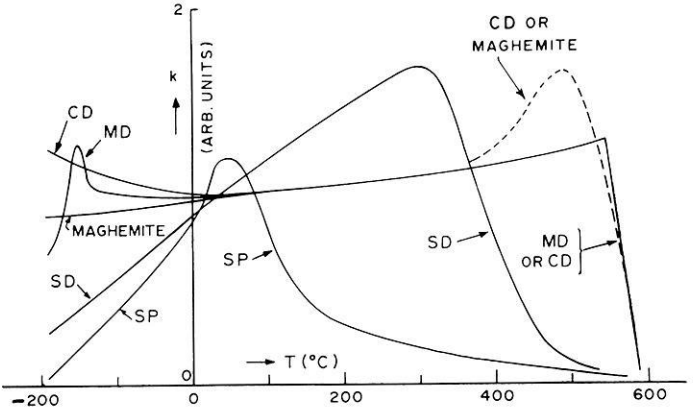

Fig. 3. Initial susceptibility as a function of temperature for basalts containing different types of grains. SP — superparamagnetic, SD — single-domain, MD — multidomain, CD — cation deficient grains of magnetite

maximum intensities of the order of 0.07, 1.0 and 2.0 emu/cc in low, medium and high fields respectively for observing distortion-free hysteresis loops with the three instruments.

3. Studies of Initial Susceptibility with Temperature

Many workers have described apparatus suitable for measuring the susceptibility (k) of rocks in low fields. The various kinds of basalts used in the present study have been measured in a field of 0.5 Oe with the apparatus described previously (Likhite and Radhakrishnamurty, 1965). With low- and high-temperature attachments (Radhakrishnamurty and Likhite, 1970a) it was possible to determine the k of most basalts at any temperature in the range -196 °C to 700 °C.

In Fig. 3 are shown curves depicting the variation of k with T for basalts containing different types of magnetic grains. These curves were based on actual measurements but somewhat idealised to bring out the salient features. Only the heating curves are shown, mainly to avoid congestion and to faciliate comparative analysis. It should be noted that the "SD" and "SP" notations on the curves refer to the respective grain state at T_r only: the actual grain state at high temperature on the "SD" curve tends towards SP, while that at low temperature on the "SP" curve tends towards SD.

All the curves are reversible in the temperature range $-196°$ to 25 °C. However, in the high temperature range, only the MD magnetite curve is

reversible, mainly because the changes taking place on heating in the composition and/or state of large magnetite grains are negligible, and the curve also shows a well defined and sharp T_c. The curves of all other types of grains are more or less irreversible in the high temperature range and some of them may change drastically due to changes in composition and/or grain growth: these features may imply that there would be ambiguity in defining any point of such curves as T_c. Some of the uncertainties in the determination of T_c of basalts were discussed in greater detail elsewhere (Radhakrishnamurty, Raja, Likhite and Sahasrabudhe, 1972).

Also, it was inferred from these magnetic observations that basalts which show SD magnetite behaviour often get oxidized to maghemite when heated beyond 200 °C; sometimes the grains become CD magnetite. Perhaps the most likely explanation for these observation is that when the grains get the necessary oxygen from their surroundings, maghemite might form and if oxygen was not available the grains might turn into CD magnetite. Cation migration in SD magnetite might start around 200 °C and the associated changes could even cause ambiguities in the determination of blocking temperature (T_b) or T_c of the relevant grains.

The following important features emerge from a comparative study of the different curves shown in Fig. 3.

1. While it may be difficult to distinguish between MD and CD magnetite from the high temperature part of the k-T curve, they may be resolved clearly from the low temperature side. MD magnetite shows the characteristic sharp k-peak at -150 °C due to phase transition and CD shows an increase in the value of k at -196 °C compared to its value at T_r.

2. SP and SD magnetite grains show a large decrease in k at -196 °C compared to their respective values at T_r. It is very difficult to identify the magnetite transition peak at -150 °C in the k-T curves of SP and SD samples, probably due to the large increase in H_c with decreasing temperature around the transition point.

3. Maghemite shows a small decrease in k at -196 °C compared with its T_r value.

The above features of the different kinds of grains can be explained by variations in the effective contributions by shape and magnetocrystalline anisotropies. Particularly, the inconspicuousness or absence of the k-peak at the transition temperature in the k-T curves of SD magnetite may be due to the undiminishing or somewhat increasing effect of shape anisotropy of the grains. The magnetic properties of CD magnetite grains are quite peculiar and at present stand out simple as experimental observations. The decrease of H_c and increase of k at low temperatures observed for CD grains are mutually supporting and consistent and it may be recorded in this context that an explanation for these, based on more fundamental properties of the material, is not yet possible.

Table 1. Magnetic granulometric data for stable basalts from Deccan and Rajmahal traps

	Flow No.	Rock type	Q_n[a]	Mineral nature	
				Virgin	After heating (600 °C)
1	2	3	4	5	6
	2	FGB	3.1	Maghemite	Maghemite
	4	PB	4.1	CD + SD	Maghemite
	5	AB	6.1	CD	Maghemite
	7	AB	5.3	CD	CD
	8	CGB	4.1	CD	CD
	9	AB	3.4	CD + SD	CD
Deccan	13	PB	6.8	CD	CD
traps	14	AB	8.0	CD	CD
	17	AB	1.3	CD	Maghemite
	21	PB	1.3	CD	CD
	22	PB	3.7	CD	CD
	24	PB	4.2	CD	Maghemite
	I	FGB	40.6	SD	Maghemite
	II	PB	71.4	SD	Maghemite
	V	FGB	36.0	SD	CD
	VI	PB	10.0	CD	CD
	VII	CGB	45.8	SD + CD	Maghemite
	X	PS	116.0	SD	SD
Rajmahal	XI	PB	7.8	CD + SD	CD
traps	XII	CGB	55.0	SD	Maghemite
	XIII	PB	24.8	SD + CD	CD
	XIV	CGB	9.9	CD	CD
	XV	PB	78.8	SD	Maghemite
	XVI	CGB	23.0	SD + CD	CD
	XVII	CGB	5.2	CD + SD	CD

[a] Ratio of remanent intensity to that induced in 0.5 Oe. FGB — Fine grained basalt, CGB — Course grained basalt, PS — Pitchstone, AB — Amygdaloidal basalt, PB — Porphyritic basalt, CD — Cation deficient, SD — Single-domain and referring to magnetite.

4. Granulometry of Basalts

Several techniques have been developed (Dunlop, 1965; Stacey, 1967; Lowrie and Fuller, 1971) for studying the domain nature of the magnetic grains in basalts. However, these are mainly meant for identifying the domain nature of part of the grains responsible for the remanent magnetization of the rocks. The techniques described in this paper are useful

for studies on the total magnetic mineral content of the basalts and include both domain nature and chemical compositional aspects of the minerals concerned.

The granulometry of several suites of basalts has been studied. In Table 1 are given magnetic data for palaeomagnetically stable rocks from the Deccan and Rajmahal traps. The important points to be noted are as follows:

1. Values of Koenigsberger ratio (Q_n) are in the range 1 to 10 for basalts containing CD and 10 to 100 for SD magnetite.

2. The mineral in some of the samples gets converted to maghemite when heated to 600 °C and cooled; this may imply that the grains in the virgin samples are less than 3000 A in size.

3. Multidomain magnetic behaviour is very rare in these basalts and this indicates that the magnetic grain size may be greatly different from the physical grain size derived from optical observations.

4. The flows not listed in Column 2 among the two suites of basalts in Table 1 were found to be unstable or partially stable, mainly due to the presence of SP particles in samples derived from the respective flows.

In Table 2 granulometric data are given for some younger and older basalts. In cases where uniformity of grain nature in rock bodies is known the totals shown in Column 3 represent flows or sites regarded as units; in all other cases, numbers refer to the total of samples or specimens. Cases like SP, SD etc. indicate that these grains predominate. Composite notations like SP+SD, MD+SD etc. mean that the magnetic characteristics of both types of grains could be clearly identified for the sample studied. More than two kinds of grains may also be present in basalts, but this would be difficult to determine and hence was not attempted.

The data presented in Table 2 indicate that in basalts younger than Cretaceous, MD behaviour is rare while it is fairly common in older basalts. CD behaviour, when its occurrences both in pure and composite form are counted, is far more prevalent than others.

5. Implications of Magnetic Granulometry to Petrography

The most important result obtained from these studies on different kinds of basalts is that SP behaviour has been found even for some coarse grained samples. This result clearly indicates that each iron oxide grain in a basalt might be behaving like a cluster of much smaller grains due to some yet unknown mechanism of subdivision.

In some Deccan trap flows and dykes, entire rock masses were found to contain SP particles. It was impossible to separate the magnetic grains from crushed samples. These cases may indicate very rapid chilling of the magmas concerned, as a result of which SP-size (100 A) magnetite particles were formed more or less uniformly in the rock bodies. The presence of even

Table 2. Magnetic granulometric data for some young and old basalt formations

Formation	Age	No. of samples (or sites)	SD	SP	CD	MD	SP+SD	SP+CD	SD+CD	MD+SD	MD+CD	SP+MD
1	2	3	4	5	6	7	8	9	10	11	12	13
Deccan Traps	Tertiary	36[a]	—	—	21	—	—	12	3	—	—	—
DT Dykes	Tertiary	15[a]	6	2	3	—	2	1	1	—	—	—
Rajmahal Traps	Cretaceous	17[a]	6	—	2	—	4	—	5	—	—	—
Columbia River Basalts	Miocene	8[b]	—	—	—	—	5	3	—	—	—	—
Greenland Basalts	Tertiary	43[b]	—	—	25	—	—	—	18	—	—	—
Ophiolites (Newfoundland)	Ordovician	56[b]	—	—	1	2	—	16	1	28	1	7
Cuddapah Traps	Precambrian	15[a]	—	—	—	—	—	—	—	15	—	—
Dykes	Precambrian	6[a]	—	—	—	—	—	—	—	—	6	—

[a] Represents sites or flows. [b] denotes samples or specimens. SD — single-domain, SP — superparamagnetic, CD — cation MD — deficient,multidomain grains.

much smaller particles which are superparamagnetic at −196 °C has been inferred in some samples of ophiolite complexes in Newfoundland (Deutsch, Radhakrishnamurty, Strong, Rao, Pätzold and Likhite, 1973). However, such small particles in these ophiolites seem to have been formed due to alteration.

It is possible to study the granulometry of a large number of samples in situ using portable instruments. The essential magnetic grain nature can be ascertained at the rate of a sample per few minutes. A few expeditions made with portable instruments to the rock outcrops have already revealed that in rock bodies such as flows or dykes the magnetic grain nature is sometimes uniform and is variable at other times. The latter case might mean that normal weathering and alteration have caused grain subdivision. Such studies in situ can aid the choice of samples best suited for palaeomagnetic work.

The magnetic grains in basalts constitute a very interesting area for future work and may contribute to a better understanding of basalt formation and subsequent alteration.

6. Implications to Geomagnetic Anomalies

As described in previous sections, the magnetic properties of basalts can be quite complex and these in turn determine the nature of the geomagnetic anomalies, especially the marine magnetic anomalies. Studies on dredged samples showed that Q_n values varied from 190 to 1 for samples taken from the axis to the edges of the Mid-Atlantic ridge (Irving, 1970); the natural remanent intensity also varied in a similar proportion. It was reported that the T_b of the grains in the samples obtained from the axis was about 200 °C and that of edge samples was around 500 °C. These features have been explained on the basis of conversion of the original titanomagnetites to titanomaghemites (Marshall and Cox, 1972) and SD titanomagnetite to SP (Butler, 1973), both operating through an oxidation process. Another somewhat different but likely explanation for such observations may be the conversion of SD grains to CD type. The change of SD to CD nature involves a sharp fall in remanent intensity and also an increase in T_b or T_c. The magnetic contrast produced by such changes could cause some anomalies in a profile and these may not be distinguishable from other anomalies caused by geomagnetic reversals.

Since the anomalies are believed to be caused by remanent intensity of the rock body, T_b of the grains is a very important parameter in estimating the thickness of the basaltic layer. Due to the increase of temperature with depth, thinner layers of low-T_b rock mass and thicker layers of high-T_b rocks would both contribute to the magnetic anomalies and this may result in underestimating the thickness of the low-T_b rock layers.

References

Bean, C.P.: Hysteresis of mixtures of ferromagnetic micropowders. J. Appl. Phys. *26*, 1381–1383, 1955

Butler, R.F.: Stable single-domain to superparamagnetic transition during low-temperature oxidation of oceanic basalts, J. Geophys. Res. *78*, 6868–6876, 1973

Chevallier, R., Bolfa, J., Mathieu, S.: Titanomagnétites et ilmenites ferromagnétiques. Bull. Soc. Franc. Mineral. Crist. *78*, 307–346 and 365–399, 1955

Deutsch, E.R., Radhakrishnamurty, C., Strong, D.F., Rao, K.V., Pätzold, R.R., Likhite, S.D.: Magnetism of ophiolite complexes in the Newfoundland mobile belt. Abstract, IAGA 2nd General Scient. Assembly, Kyoto, 1973

Dunlop, D.J.: Grain distribution in rocks containing single domain grains. J. Geomag. Geoelectr. *17*, 459–471, 1965

Evdokimov, V.B.: The magnetic interaction of superparamagnetic particles. Russ. J. Phys. Chem. (English Transl.) *37*, 1018–1019, 1963

Feitknecht, W., Gallagher, K.G.: Mechanisms for the oxidation of Fe_3O_4. Nature *228*, 548–549, 1970

Irving, E.: The Mid-Atlantic Ridge at 45 N. XIV. Oxidation and magnetic properties of basalt; review and discussion. Can. J. Earth Sci. *7*, 1528–1538 1970

Lepp, H.: Stages in the oxidation of magnetite. Am. Mineralogist *42*, 679–681, 1957

Likhite, S.D., Radhakrishnamurty, C.: An apparatus for the determination of susceptibility of rocks at different frequencies. Bull. N.G.R.I. *3*, 1–8, 1965

Likhite, S.D., Radhakrishnamurty, C.: Initial susceptibility and constricted Rayleigh loops of some basalts. Current Sci. *35*, 534–536, 1966

Likhite, S.D., Radhakrishnamurty, C., Sahasrabudhe, P.W.: Alternating current electromagnet type hysteresis loop tracer for minerals and rocks. Rev. Sci. Instr. *36*, 1558–1560, 1965

Lowrie, W., Fuller, M.: On the alternating field demagnetization characteristics of multidomain thermoremanent magnetization in magnetite. J. Geophys. Res. *76*, 6339–6349, 1971

Marshall, M., Cox, A.: Magnetic changes in pillow basalt due to sea floor weathering. J. Geophys. Res. *77*, 6459–6469, 1972

Morrish, A.H., Watt, L.A.K.: Coercive force of iron oxide micropowders at low temperatures. J. Appl. Phys. *29*, 1029–1033, 1958

Néel, L.: Some theoretical aspects of rock-magnetism. Advanc. Phys. *4*, 191–243, 1955

Néel, L.: Interpretation des cycles d'hystérésis entranglés de certaines basalts. C. r. hebd. Séanc. Acad. Sci. Paris, *270*, 1125–1130, 1970

Radhakrishnamurty, C. Likhite, S.D.: Hopkinson effect, blocking temperature and Curie point in basalts. Earth Planet. Sci. Lett. *7*, 389–396, 1970a

Radhakrishnamurty, C., Likhite, S.D.: Relation between thermal variation of low field susceptibility and magnetic hysteresis of basalts. Earth Planet. Sci. Lett. *9*, 294–298, 1970b

Radhakrishnamurty, C., Sastry, N.P.: A single-domain grain model for the low field constricted hysteresis loops of some basalts. Proc. Indian Acad. Sci. *72*, 94–102, 1970

Radhakrishnamurty, C., Likhite, S.D., Raja, P.K.S., Sahasrabudhe, P.W.: Magnetic grains in Bombay columnar basalts. Nature, Phys. Sci. *235*, 33–35, 1971

Radhakrishnamurty, C., Raja, P. K. S., Likhite, S. D., Sahasrabudhe, P. W.: Problems concerning the magnetic behaviour and determination of Curie points of certain basalts, Pure Appl. Geophys. *93*, 129–140, 1972

Readman, P. W., O'Reilly, W.: Magnetic properties of oxidized (cation-deficient) titanomagnetites (Fe, Ti, □)$_3$O$_4$. J. Geomag. Geoelectr. *24*, 69–90, 1972

Stacey, F. D.: The Koenigsberger ratio and the nature of thermoremanence in igneous rocks. Earth Planet. Sci. Lett. *2*, 67–68, 1967

Uyeda, S.: Thermo-remanent magnetism as a medium of palaeomagnetism, with special reference to reverse thermo-remanent magnetism. Japanese J. Geophys. *2*, 1–123, 1958

C. Radhakrishnamurty
Tata Institute of Fundamental Research
Bombay 400005, India

E. R. Deutsch
Department of Physics
Memorial University
of Newfoundland
St. Johns, Canada

J. Geophys. 40, 467–487, 1974

Integrated Effect of Repeated Mechanical Shocks on Shock Remanent Magnetization and Shock Demagnetization

Takesi Nagata

National Institute of Polar Research, Tokyo, and Department of Earth and Planetary Sciences, University of Pittsburgh, Pittsburgh

Received March 12, 1974

Abstract. The integrated effect of n repeated shocks on the shock remanent magnetization (SRM) of igneous rocks is empirically expressed as

$$J_R(H_+S_1H_0, \ldots, H_+S_nH_0) = J_R(\infty)[1-(1-K)\exp\{-\alpha(n-1)\}],$$
$$(S_1 = \ldots\ldots = S_n = S \text{ and } \alpha > 0),$$

where

$$J_R(H_+SH_0) = KJ_R(\infty) \quad (K < 1),$$

and $J_R(\infty)$ is approximately proportional to H for its small values and also to S for its large values.

The integrated effect of n repeated shocks on the shock demagnetization of SRM is experimentally summarized as

$$J_R(H_+S^*H_0S_1 \ldots S_n) = J_R(H_+S^*H_0)[K_\infty + (K_1 - K_\infty)\exp\{-\beta(n-1)\}],$$
$$(S_1 = \ldots\ldots = S_n = S \text{ and } \beta > 0),$$

where

$$J_R(H_+S^*H_0S) = K_1J_R(H_+S^*H_0) \quad (K_\infty < K_1 < 1),$$

and $J_R(H_+S^*H_0S)/J_R(H_+S^*H_0)$ is a monotonically decreasing function of S/H.

However, there is no integrated effect of repeated shocks on the advanced effect of mechanical shock on IRM. Namely, $J_R(S_1 \ldots S_nH_+H_0) = J_R(SH_+H_0)$, where $J_R(SH_+H_0)$ is a monotonically increasing function of S/H and becomes approximately proportional to S/H for large values of S/H.

Assuming a theoretical model that individual shocks are associated with statistical fluctuations in regard to their effect on the magnetic domain walls and the fluctuations can affect the domain walls to move only if the movement results in a decrease of the magnetostatic energy, the observed integrated effects of repeated shocks on SRM and the shock demagnetization and no repetition effect in the case of advanced shock can be reasonably well interpreted.

Key words: Shock-Remanent Magnetization (SRM) — Advanced Shock Effect on the Isothermal Remanent Magnetization — Shock Demagnetization — Integrated Effect of Repeated Shocks on SRM, etc. — Piezo-Remanent Magnetization (PRM) — Nagata-Carleton Theory of PRM.

1. *Introduction*

In his previous paper (Nagata, 1971), the author described the general characteristics of shock remanent magnetization $J_R(H_+SH_0)$, the advanced shock effect on IRM, $J_R(SH_+H_0)$, and the shock demagnetization, $J_R(H_+H_0S)$ of igneous rocks. Here, $J_R(H_+SH_0)$ represents the remanent magnetization acquired by giving a compressive shock momentum S on a rock sample in the presence of a magnetic field H; $J_R(SH_+H_0)$ the isothermal remanent magnetization acquired in H of a rock sample which was shocked by S in non-magnetic space before the magnetic field is applied; $J_R(H_+H_0S)$, the remanent magnetization after the ordinary isothermal remanent magnetization, $J_R(H_+H_0)$, is shocked by S in non-magnetic space. In this notation, H_+ means an application of H and H_0 a release of a sample from H, while S is given by

$$S = \int_t P(t)\, dt, \tag{1}$$

where $P(t)$ represents a mechanical compressive shock of a short duration as a function of time (t).

As for the shock remanent magnetization, $J_R(H_+SH_0)$, experimental results have been summarized for small values of H and large values of S as

$$\begin{aligned} J_R^{\prime\prime}(H_+SH_0) &= K^{\prime\prime}H\cdot S\ , \\ J_R^{\perp}(H_+SH_0) &= K^{\perp}H\cdot S\ , \end{aligned} \tag{2}$$

where // and $\perp$ represent respectively the case where the direction of H is parallel to the axis of unaxial shock momentum S and another case where the direction of H is perpendicular to the axis of S, and $K^{\prime\prime}$ and $K^{\perp}$ denote material constants Here

$$K^{\perp} \simeq \frac{3}{4} K^{\prime\prime}\ . \tag{3}$$

As for the advanced shock effect on IRM, $J_R(SH_+H_0)$, experimental results are summarized as

$$J_R(SH_+H_0)/J_R(H_+H_0) = F(S/H)\ , \tag{4}$$

where $F(S/H) \geqq 1$ with $F(0) = 1$ and $F(S/H) \simeq NS/H$ for large values of S/H, N denoting a positive numerical constant.

The shock demagnetization of IRM, $J_R(H_+H_0S)$, has been empirically expressed as

$$J_R(H_+H_0S)/J_R(H_+H_0) = G(S/H)\ , \tag{5}$$

with $\dfrac{dG(S/H)}{d(S/H)} = -M < 0$ for small values of S/H, and $\lim_{(S/H)\to\infty} G(S/H) = 0$.

The dependences of $J_R(H_+SH_0)$, $J_R(SH_+H_0)$ and $J_R(H_+H_0S)$ on H and S thus obtained are essentially the same as those on H and P of the piezoremanent magnetization, $J_R(H_+P_+P_0H_0)$, the advanced compression effect on IRM, $J_R(P_+P_0H_+H_0)$, and the pressure demagnetization, $J_R(H_+H_0P_+P_0)$, respectively, where P is a static uniaxial compression, (Nagata and Carleton 1968, 1969(a)(b): Nagata 1970). Since the duration of shock pressure $P(t)$ in (1) is very short, being about 0.4 m. sec, and the functional form of $P(t)$ with t can be approximated by a single pulse, (Nagata 1971), the effects of S in (2), (4) and (5) could be approximately replaced by those of an application of $\overline{P}$ during a short time Δt, where $\overline{P} \cdot \Delta t = \int_t P(t)dt$; namely, S in (2), (4) and (5) could be replaced by an operation $(\overline{P}_+\overline{P}_0)$ with a special condition that Δt is so short that the effect of $(\overline{P}_+\overline{P}_0)$ on the remanent magnetization might be incomplete in comparison with that of an application and a following release of a static pressure P with a sufficiently long time interval between operations P_+ and P_0.

Actually, the most conspicuous difference of the shock effects $J_R(H_+SH_0)$ and $J_R(H_+H_0S)$ from the static effects $J_R(H_+P_+P_0H_0)$ and $J_R(H_+H_0P_+P_0)$ is a large integrated effect of repeated shocks. The integrated effect of repeated mechanical shocks was first studied by Shapiro and Ivanov (1967), who pointed out that the shock remanent magnetization acquired by n repeated shocks in a magnetic field exponentially increases with n to approache a saturated value. Similarly, the effect of repeated shock demagnetization of IRM was represented by an exponential decrease of the remanent magnetization with n, approaching the final steady value. In the results of the previous preliminary study (Nagata, 1971), however, an increase of n repeated shock remanent magnetization with n is not simply exponential, and likewise a decrease of IRM by n repeated shock demagnetization with n is not of a simple exponential form.

It is then obvious that a critical problem in the analysis of the shock remanent magnetization and shock demagnetization is concerned with studies in detail on the integrated effect of repeated shocks on the remanent magnetization. In the present report, therefore, further experimental data of the effect of repeated shocks on $J_R(H_+SH_0)$ and $J_R(H_+H_0S)$ are summarized, together with new experimental results on the effect of repeated shocks on $J_R(SH_+H_0)$. A theoretical interpretation of the physical mechanism of the observed integrated effect of repeated shocks also is added.

2. *General Magnetic Properties and SRM Characteristics of Samples*

For the purpose of the present study, two typical samples, NV—B (basalt) and NV—K (andesite), have been selected from a number of igneous rocks whose piezo-magnetic characteristics were already examined in some

Table 1. General magnetic properties of examined samples

Sample / properties	NV—B	NV—K	Unit
Rock	Homogeneous basalt (New York, USA)	Andesite intrusion (Antarctica)	
Saturation Magnetization (J_s)	1.10	2.99	emu/cc
Saturation remanent Magnetization (I_R)	0.320	0.395	emu/cc
Coercive force (H_c)	68	97	Oersteds
Magnetic Susceptibility (χ_0)	2.6×10^{-3}	3.1×10^{-3}	emu/cc/Oe
b	1.0×10^{-4}	3.0×10^{-6}	emu/cc/Oe^2
C	9.2×10^{-6}	1.6×10^{-6}	emu/cc/Bar. Oe
b_c	8.9×10^{-2}	5.2×10^{-1}	Oe/Bar
K	2.3×10^{-2}	8.2×10^{-3}	emu/cc/Bar. Sec. Oe

detail (Nagata and Carleton 1968, 1969(a)). In Table 1, saturation magnetization (J_s), saturation remanent magnetization (J_R), coercive force (H_c), initial magnetic susceptibility (χ_0) and the coefficient of isothermal remanent magnetization (b) of these two samples are summarized, where b is the coefficient of isothermal remanent magnetization (IRM) in its well established parabolic dependence on weak external magnetic fields (H_{ex}): namely $b = (\text{IRM})/H_{ex}^2$. As shown in Table 1, the coefficient (b) of IRM is much smaller in sample NV—K than in sample NV—B, though the magnetic susceptibilities are roughly the same in the two samples.

On the other hand, characteristics of the piezo-remanent magnetization (PRM) and the pressure demagnetization effect of samples NV—B (Nagata and Carleton 1968) and NV—K (Nagata and Carleton, 1969(a)(b)), acquired by static uniaxial compressions, have already been studied in detail. In these previous studies, a linear relationship between PRM, $J_R(H_+P_+P_0H_0)$, and the product $P \times H$ for small values of H and large values of P was established; namely,

$$J_R(H_+P_+P_0H_0) = C \cdot H \cdot P \ . \tag{6}$$

The coefficient C of the two samples is given in Table 1. The coefficient, C, also is smaller in Sample NV—K than in sample NV—B, but the ratio, C(NV—K)/C(NV—B) is considerably larger than the ratio b(NV—K)/

b(NV—B). This result may suggest that the effect of mechanical pressure relative to that of an applied magnetic field in the acquisition of remanent magnetizations is considerably larger in sample NV—K than in sample NV—B. $J_R(H_+P_+P_0H_0)$ is theoretically expressed (Nagata and Carleton 1969(b)) as

$$J_R(H_+ P_+ P_0 H_0) = \frac{16}{5\pi} bHH_c \ , \tag{7}$$

with

$$H_c = \frac{3\lambda_s}{\sqrt{2}J_s} P = h_c P \ , \tag{8}$$

where λs represents the isotropic magnetostriction coefficient. h_c thus defined represents the rate of contribution of a unit uniaxial pressure to the acquisition of piezo-remanent magnetization. In Table 1, the numerical value of h_c is considerably larger in NV—K than in NV—B.

In accordance with the general magnetic properties and the PRM characteristics thus obtained in the previous studies, sample NV—K has been selected as a typical igneous rock which has a comparatively large effect of mechanical pressure on remanent magnetization, while sample NV—B has been chosen as an igneous rock whose magnetoelastic dependence is comparatively small but whose basic isothermal remanent magnetization is sufficiently large for detecting the comparatively small magnetoelastic effect.

In Fig. 1, examples of the dependence of $J_R(H_+SH_0)$ upon S in a constant magnetic field for the two samples are illustrated. As anticipated, $J_R(H_+H_0)$ is much smaller in NV—K than in NV—B, but the rate of increase of $J_R(H_+SH_0)$ with increasing values of S is much larger in the former than in the latter. For small values of H with a sufficiently large value of S, $J_R(H_+SH_0)$ of these samples is approximately proportional to H as summarized by (2). Numerical values of coefficient K'' defined by (2) of the two samples are given in Table 1. Again, the ratio K''(NV—K)/K''(NV—B) is considerably larger than b(NV—K)/b(NV—B).

In Fig. 2, the dependence of $J''_R(SH_+H_0)/J_R(H_+H_0)$ upon S/H is illustrated for the two samples. As shown in the figure, the advanced shock effect on IRM also is markedly larger in NV—K than in NV—B.

3. Integrated Effect of Repeated Mechanical Shocks on Shock-Remanent Magnetization

In Fig. 3, results of experimental tests of the integrated effect of repeated mechanical shocks on the shock remanent magnetization of sample NV—B are illustrated for two different values of S in a same magnetic field H. In this case, the experimental procedure to obatin the repeated shock remanent

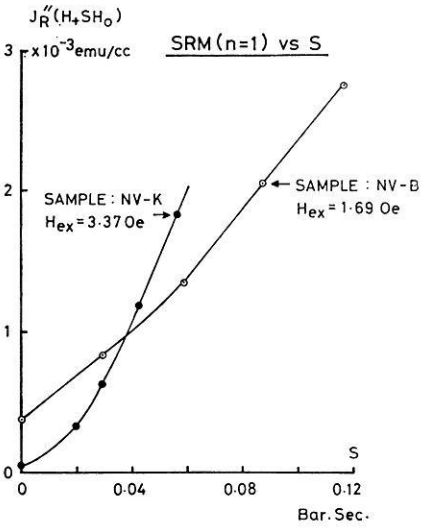

Fig. 1

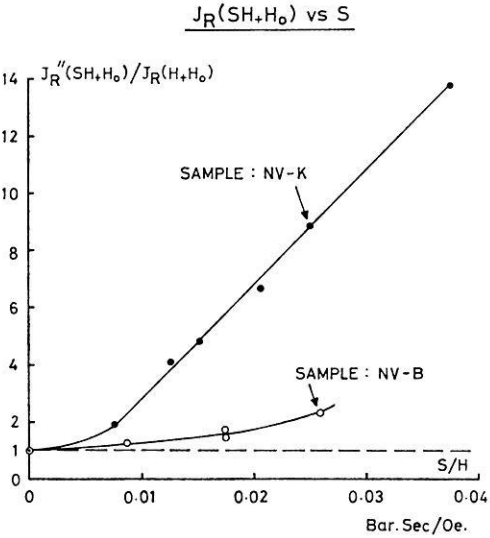

Fig. 2

Fig. 1. Dependence of shock remanent magnetization acquired by a single uniaxial shock in the presence of a magnetic field (H_{ex}) upon shock momentum (S).

Fig. 2. Relationship between ratio S/H and ratio of IRM acquired by a sample which is impacted by a single uniaxial shock in advance of the acquisition of IRM, J_R (SH_+H_0), to the ordinary IRM, $J_R(H_+H_0)$

magnetization is symbolically expressed as $J_R(H_+S_1H_0,\cdots\cdots, H_+S_nH_0$ where $S_1=S_2=\cdots\cdots=S_n=S$: that is, H is applied on the sample before individual shocks S_i ($1\leqq i\leqq n$) and H is removed after the individual S_i operations. The other definition of the repeated shock remanent magnetization may be symbolically expressed as $J_R(H_+S_1\cdots S_nH_0)$. Within the limit of experimental errors, however, no difference has been found between $J_R(H_+S_1H_0,\cdots\cdots, H_+S_nH_0)$ and $J_R(H_+S_1\cdots\cdots S_nH_0)$. We may conclude therefore that

$$J_R(H_+S_1H_0,\cdots\cdots, H_+S_nH_0)=J_R(H_+S_1\cdots S_nH_0). \tag{9}$$

In Fig. 4, the dependence of $J_R(H_+S_1\cdots\cdots S_nH_0)$ of sample NV—K upon n is illustrated for two different values of S in the same magnetic field. It is shown in these figures that $J_R(H_+S_1H_0,\cdots, H_+S_nH_0)$ or $J_R(H_+S_1\cdots\cdots S_nH_0)$ increases with an increase of n and tends to approach the final saturated value. In general, the larger part of SRM is acquired by the first shock and then $J_R(H_+S_1H_0,\cdots, H_+S_nH_0)$ or $J_R(H_+S_1\cdots\cdots S_nH_0)$ gradually increases with $n>1$, whence it does not seem possible to represent the dependence of $J_R(H_+S_1H_0,\cdots, H_+S_nH_0)$ or $J_R(H_+S_1$

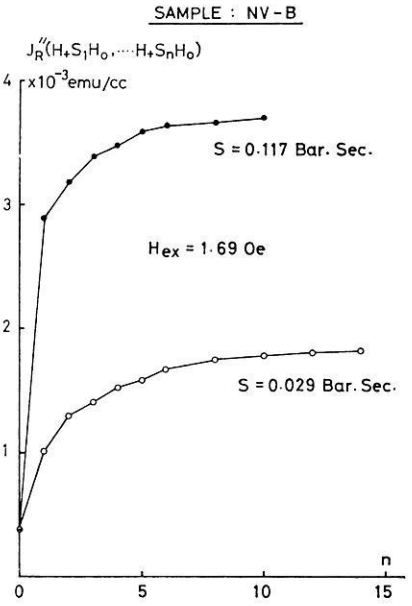

Fig. 3

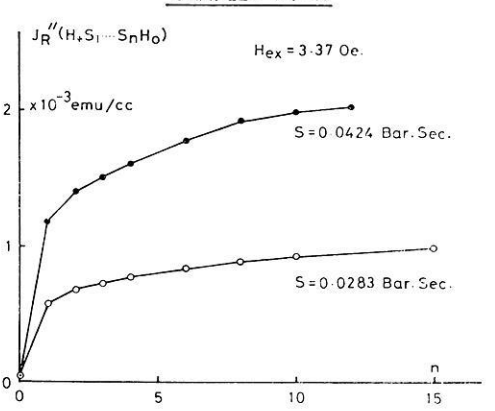

Fig. 4

Fig. 3. Dependence of repeatedly shocked SRM, $J_R(H_+S_1H_0,\ldots, H_+S_nH_0)$, on n. Sample: NV−B

Fig. 4. Dependence of repeatedly shocked SRM, $J_R(H_+S_1\ldots S_nH_0)$ on n. Sample: NV−K

SnH_0) upon n by a simple functional form for the whole range from $n=0$ to $n=\infty$. Then, it is natural to assume that the n repeated SRM consists of the effect of the first shock and the additional integrated effect of n—1 succeeding shocks. Namely,

$$J_R(H_+S_1H_0,\cdots\cdots H_+S_nH_0) = J_R(H_+S_1H_0) + J_R^*(n), \qquad (10)$$

where

$$J_R^*(n\to\infty) = J_R^*(\infty). \qquad (11)$$

$J_R^*(\infty)-J_R^*(n)$ values of the two samples are plotted against $n\geqq 1$ for different values of S in Fig. 5 and 6, which may lead to an empirical dependence of $J_R^*(n)$ upon n, expressed by

$$J_R^*(n) = J_R^*(\infty)[1-\exp\{-\alpha(n-1)\}]\ , \qquad (12)$$

where α is a material constant depending also on H and S.

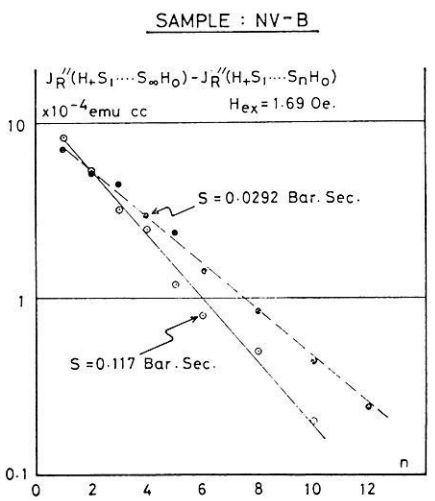

Fig. 5

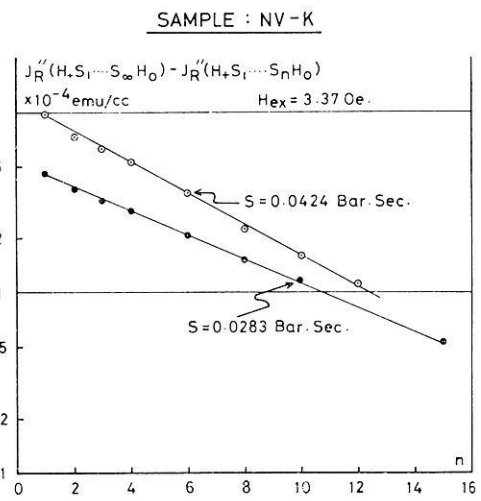

Fig. 6

Fig. 5. A linear dependence of log $[J_R(\infty)-J_R(H_+S_1\ldots S_nH_0)]$ on n for sample NV−B

Fig. 6. A linear dependence of log $[J_R(\infty)-J_R(H_+S_1\ldots S_nH_0)]$ on n for sample NV−K

Putting

$$J_R(H_+S_1H_0)+J_R^*(\infty)=J_R(\infty)\ , \tag{13}$$

and

$$J_R(H_+S_1H_0)=KJ_R(\infty),\ (K<1)\ , \tag{14}$$

we get from (10), (12), (13) and (14) that

$$J_R(H_+S_1H_0,\cdots\cdots H_+S_nH_0)=J_R(\infty)[1-(1-K)\exp\{-\alpha(n-1)\}]. \tag{15}$$

Numerical values of coefficients K and α in (15) derived from observed data shown in Figures 3 through 6 are summarized in Table 2.

Table 2. Shock remanent magnetization parameters

	H	S	K	α
	(Oe)	(Bar. Sec)		
(Sample NV–B)	1.69	0.117	0.779	0.414
	1.69	0.0292	0.552	0.301
(Sample NV–K)	3.37	0.0424	0.550	0.198
	3.37	0.0283	0.550	0.157
	4.50	0.0200	0.733	0.343

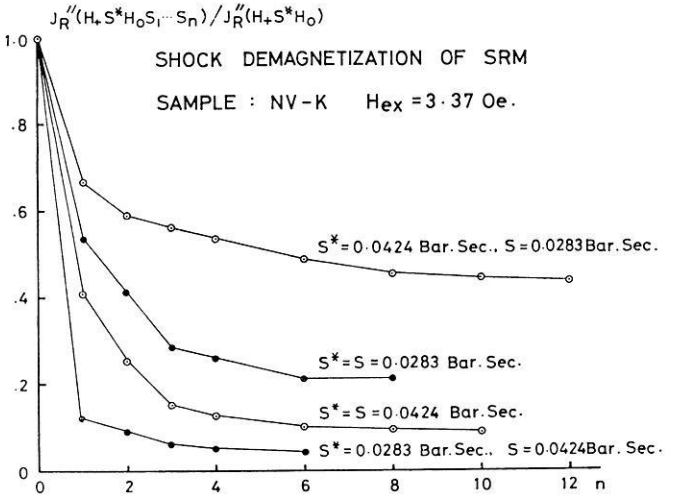

Fig. 7. Dependence of ratio $J_R(H_+S^*H_0S_1 \ldots S_n)$ to $J_R(H_+S^*H_0)$ upon n, where $J_R(H_+S^*H_0S_1 \ldots S_n)$ denotes the intensity after repeatedly shock demagnetized by S of SRM acquired by S^* in H. Sample: NV−K

4. Integrated Effect of Repeated Mechanical Shocks on Shock Demagnetization

The shock demagnetization effect was originally defined in terms of the demagnetization of IRM, $J_R(H_+H_0)$, by a mechanical shock in non-magnetic space (Nagata 1971). The remaining magnetization after n repeated mechanical shocks on $J_R(H_+H_0)$ has been noted by $J_R''(H_+H_0S_1\cdots S_n)$, $S_1=S_2=\cdots=S_n=S$, when the axis of shock momentum S is parallel to the direction of J_R (H_+H_0). When the axis of S is perpendicular to the direction of $J_R(H_+H_0)$, J_R'' in the above-notation is replaced by $J_R^{\perp}$. In both cases of J_R'' and $J_R^{\perp}$, $J_R(H_+H_0S_1\cdots S_n)$ decreases with an increase of n and approaches a final steady value. In this case also, the major decrease of remanent magnetization takes place with the first shock and succeeding shocks cause an exponential decrease with increasing values of n.

In the present sequence of experiments, the repeated shock demagnetization effect on the SRM acquired by a single shock (S^*) in the presence of a magnetic field (H) has been studied. The remanent magnetization after repeated shocks in non-magnetic space of a rock sample having an initial SRM, $J_R(H_+S^*H_0)$, will be noted by $J_R''(H_+S^*H_0S_1\cdots S_n)$ where $S_1=\cdots=S_n=S$. Here J_R'' represents that the axes of S^* and S and the direction of H are all parallel to one another. Fig. 7 illustrated four examples of the dependence of $J_R''(H_+S^*HS_1)\cdots Sn)/J_R''(H_+S^*H)$ on n for Sample NV—K, where H is the same in all the four cases but two cases of $S^*=S$ are illustrated together with cases of $S^*>S$ and $S^*<S$. As

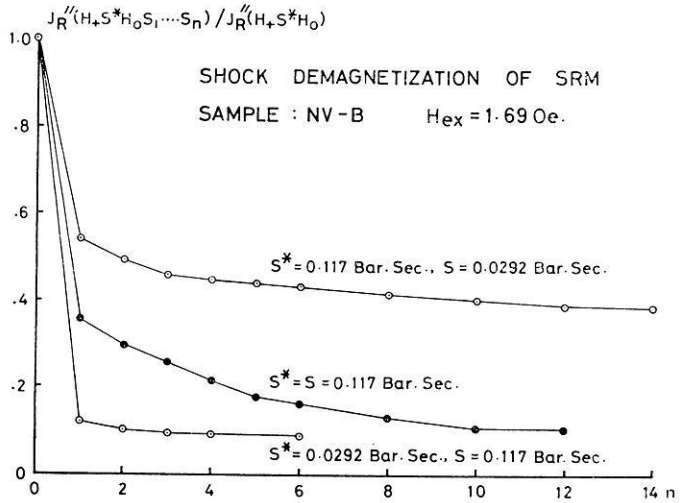

Fig. 8. Dependence of ratio $J_R(H_+S^*H_0S_1 \ldots S_n)$ to $J_R(H_+S^*H_0)$ upon n, where $J_R(H_+S^*H_0S_1 \ldots S_n)$ denotes the intensity after n-time repeatedly shock-demagnetized by S of SRM acquired by S^* in H. Sample: NV−K

shown in Fig. 1, the intensity of $J_R(H_+S^*H_0)$ is larger for a larger value of S^* in a same magnetic field (H). In Fig. 8, similar examples of the dependence of $J_R(H_+S^*H_0S_1\cdots\cdots S_n)/J_R(H_+S^*H_0)$ on n are illustrated for sample NV—B.

In all these experimental data, the relationship of $J_R(H_+S^*H_0S_1\cdots S_n)$ with n is found to consist of an initial sharp decrease caused by the first shock and a gradual exponential decrease by succeeding shocks toward the final steady value. These results may be empirically summarized as

$$J_R(H_+S^*H_0S_1) = K_1J_R(H_+S^*H_0) \quad (K_1 < 1). \tag{16}$$

$$\lim_{n\to\infty} J_R(H_+S^*H_0S_1\cdots S_n) = J_R(\infty) = K_\infty J_R(H_+S^*H_0), \quad (K_1 - K_\infty < 1), \tag{17}$$

and

$$J_R(H_+S^*H_0S_1\cdots S_n) - K_\infty J_R(H_+S^*H_0) = (K_1 - K_\infty)J_R(H_+S^*H_0)\exp\{-\beta(n-1)\}, \text{ (for } n \geqq 1). \tag{18}$$

Hence,

$$J_R(H_+S^*H_0S_1\cdots Sn) = J_R(H_+S^*H_0)[K\infty + (K_1 - K\infty) \times \exp\{-\beta(n-1\}]. \tag{19}$$

The empirical formula (19) describes the experimental results of shock demagnization effect shown in Figs. 7 and 8. Numerical values of parameters K_1, K_∞ and β for various different cases are summarized in Table 3. It may be generally concluded from Figs. 7 and 8 and in Table 3 that K_1 and K_∞ are smaller for larger values of S when S^* and H are kept invariant. This is one of general characteristics of the shock demagnetization effect. It must be further noted that $(K_1 - K_\infty)/(1 - K_\infty)$, which represents a part of the integrated effect of succeeding repeated shocks for $n > 1$ among the total shock demagnetization, becomes considerably smaller in the case that S is appreciably larger than S^*. This result may indicate that the first shock (S_1) in non-magnetic space can result in a nearly complete shock demagnetization effect so far as S is appreciably larger than S^*.

5. *Integrated Effect of Repeated Advanced Mechanical Shocks on* IRM

It seems that the most significant key phenomenon in a direct connection with the physical mechanism of various effects of a static pressure or a mechanical shock on the remanent magnetization of rocks would be the advanced compression effect (Nagata and Carleton 1968, 1969(a)(b)) and the advanced shock effect (Nagata, 1971) on IRM, which are symbolically noted by $J_R(P_+P_0H_+H_0)$ and $J_R(SH_+H_0)$ respectively. These phenomena can not be interpreted by the irreversible rotation theory of spontaneous magnetization of single domains proposed by Nagata (1966), Kinoshita (1969), Dunlop *et al.* (1969), but they can be reasonably well understood, together with all the other effects of P or S upon the remanent magnetization, by the irreversible movement theory of the 90° domain walls proposed by Nagata and Carleton (1969(a)(b)). As already shown in Fig. 2, $J_R(SH_+H_0)$ markedly increases with an increase of S beyond a certain critical value when H is kept constant, whereas $J_R(S)$ is always zero just as $J_R(P_+P_0) = 0$ regardless of the magnitude of P. However, the inner condition of $J_R(S)$ of a sample must not be the same as that of the initial virgin state which has not yet been shocked by S in non-magnetic space, because $J_R(SH_+H_0) > J_R(H_+H_0)$ as summarized by (4). It has been experimentally proved that the inner condition of $J_R(S)$ state can be practically reduced to the initial virgin state, $J_R(0)$, by the ordinary AF demagnetization procedure, because IRM acquired by any shocked rock sample after a sufficient AF-demagnetization procedure is always identical to $J_R(H_+H_0)$.

Another problem is concerned with the integrated effect of repeated shocks in non-magnetic space in advance of an acquisition of IRM, i.e. a possible dependence of $J_R(S_1 \cdots S_nH_+H_0)$ upon n. Fig. 9 shows a summary of results of experimental studies on the dependence of $J_R(S_1S_2 \cdots S_nH_+H_0)/J_R(H_+H_0)$ on n of sample NV–K for different values of S

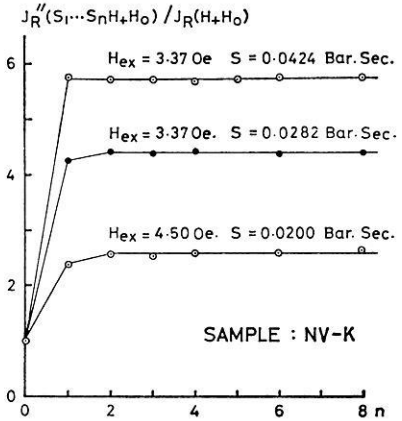

Fig. 9. Constancy of repeated advanced shock effect, which is practically independent of n. Sample: NV−K

and H, where $S_1 = \cdots = S_n = S$. It seems in Fig. 9 that $J_R(SH_+H_0)$ is slightly smaller than $J_R(SSH_+H_0)$ for smaller values of S/H but $J_R(S_1 \cdots S_nH_+H_0)$ is practically constant for $n \geqq 2$. Approximately speaking, therefore, there is no appreciable integrated effect of repeated advanced mechanical shocks on IRM, that is,

$$J_R(S_1 \cdots S_nH_+H_0) = J_R(SH_+H_0) \tag{20}$$

Results of the similar experiments on sample NV—B have led to the same conclusion, though the accuracy of measurements for this sample is less than that for sample NV—K.

6. Theoretical Discussions of Experimental Results

In summarizing the foregoing experimental results, one may conclude that both phenomena of the shock remanent magnetization and the shock demagnetization are subjected to the integrated effect of repeated shocks; the effect of repeated shocks in the two phenomena can be divided into the major effect of the first shock and the additional integrated effect of succeeding shocks approaching in an exponential form to a final saturated value. On the other hand, no appreciable effect of an integration of succeeding repeated shocks can be observed for the effect of advanced shocks on the acquisition of IRM. The most significant difference of the effects of repeated shocks on $J_R(H_+S_1 \cdots S_nH_0)$ and $J_R(H_+S^*H_0S_1 \cdots S_n)$ from that on $J_R(S_1 \cdots S_nH_+H_0)$ would be that the spontaneous magnetization (J_s) in individual domains in the former case is subjected to the magnetostatic

energy when the mother sample is repeatedly shocked, while in the latter case there is no magnetic field and no bulk magnetization and consequently no bulk magnetostatic energy is involved in the mechanism for possible changes of domain configurations to be caused by repeated shocks in non-magnetic space.

As already discussed (Nagata 1971), it seems that the most reliable and unified theoretical interpretation of the phenomena of shock remanent magnetization, shock demagnetization and advanced shock effect on remanent magnetization is based on the idea that both the magnetostatic force introduced by a magnetic field and the magnetoelastic force introduced by a mechanical shock or pressure irreversible drive the 90° domain walls so that the total potential energy takes the minimum possible value at individual stages during the whole course of respective experimental procedures. The basic condition required for acquiring the remanent magnetization in the above theory is based on the Rayleigh's parabolic relationship between H and IRM, i.e. $J_R(H_+H_0)=bH^2$.

In the present case dealing with the effects of mechanical shocks of a short duration time ($\sim$0.4 m.sec.), the dynamic motion of the domain walls passing over the internal energy barriers should be subjected not only to the magnitude of a pressure peak of a given shock but also to the kinetic energy of propagation of the shock pressure peak and the thermal fluctuation of energy barriers themselves. In brief, individual shocks (S_i) may be associated with fluctuations in both positive and negative sides. (A) Let us now assume that the effective value of Hc working on individual 90° domain walls has statistical fluctuations in each shocks, an individual Hc value being expressed as

$$H_c = H_c{}^0 + \xi \ , \tag{21}$$

where the distribution function $P(\xi)$ of ξ is represented by a finite symmetric function around $\xi=0$ such as

$$\left.\begin{aligned} p(\xi) &= \frac{1+\gamma}{2h_0{}^{1+\gamma}}(h_0-\xi)^\gamma \text{ for } 0\leqq\xi\leqq h_0 \ , \\ &= \frac{1+\gamma}{2h_0{}^{1+\gamma}}(h_0+\xi)^\gamma \text{ for } -h_0\leqq\xi\leqq 0 \ . \end{aligned}\right\} \tag{22}$$

For the whole set of 90° domain walls, the average value of Hc is $H_c{}^0$, and

$$\int_{-h_0}^{0} p(\xi)d\xi = \int_{0}^{h_0} p(\xi)d\xi = \frac{1}{2}.$$

(B) As the second assumption, we may consider that repeated shocks following the first shock give rise to additional effects on individual walls only

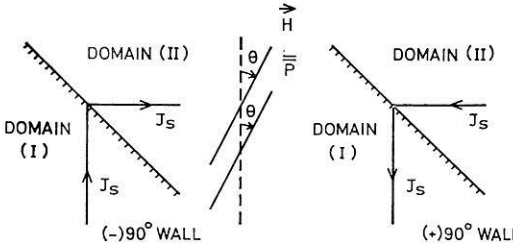

Fig. 10. Schematic model of a pair of (+) and (−) 90° domain walls

when the effects result in decrease of the magnetostatic energy. These two basic assumptions, (A) and (B), seem to be reasonably acceptable.

In the Nagata-Carleton theory of the piezoremanent magnetization, a set of pairs of 90° domain walls as illustrated in Fig. 10 is considered as a set of basic elements: the direction of spontaneous magnetization (Js) is antiparallel to each other between the two elemental domain configurations in a pair. When the direction of $\vec{H}$ makes an angle $\theta(0 \leqq \theta = \pi/4)$ with the Js direction in domain (I) on the left side of Fig. 10, (−)90° domain wall moves from the domain (I) side to the domain (II) side, while (+)90° domain wall does from the domain (II) side to the domain (I) side, both movements resulting in an increase of magnetization along the direction of H. If the axis of an applied mechanical compression P is parallel to the direction of H and the material compressed has a positive value of isotropic magnetostriction coefficient (λs), a (−)90° domain wall is derived by P from the domain (II) side to the domain (I) one, while a (+)90° wall also from the domain (II) side to domain (I) one, provided $0 \leqq \theta \leqq \pi/4$. Namely, both H and P affect the (+) domain wall to increase the magnetization along H, while P affects the (−) domain wall to decrease the magnetization along H though H always affects the (−) domain wall to increase the magnetization along H. Thus, Hc's defined by (8) which are working on the (+) and (−) 90° domain walls can be noted by $Hc^{(+)}$ and $Hc^{(-)}$ respectively.

(a) Integrated Effect of Repeated Shocks on Shock Demagnetization

Since the mechanism of shock demagnetization of a remanent magnetization is simpler then the other two cases, the integrated effect of repeated shocks on the demagnetization will first be theoretically discussed. In the case of a static pressure demagnetization, $J_R''(H_+H_0P+P_0)$ is theoretically expressed (Nagata and Carleton 1969(b)) as

$$J_R''(H_+H_0P_+P_0) = J_R(H_+H_0)\left(1-\frac{16}{15\pi}\frac{Hc}{H}\right) \text{ for } Hc \leqq H \qquad (23)$$

which consists of

$$J_R^{'}(H_+H_0P_+P_0) = \frac{1}{2} J_R(H_+Hc) + \frac{1}{2} J_R(H_+Hc) \left(1-\frac{32}{15\pi}\frac{H_c^{(-)}}{H}\right) . \quad (24)$$

Namely, only the $(-)90°$ domain walls are affected by the demagnetizing compression, as far as $Hc \leqq H$. As for an individual pair of 90° domain walls also, only the $(-)90°$ domain walls are affected by the demagnetizing compression provided that the component of Hc along the direction of Js in domain (I) is smaller than the component of H along the same direction; when the former becomes equal to or larger than the latter, the remanent magnetization of the pair is completely demagnetized, becoming zero.

Let us now consider the integrated effect of repeated shocks which are represented by (21) and (22). The probability that nth shock is larger than $(n-1)$th shock is 1/2. i.e.

$$p(S > S_{n-1}) = 1/2.$$

Then, expressing the average value of H_c of all $(S_2 > S_1)$ walls by

$$H_c = H_c^0 + h_2,$$

we get

$$h_2 = h_0 \left\{1 - \left(\frac{1}{2}\right)^{\frac{1}{1+\gamma}}\right\}. \quad (25)$$

Further, we can get in general

$$h_n = h_0 \left\{1 - \left(\frac{1}{2}\right)^{\frac{n-1}{1+\gamma}}\right\}. \quad (26)$$

Then, replacing $J_R\ (H_+H_0P+P_0)$ in (24) by $J_R\ (H_+H_0S_1 \ldots . S_n)$, $H_c^{(-)}$ in (24) can be written as

$$\begin{aligned} H_c^{(-)}(n) &= Hc^0 + h_n = Hc^0 + h_0 \left\{1 - \left(\frac{1}{2}\right)^{\frac{n-1}{1+\gamma}}\right\} \\ &= Hc^0 + h_0 \left[1 - \exp\left\{-\frac{ln2}{1+\gamma}(n-1)\right\}\right]. \end{aligned} \quad (27)$$

Thus,

$$\begin{aligned} J_R^{'}(H_+H_0S_1 \ldots S_n) &= J_R(H_+H_0) \times \\ &\left\{\left(1-\frac{16}{15\pi}\frac{Hc^0+h_0}{H}\right) + \frac{16}{15\pi}\frac{h_0}{H}\exp\left[-\frac{ln2}{1+\gamma}(n-1)\right]\right\}. \end{aligned} \quad (28)$$

If we put $1-\frac{16}{15\pi}\frac{H_c^0+h_0}{H} \equiv K_\infty$, $1-\frac{16}{15\pi}\frac{Hc^0}{H} \equiv K_1$, $\frac{\ln 2}{1+\gamma} \equiv \beta$, then the theoretical expression (28) becomes identical to the empirical formula (19).

(b) Integrated Effect of Repeated Shocks on the Acquisition of SRM

In the case of a static piezoremanent magnetization, J_R'' $(H_+P_+P_0H_0)$ for large values of P and small values of H can be represented by (7), which consists of two components (Nagata and Carleton [8]) in such a form as

$$J_R''(H_+P_+P_0H_0) = \frac{16}{5\pi}\, b\, H\, Hc = \frac{16}{15\pi}\, b\, H\, Hc^{(+)} + \frac{32}{15\pi}\, b\, H\, Hc^{(-)}. \quad (29)$$

In the presence of a magnetic field H, an increase of magnetization causes a decrease of the magnetostatic energy. In regard to an individual pair of $(+)90°$ and $(-)90°$ domain walls, the piezoremanent magnetization of the pair in the case of $Hc^* \geqq 2\,H^*$ is expressed as

$$\begin{aligned} J_R''(H_+P_+P_0H_0) &= \frac{b}{2}\{(H_c^{*(+)})^2 + 2H_c^{*(+)}H^*\} \\ &+ \frac{b}{2}\{4H_c^{*(-)}H^* - (H_c^*)^2\} - bH^2, \end{aligned} \quad (30)$$

where Hc^* and H^* denote respectively the components of Hc and H along the direction of Js in domain (I) relative to those along the direction of Js in domain (II). If $Hc^* > 4H^*$ in (30), an increase of $Hc^{*(-)}$ results in a decrease of the remanent magnetization so that an increase of $Hc^{*(-)}$ by repeated shocks is forbidden in the present model. If $4H^* > Hc^* \geqq 2H^*$ on the other hand, an increase of $Hc^{*(-)}$ also is allowable. Since the case of large values of Hc and small values of H (i.e. the case that H^2 can be neglected in comparison with $3HH_c$) is experimentally dealt with, we may consider that $Hc^* > 4H^*$ in the present case.

Thus, similarly to the case of shock demagnetization, the integrated effect of repeated shocks on SRM can be theoretically given by

$$\begin{aligned} J_R''(H_+S_1 \ldots S_nH_0) &= \frac{32}{15\pi}\, bHH_c^0 + \frac{16}{15\pi}\, bH(H_c^0 + h_n) \\ &= \frac{16}{5\pi}\, bHH_c^0 + \frac{16}{15\pi}\, bHb_0\left[1 - \exp\left\{-\frac{\ln 2}{1+\gamma}(n-1)\right\}\right]. \end{aligned} \quad (31)$$

Putting then, $\frac{16}{15\pi}\, bHH_c^0 = J_R(H_+S_1H_0) \equiv K\ J_R(\infty)$, $\frac{16}{15\pi}\, bHb_0 \equiv J_R^*(\infty)$, and $\frac{\ln 2}{1+\gamma} \equiv \alpha$, the theoretical result (31) is found to be identical to empirical formula (15).

(c) Integrated Effect of Repeated Advanced Shocks on IRM

The integrated effect of repeated advanced shocks on IRM is essentially different front the above-mentioned two cases, because there is no bulk

magnetostatic energy in $J_R(S)$ nor $J_R(S_1 \cdots S_n)$; namely, $J_R(S) = J_R(S_1 \cdots S_n) = 0$ in $H = 0$ space. However, the domain configuration of state $J_R(S)$ should be different from the initial state $J_R(0)$, which represents the vergin state before an application of S in $H = 0$ space. In Nagata-Carleton theory of the effect of advanced static compression on IRM, $J_R(P_+P_0)$ for large values of P can be decomposed into two components such as

$$J_R(P_+P_0) = \frac{16}{15\pi} b(H_c^{(+)})^2 - \frac{16}{15\pi} b(H_c^{(-)})^2 = 0. \tag{32}$$

If $H_c^{(+)} \neq H_c^{(-)}$, $J_R(P_+P_0)$ must have either positive or negative remanent magnetization and consequently a certain finite amount of the magnetostatic energy must appear, whence $H_c(^-)$ must be equal to $H_c^{(+)}$ as far as any acquisition of a finite magnetostatic energy is forbidden in $H = 0$ space. In the case of $J_R(S)$ or $J_R(S_1 \cdots S_n)$, the situation must be the same as in the case of $J_R(P_+P_0)$. Namely, the magnetically neutral state, $J_R(S)$ or $J_R(S_1 \cdots S_n)$, can be considered as an assemblage of a large number of pairs of $H_c^{(+)}$ and $H_c^{(-)}$ domain walls, where $H_c^{(+)} = H_c^{(-)}$ in each pair. Even if we assume that both $H_c^{(+)}$ and $H_c^{(-)}$ are allowed to take any value between $H_c^0 - h_0$ and $H_c^0 + h_0$, the required condition of $H_c^{(+)} = H_c^{(-)}$ for individual pairs may strictly limit alowable values for $H_c^{(+)}$ and $H_c^{(-)}$, i.e. the allowable values for individual shocks must to $Hc^{(+)} = Hc^{(-)} = H_c^0 + \xi$ $(-h_0 \leqq \xi \leqq h_0)$ for each pair. The probability that both $H_c^{(+)}$ and $H_c^{(-)}$ simultaneously take the same value of $H_c^0 + \xi$ is negligibly small. Since the average value of $H_c^0 + \xi$ is H_c^0, we may write

$$J_R(S_1 \cdots S_n) = J_R(S) = \frac{16}{15\pi} b\,[(H_c^0)^2 - (H_c^0)^2] = 0. \tag{33}$$

Then, (33) theoretically leads to

$$J_R''(S_1 \cdots S_n\, H_+H_0) = J_R''(SH_+H_0) = \frac{16}{15\pi} b\, HH_c^0, \tag{34}$$

for sufficiently large values of H_c^0/H. (Nagata and Carleton 1969(b)). Namely, there is no integrated effect of advanced repeated shocks on IRM.

7. *Concluding Remarks*

In the previous section, $J_R''(H_+H_0S_1 \cdots S_n)$, $J_R''(H_+S_1 \cdots S_nH_0)$ and $J_R''(S_1 \cdots S_nH_+H_0)$ are theoretically discussed. In Section, 3, 4 and 5, however, experimental results on $J_R''(H_+S_1H_0, \cdots H_+S_nH_0)$, $J_R''(H_+S \cdots S_nH_0)$, $J_R''(H_+S^*H_0S_1 \cdots S_n)$ and $J_R''(S_1 \cdots S_nH_+H_0)$ are described. As already mentioned in Section 3, it has been experimentally demonstrated

that $J_R(H_+S_1H_0, \cdots H_+S_nH_0) = J_R(H_+S_1\cdots S_nH_0)$. From the theoretical viewpoint also, this equality between $J_R(H_+S_1H_0, \cdots, H_+S_nH_0)$ and $J_R(H_+S_1\cdots S_nH_0)$ can be easily obtained, because $J_R(H_+S_1H_0, \cdots, H_+S_n) = J_R(H_+S_1\cdots S_n)$ in repeated Rayleigh's hysteresis loops. Hence, the theoretical expression of $J_R(H_+S_1\cdots S_nH_0)$ can stand for experimental results for $J_R(H_+S_1H_0, \cdots, H_+S_nH_0)$ and $J_R(H_+S_1\cdots S_nH_0)$. As for the repeated shock demagnetization on IRM, experimental results on $J_R(H_+H_0S_1\cdots S_n)$ have already been reported in a previous paper (Nagata, 1971). In Section 3 of the present paper, new experimental results on the repeated shock demagnetization on SRM, $J_R(H_+S^*H_0\ S_1\cdots S_n)$, are described. As far as $S^* \geqq S$, however, the general characteristics of $J_R(H_+S^*H_0S_1\cdots S_n)$ can not be different from those of $J_R\ (H_+H_0S_1\cdots S_n)$, because $J_R(H_+S^*H_0)$ simply corresponds to $J_R(H'_+H'_0)$ for H' which is larger than H. Hence, the present theory of $J_R(H_+H_0S_1\cdots S_n)$ can stand for both $J_R(H_+H_0S_1\cdots S_n)$ and $J_R(H_+ + S^*H_0S_1\cdots S_n)$ for $S^* \geqq S$. If $S^* < S$, however, the demagnetization characteristics become a little complicated. If $H_c{}^0(S)$ is larger than $H_c{}^{0*}(S^*)+H$, $J_R(H_+S^*H_0)$ is completely demagnetized by the first shock S. Namely,

$$J_R(H_+S^*H_0S) = 0 \text{ for } H_c{}^0(S) > H_c{}^{0*}(S^*)+H.$$

If $H_c{}^{0*}(S^*) < H_c{}^0(S) < H_c{}^{0*}(S^*)+H$, on the other hand, the equivalent expression in terms of the pressure demagnetization of piezoremanent magnetization can be written as

$$J_R(H_+P_+{}^*P_0{}^*H_0P+P_0) = \frac{1}{2}J_R(H_+P_+{}^*P_0{}^*H_0) + \frac{1}{2}J_R\,(H_+P_+{}^*P_0{}^*H_0)\left[1-\frac{32}{15\pi}\frac{H_c{}^{(-)}(P)}{H}\right]. \tag{35}$$

The mathematical form of (35) is the same as that of (24), whence $J_R(H_+ S^*H_0S_1\cdots S_n)$ can be theoretically represented by (28) in the present case also, where $J_R(H_+H_0)$ on the right hand side of (28) must be replaced by $J_R(H_+S^*H_0)$. In experimental results for $S \gg S^*$ in Table 3, the observed values of K_1 are very small and $K_1 - K_\infty$ values are further smaller compared with the cases of $S < S^*$. This would be the case of $H_c{}^0(S) \sim H_c{}^{0*}(S^*)+H$ and consequently $J_R(H_+S^*H_0S) \simeq 0$.

In the present model, α and β in empirical formulae (15) and (19) respectively are theoretically represented by

$$\alpha = \beta = \frac{\ln 2}{1+\gamma}. \tag{36}$$

Table 3. Shock demagnetization parameters

	H	S^*	S	K_1	$K\infty$	β	$\frac{(K_1-K\infty)}{(1-K\infty)}$
	(Oe)	(Bar. Sec)	(Bar. Sec)				
(Sample NV−B)	1.69	0.117	0.117	0.356	0.098	0.326	0.286
	1.69	0.117	0.0292	0.540	0.360	0.142	0.281
	1.69	0.0292	0.117	0.128	0.121	0.428	0.008
	1.69	0.0584	0.117	0.119	0.088	0.935	0.031
(Sample NV−K)	1.37	0.0424	0.0424	0.408	0.085	0.595	0.353
	3.37	0.0424	0.0272	0.664	0.420	0.272	0.421
	3.37	0.0283	0.0283	0.535	0.210	0.552	0.411
	3.37	0.0283	0.0424	0.122	0.027	0.364	0.098

Experimentally observed values of α in Table 2 and those of β for cases of $S \leqq S^*$ in Table 3 range between 0.16 to 0.41 and between 0.14 to 0.60 respectively. These ranges of α and β correspond to $\gamma = 3.3 \sim 0.7$ and $\gamma = 4.0 \sim 0.2$ respectively. It seems likely in the observed values of α and β that the larger values of S correspond to the larger values of α or β and consequently the smaller values of γ, if the other parameters, H and S^*, are kept constant. As defined by (22), the probability function $p(\xi)$ has a flatter distribution with respect to ξ with a decreasing value of γ. It may be concluded therefore that a larger shock is associated with a broader distribution of fluctuation (ξ).

The present theoretical interpretation of the integrated effect of repeated shocks on the shock remanent magnetization, the shock demagnetization and the advanced shock on IRM is based on an idealistically simplified model (A) that any additional movement of the 90° domain walls which gives rise to an increase of the magnetostatic energy is forbidden as far as the driving force is due to statistical fluctuations of applied shocks, and (B) that the fluctuations ξ in Hc are assumed to be distributed between $-h_0$ and $+h_0$ around the average value $H_c{}^0$in such a form as represented by (22). The first assumption seems to be too strict; that is, an increase in the magnetostatic energy could be allowed to a certain small extent in actual cases. Quantitatively speaking, therefore, the theoretical results given by (28), (31) and (34) can be more or less unsatisfactory for explaining details of the experimental results represented by (15), (19) and (20) respectively. As far as general characteristics are concerned, however, it may be concluded that the present theoretical model can reasonably well explain the observed characteristics of the integrated effect of repeated shocks in the three types of process.

Another problem in relation to the effect of repeated mechanical shocks on rock magnetization would be possible effects of natural or artificial seismic shocks on the magnetization of the earth's crust, as already pointed out by the author (Nagata 1969). Actually, Undzendov and Shapiro (1967) observed irreversible changes in the geomagnetic field caused by artificial seismic shocks. In their studies, artificial explosions using gunpowder were operated five times nearby two magnetograph stations to give the seismic shocks to the subterranean magnetized body which is associated with a geomagnetic anomaly of about 15,000 γ in vertical component. The observed geomagnetic field changes consist of (a) magnetic spike which takes place simultaneously with a seismic shock and (b) an irreversible change of several gammas in magnitude. The first type change may be largely due to mechanical vibrations of the magnetograph, tough a part of the change is to be due to the reversible effect of a mechanical shock on the magnetic susceptibility of rocks. However, the second type irreversible change can be considered to be due to the shock remanent magnetization or the shock demagnetization of the magnetized subterranean body. According to the investigators' estimate, the shock stress induced by the seismic waves is in the order of magnitude of $1 \sim 2$ kg/cm^2. If the observed irreversible change is assumed to be attributable to the shock demagnetization effect, a decrease in the geomagnetic anomaly by about 10 γ could be expected. It seems that studies in detail on possible effects of destructive natural earthquakes on the earth crust's magnetization would be extremely interesting.

In the end of this short paper, the author wishes to express his sincere thanks to Dr. M. D. Fuller of University of Pittsburgh for his fruitful discussions on this work.

References

Dunlop, D. J., Ozima, M., Kinoshita, H.: Piezo magnetization of single-domain grains: a graphical approach, J. Geomag. Geoelectr. *21*, 513–518, 1969

Kinoshita, H.: Studies on piezo-magnetization (IV) Interpretations of PRM production for single domain grains. J. Geomag. Geoelectr. *21*, 409–425, 1969

Nagata, T.: Main characteristics of piezo-magnetization and their qualitative characteristics. J. Geomag. Geoelectr. *18*, 81–97, 1966

Nagata, T.: Tectonomagnetism IAGA Bull. *27*: Transact. General Assembly, Madrid, 12–43, 1969

Nagata, T.: Basic magnetic properties of rocks under the effects of mechanical stresses. Tectonophysics *9*, 167–195, 1970

Nagata, T.: Introductory notes on shock remanent magnetization and shock demagnetization of igneous rocks. Pure. Appl. Geophys. *89*, 159–177, 1971

Nagata, T., Carleton, B. J.: Notes on piezo-remanent magnetization. J. Geomag. Geoelectr. *20*, 115–127, 1968

Nagata, T., Carleton, B. J.: Notes on piezo-remanent magnetization of igneous rocks II. J. Geomag. Geoelectr. *21*, 427–445, 1969a

Nagata, T., Carleton, B. J.: Notes on piezo-remanent magnetization of igneous rocks III; Theoretical interpretation of experimental results. J. Geomag. Geoelectr. *21*, 623–645, 1969b

Shapiro, V. A., Ivanov, N. A.: Dynamic remanence and the effect of shocks on the remanence of strongly magnetic rocks. Doklady Akad. Nauk, USSR, *173*, 1065–1068, 1967

Undzendov, B. A., Shapiro, V. A.: Seismomagnetic effect in a magnetite deposit. Izvestia Earth Phys., USSR, No *1*, 121–123, 1967

Takesi Nagata
National Institute of Polar Research
Ministry of Education
1-9-10, Kaga, Itabashi-ku
Tokyo, 173 Japan

J. Geophys. 40, 489–500, 1974

A Test of Paleomagnetic Intensity Methods Using Recent Lavas, and Implications for Anomaly Interpretation

C. M. Carmichael

University of Western Ontario, London, Canada

Received March 12, 1974

Abstract. Measures of the intensity of the paleomagnetic field derived by studying lava from the 1963 and 1967 eruptions on Surtsey and the 1971 eruption on Etna, have been compared to the known field. Methods used were the comparison of the partial TRM removed from the NRM with the partial TRM produced in a known field, in increasing temperature steps, as described by Thellier and the NRM as a fraction of the saturation remanence compared to the TRM in a known field, as a fraction of the saturation remanence after heating, all in increasing AF demagnetization steps, as described by Carmichael.

The single heating of the second method caused less alteration in general, but in most cases additional magnetic oxide was produced and in some samples the composition was changed as detected by the zero field Curie point curves and the AF profiles of the various remanences. In spite of the changes detected in some samples, measures of the field judged to be reliable to about 10%, were obtained from all the lavas.

The results from these recent lavas lend credibility to paleomagnetic field intensity measures showing the earth's magnetic field to have been similar in strength to the present field except during the Paleozoic era when it was much weaker. In magnetic anomaly interpretation, it is only for rocks of the Paleozoic era that it is safe to assume that the remanent component is negligible compared to the induced component.

Key words: Paleomagnetic Field Intensity — Remanent Component.

Introduction

Magnetic anomaly interpretation attempts to infer the properties of the rock bodies causing the anomalies. In any such procedure some assumption must be made about the contribution of remanent magnetization. Frequently it is assumed that the remanent component is negligible and this is often valid as a first approximation.

There are numerous instances however, where remanent magnetization cannot be ignored, perhaps the most notable being the anomalies due to the remanent magnetization of the thin veneer of basalt on the ocean floor. Almost everyone can draw on personal experience for other examples

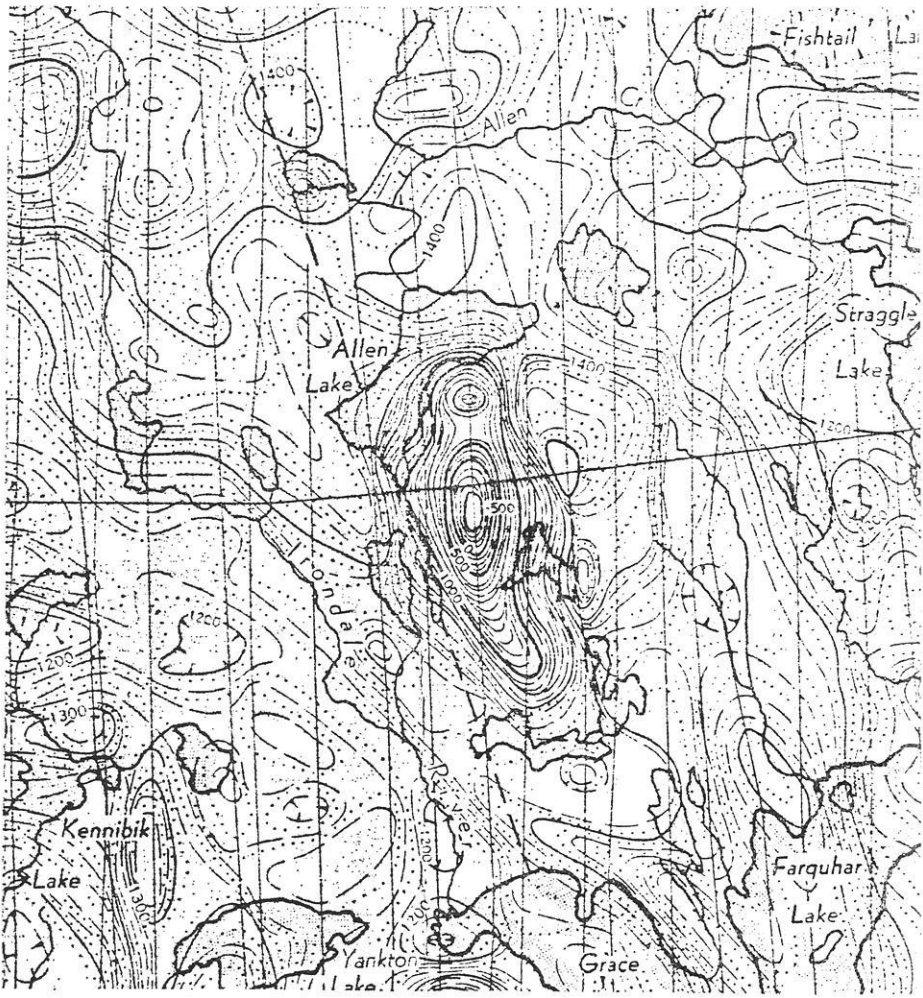

Fig. 1. A portion of the aeromagnetic map 110G, Geological Survey of Canada 1953, showing the negative anomaly near Wilberforce, 45° 7′N 78° 15′W. It is due to the inverse remanence of less than 1% magnetite in the form of small needles in pyroxene

where remanent magnetization has been important. Fig. 1 shows the anomaly over a pyroxenite body near Wilberforce, Ontario, Canada that was drilled in the hope of finding a massive hemoilmenite deposit. The anomaly is due entirely to the strong inverse remanence of magnetite needles in the pyroxenite even though the magnetite content is less than 1% (Palmer and Carmichael, 1973). Another example is the case of a deposit

containing up to 20% iron oxide in the Allard Lake region of Quebec, Canada, (Carmichael, 1964) in which a balance of induced and remanent magnetization produced a negligible anomaly.

There are a number of magnetic parameters that determine whether remanent magnetization contributes significantly to an anomaly but only the intensity of the earth's magnetic field at the time the rock formed is being considered here. The intensity of the field has varied over the past few thousand years by a factor of 4, from about one half to twice its present value and this has probably been the case in the past (Smith, 1967). Such field intensity changes will have a noticeable effect on the ratio of remanent to induced component but larger changes will be more significant.

Intensity Methods

In general paleomagnetic intensity methods involve a comparison of the natural remanence of a sample with the thermoremanence produced in a known field. Difficulties arise with samples whose magnetic oxides have undergone chemical change after they received their original magnetization or during the heating to produce a thermoremanence in a known field. Metamorphism that involves heating above the Curie point of the magnetic minerals is not a problem except that the field being measured is that present during the final cooling at the end of the metamorphic episode, not the field when the rock was originally formed. Chemical change at temperatures below the Curie point can cause considerable difficulty since these can alter the amount of magnetic oxide and its magnetic properties. The most common alteration of this sort is the low temperature oxidation of magnetite to maghemite. The maghemite is magnetically soft but can account for a considerable portion of the natural remanence. Heating to produce a thermaremanence will usually convert the maghemite to hematite which has a much lower specific magnetization. Unless the problem is recognized, such samples can give measures of plaeomagnetic field intensity that are too high.

Chemical changes taking place during heating to produce a thermoremanence can either reduce the magnetization by such changes as converting a magnetite phase to a less magnetic hematite phase or can increase it by precipitating a magnetite phase out of the silicates. Small changes of this sort, less than 15% say, can be allowed for provided one knows they have taken place. Techniques of alteration detection involve direct examination of the magnetic minerals by ore microscopy, X-ray diffraction and microprobe analysis and indirect examination by comparing Curie point curves, saturation remanence and coercivity spectra of the sample before and after heating.

There are many different procedures used for calculating paleomagnetic field intensity but most are variations of two general techniques. The first

was developed by Thellier (Thellier and Thellier, 1959) and involves a comparison of the partial natural remanence destroyed by heating in steps to higher temperatures and cooling in zero field, to the partial thermoremanence produced in a demagnetized sample upon heating it over the same temperature intervals and cooling in a known field. This procedure was devised for bricks, tiles and pottery in which the magnetic oxide is usually a magnetically hard and very stable hematite. It can also work well with rocks that are unaltered by repeated heating. The second general method uses a single heating and cooling in a known field with some form of demagnetization to remove soft components and various ways of detecting chemical change. The procedure used here (Carmichael, 1968) corrects for some destruction of magnetic oxide or production of new oxide in the heating process, and computes the intensity as recorded in a range of coercive force components Chemical change is detected by microscopic examination of the oxides, by comparing curves of the thermal decay of the natural remanence in zero field with that after heating and by comparing curves of alternating field demagnetization. Changes in shape of the thermal decay curves and changes in the zero field Curie temperature indicate chemical alteration of the magnetic minerals, and changes in the saturation remanence by the heating indicates changes in the amount of these minerals. Thermoremanence is produced by cooling in a 0.5 oersted field from a temperature 50 °C above the temperature at which the natural remanence is destroyed. This minimizes alterations due to heating and avoids magnetizing higher Curie point components, such as hematite formed from maghemite, that did not contribute to the natural remanence. The paleomagnetic field intensity is calculated as a factor relative to the present field intensity as *1* by

$$\frac{\text{NRM}}{\text{SRMn}} \Big/ \frac{\text{TRM (0.5 oe)}}{\text{SRMh}} \times \text{latitude factor}$$

where NRM is the natural remanent magnetization, TRM (0.5 oe) is the thermoremanence produced in a field of 0.5 oersteds, SRMn is the saturation remanent magnetization of a natural sample and SRMh is the saturation remanent magnetization after heating to produce the thermoremanence. The latitude factor corrects for the variation of the magnetic field intensity with latitude using the relative variation of the present earth's field and the inclination of the natural remanence. This assumes that the paleomagnetic field had a similar variation in intensity with inclination as the present field has, using as the present field the charts published by the United States Naval Oceanographic Office, 5th edition, epoch 1965.0. Values of total field intensity along inclination contours 10° apart north and south, were read at intervals of 15° of longitude and averaged. These averaged values

Table 1. Average intensity of present earth's field at 10° inclination intervals and latitude factor for a thermoremanence produced in 0.5 oersteds

Inclination (+ve or −ve)	0°	10°	20°	30°	40°	50°	60°	70°	80°	90°
Intensity (oersteds)	0.347	0.356	0.359	0.375	0.399	0.436	0.494	0.558	0.609	0.632
Latitude factor	1.44	1.41	1.39	1.33	1.25	1.15	1.01	0.90	0.82	0.79

are listed in Table 1 along with the values of the latitude factor to be used in the equation for paleomagnetic field intensity where the thermoremanence was produced in a field of 0.5 oersteds. The value of the factor to be used is that corresponding to the inclination of the natural remanence.

Each of the four remanent magnetizations are subjected to alternating field demagnetization in stages of 50 or 100 oersteds and a value of paleomagnetic field intensity is calculated for each step. These values are usually similar and the value of the paleomagnetic intensity chosen is a mean of those for steps of demagnetization that produced the best grouping of directions.

Intensity Methods Applied to Recent Lavas

As a test of applicability to older lavas the intensity methods as described by Thellier and by Carmichael were applied to samples from the 1963 and 1967 eruptions on Surtsey and the 1971 eruption on Etna. It was hoped that a wide range of oxidation states could be found and criterion of suitability could be established for use with older lavas.

In the field, redness of the flows was used as an indication of conditions of high oxidation and blackness as an indication of conditions of low oxidation. As it turned out the red colour was mostly a thin layer on the surface and on the walls of vesicles and not a very good indicator. Polished thin sections showed that there was a wide range of oxidation state of the magnetic oxides particularly in the Etna samples. It is difficult to attach a general oxidation state to each sample since all had generally greygreen silicates with single phase magnetite grains, along with local reddish silicates in which the magnetite was oxidized, often to hematitic relicts. The oxide grains were in three distinct sizes, a few large subhedral magnetite grains up to 1 mm across, abundant euhedral magnetite from 1 to 20 microns but mostly in the 5 to 10 micron range, and fine dust in the silicates and along silicate grain boundaries. In about a third of the samples the large magnetites were single phase except for some maghemitization along cracks.

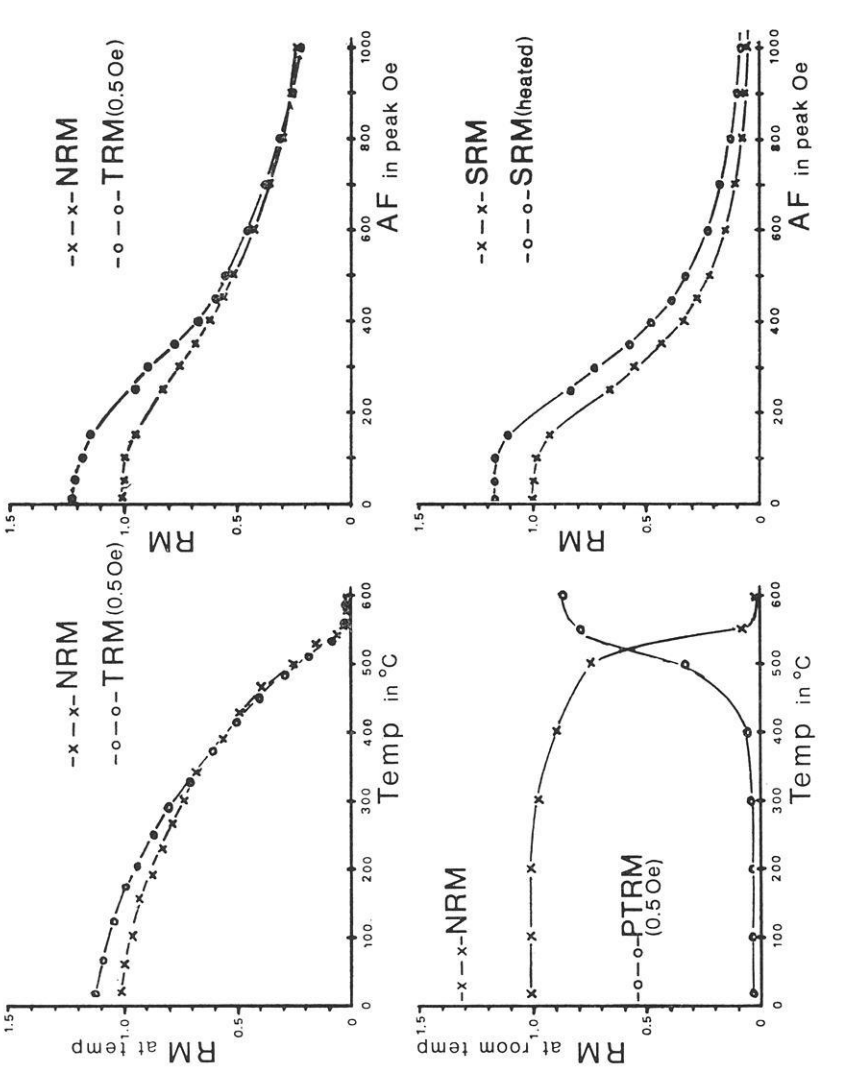

Fig. 2
Curves showing the magnetic properties of two samples of Surtsey lava. Sample S-2 is much more extensively oxidized than is sample S-5

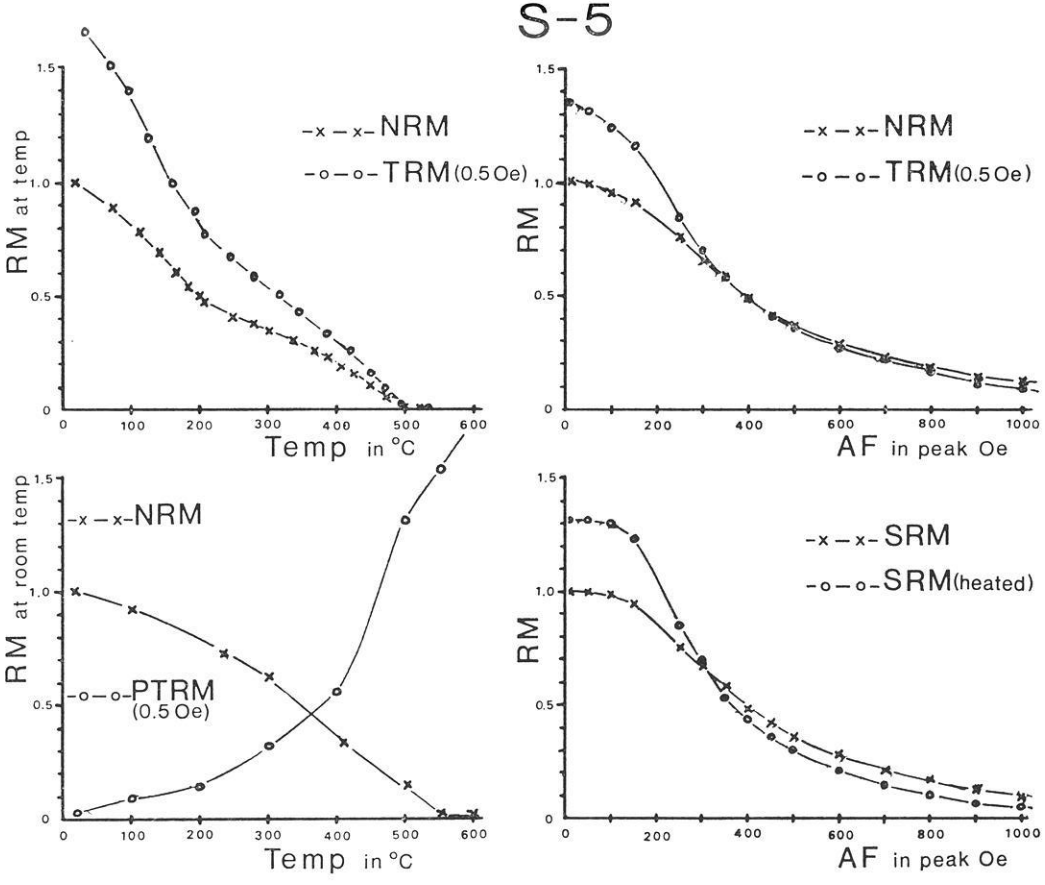

(Fig. 2 continued)

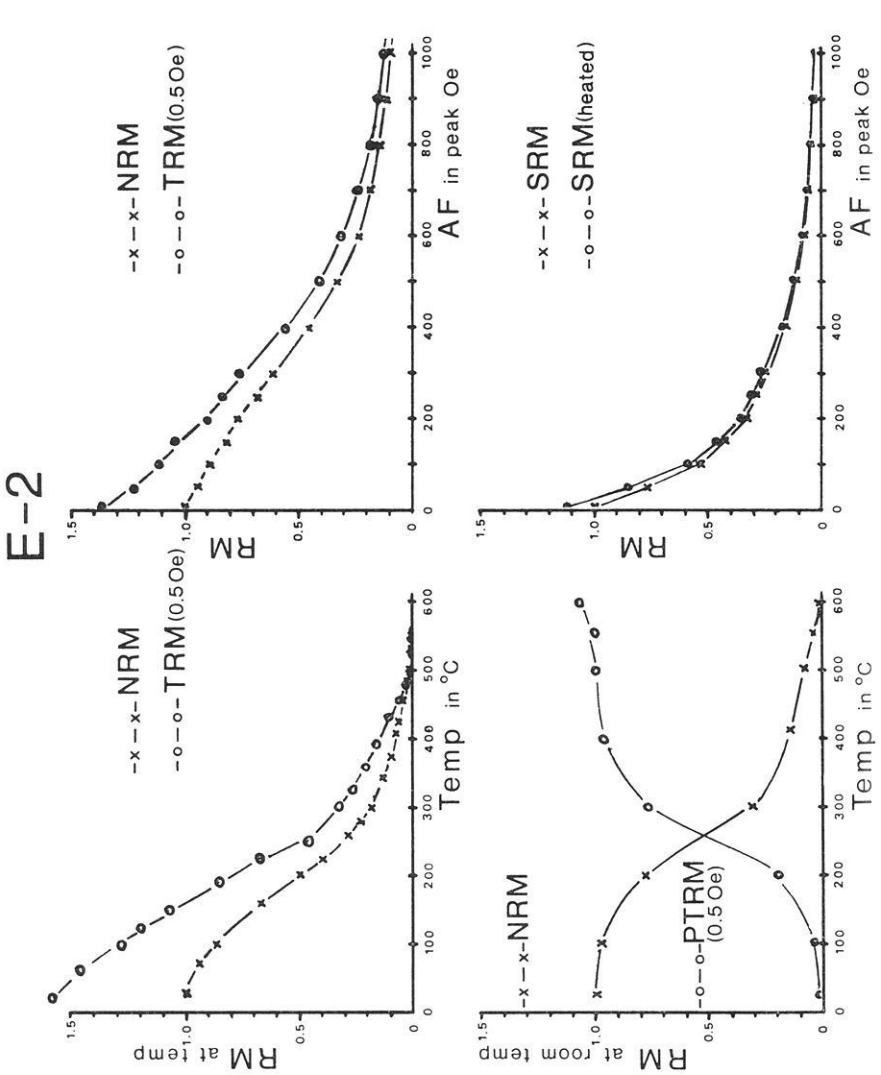

Fig. 3 Curves showing the magnetic properties of two samples of Etna lava. Sample E-2 shows the least oxidation of the Etna samples

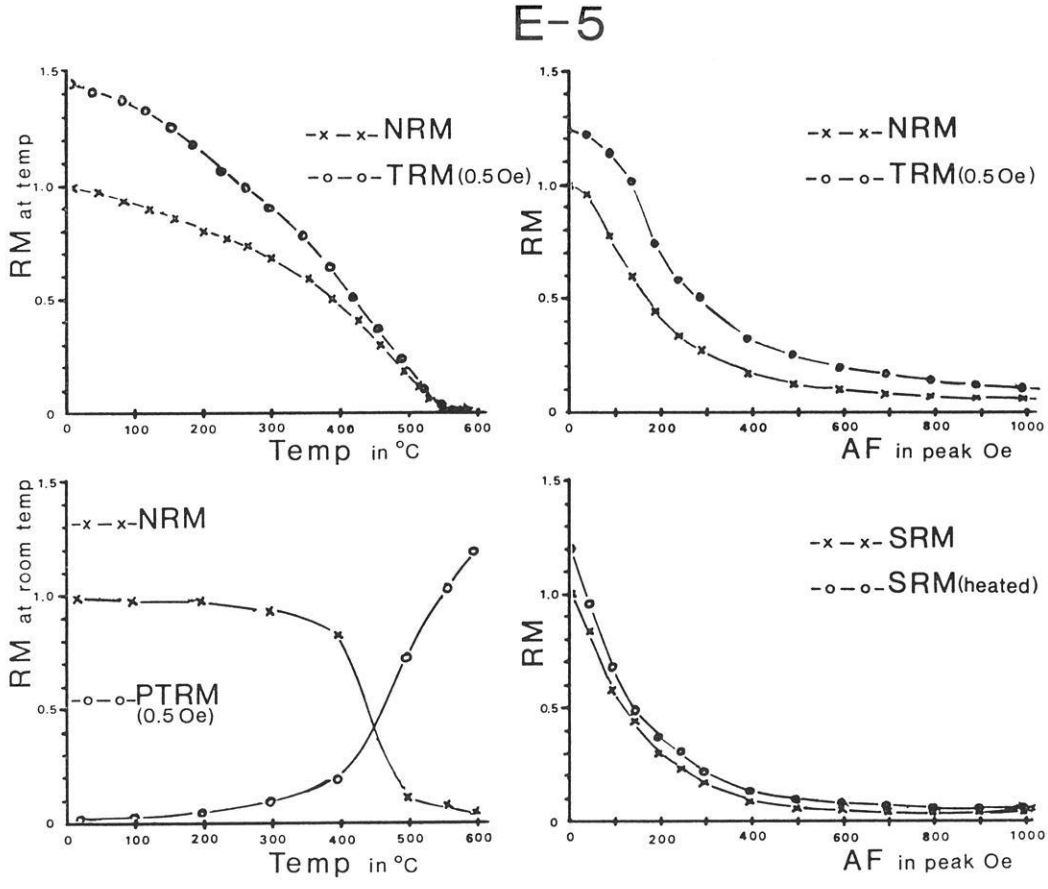

(Fig. 3 continued)

Table 2. Paleomagnetic Field Intensity from Recent Lavas (Relative to the IGRF 1965.0 IAGA Bulletin No. 29, field at the site as 1.0)

	Surtsey 1963–67							Etna 1971					
AF (Peak Oe)	S-2	S-5	S-11	S-16	S-17	S-21	S-23	E-1	E-2	E-3	E-4	E-5	E-8
	(Method as described by Carmichael)												
0	0.94	0.97	1.51	1.27	0.97	1.13	1.09	1.44	0.92	0.76	0.83	1.08	0.74
100	1.00	0.98	1.74	1.14	0.95	1.06	1.01	0.89	1.00	0.81	0.63	0.91	0.77
200	1.02	1.01	1.78	1.12	0.98	1.05	0.95	0.74	1.01	0.85	0.86	0.90	0.78
300	1.07	1.01	1.31	1.08	1.08	0.98	0.93	1.12	0.94	0.69	0.87	0.92	0.79
400	1.32	0.95	1.21	1.06	1.02	1.03	0.90	1.15	0.95	1.02	0.80	0.92	0.67
500	1.36	0.90	1.19	1.03	1.02	0.99	0.97	—	0.91	0.90	0.89	0.96	0.84
600	1.44	0.82	1.24	0.99	1.01	0.90	0.95	0.75	0.90	0.89	0.93	0.98	0.83
700	1.55	0.82	1.14	0.98	1.08	1.02	0.96	1.15	0.87	1.08	0.83	1.00	0.86
800	1.73	0.76	1.16	0.96	1.00	0.74	1.10	1.69	0.91	0.85	0.88	0.93	0.81
PTRM (Temp °C)	(Method as described by Thellier)												
400	3.1	0.83	2.1					1.36		1.46			
500	1.2	1.55	0.79					1.29		0.96			
550	0.82	1.55	0.91					1.21		1.35			
600	0.85	2.04	1.06					1.23		1.37			

There are no separate ilmenite grains and only minor indications of exsolution of some magnetites into broad ilmenite bearing areas.

The Surtsey samples contained small skeletal magnetite grains with euhedral segments in the 1 to 10 micron range. With such small size it is difficult to be specific about composition but they appeared to be single phase magnetite except where local oxidation produced red silicates and converted the magnetite to hematite. There was no noticeable maghemite and only rare ilmenite grains.

Results

There was some change in shape of the zero field demagnetization curves after heating, part of which is due to destruction of maghemite. All the samples had higher saturation remanence after heating indicating production of new magnetic oxide. Some representative sets of curves are shown in Figs. 2 and 3. Both techniques gave satisfactory measures of the known field intensity when the eruptions took place. The Thellier method was less satisfactory, partly because of the maghemite present and partly because of an unidentified soft component with a high Curie point. A standard 100 oersted AF demagnetization step was used with each heating

but a more comprehensive demagnetization sequence might have improved the results.

The mean values of intensity obtained were within 10% of the known field (Table 2) even for samples in which changes in zero field thermal demagnetization curves and saturation remanence curves would have led to their rejection of they were ancient samples. The assumed reliability for paleointensity purposes of samples showing high temperature oxidation states could not be tested very well since those samples with high temperature oxidation phases also contained low temperature oxidation phases as well. In the case of the Surtsey samples the reddest and most oxidized sample was S-2 and yet it gave the poorest value of field intensity.

Conclusions

Measures of field intensity obtained from the recent Surtsey and Etna lavas are closer to the known intensity when they were erupted than I had expected. Even samples with appreciable maghemite, and those in which there was a change in the amount of oxide and its coercive force spectrum, gave acceptable results. This is encouraging and suggests that measures of paleofield intensity made on similar lavas by the same methods should give results that can be compared.

Paleomagnetic field intensity values are inherently more variable than are directions. The large scatter among values for a series of lavas suggests that the known four fold intensity variation over the last few thousand years has been present in the past as well. When this is taken into account there are enough measures of intensity to conclude that the intensity of the earth's magnetic field has been similar to the present since early pre-Cambrian time except for the early to middle Paleozoic era when it was much weaker, say 5 to 10% of present (Carmichael, 1968).

Though there are large time gaps in the measured values of intensity in the pre-Cambrian, anyone doing aeromagnetic interpretation in areas where pre-Cambrian rocks are present should never assume that remanence is negligible. In areas where paleozoic rocks are present it would be unusual to find remanent magnetization significant and as a first approximation remanence can be ignored. For areas where there are Mesozoic and Recent rocks remanence should again not be considered negligible.

Acknowledgements. It is a pleasure to acknowledge the assistance of Dr. Sigurgeirsson and the National Research Council of Iceland who made the collection of samples on Surtsey possible. Most of the measurements were made by Mr. Brian McParland whose contribution is acknowledged. The work was supported by a research grant from the National Research Council of Canada.

References

Carmichael, C. M.: The magnetization of a rock containing Magnetite and Hemoilmenite, Geophysics *XXXIX*, 87–92, 1964

Carmichael, C. M.: An outline of the intensity of the paleomagnetic field of the earth. Earth Planet. Sci. Lett. *3*, 351–354, 1968

Palmer, H. C., Carmichael, C. M.: Paleomagnetism of some Grenville province rocks. Can. J. Earth Sci. *10*, 1175–1190, 1973

Smith, P. J.: The intensity of the tertiary geomagnetic field. Geophys. J. *12*, 239–258, 1967

Thellier, E., Thellier, O.: Sur l'intensité du champ magnetique terrestre dans la passe historique et geologique. Ann. Géophys. *15*, 285–376, 1959

C. M. Carmichael
Department of Geophysics
University of Western Ontario
London, Ontario, Canada

J. Geophys. 40, 501–512, 1974

3. Aspects of Rock Magnetism — Oceanic Material

Ferromagnetic Minerals in the Sediment Cores Collected from the Pacific Basin

Kazuo Kobayashi and Masafumi Nomura

Ocean Research Institute, University of Tokyo

Received March 12, 1974

Abstract. The magnetic properties, crystallographic features and chemical composition of ferromagnetic minerals contained in the deep-sea sediment cores from the Pacific Ocean and adjacent seas are examined by means of thermomagnetic analysis, X-ray diffraction, X-ray fluorescence analysis and microscopic observation. It has so far been proved that ferromagnetic constituents of the oceanic sediments, except those of certain depths of the Japan Basin cores, are composed of titaniferous magnetite with or without ilmenite exsolution lamellae. The titaniferous magnetite is classified into three groups, I, II and III according to its bulk Ti-content. The type I is Ti-poor magnetite which originated from the continental granite. The type II is most widespread in the Pacific Basin and may possibly be attributed to the andesitic volcanoes in the island arcs. The origin of type III seems to be the mid-Pacific oceanic volcanoes. None of these three types show any trace of complete recrystallization. It is therefore safely to say that the paleomagnetic records of the deep-sea sediment cores relies upon the DRM of these ferromagnetics. The result also indicates that the type III Ti-rich magnetite can be used as a paleo-geographical indicator of the hot-spots and the mid-oceanic ridges when the longer cores are examined, although no variation of occurrence of ferromagnetics is found in the Pacific cores 10 m long. Occurrence of iron sulfides in some depths of the Japan Basin cores indicates a strongly reducing paleoenvironment of the Sea of Japan during the glacial periods.

Key words: Ferromagnetic Minerals — Pacific Sediment Cores.

Introduction

The present study has been initiated with two principal aims: (1) to determine the origin of natural remanent magnetization of sediment cores and (2) to identify the source of at least a coarse fraction of the deep-sea sediments as well as to presume the sedimentary environment.

It has been known a large fraction of sediments is biogenic. In some shallow seas more than 80 per cent is carbonate composed predominantly of tests of foraminifera and coccoliths. In the sea floor deeper than about 4500 m the biogenic carbonate is dissolved into sea water. The biogenic silicate composed of diatom and radiolaria is also dissolved in the deeper

basins. Content of biogenic material in the sediments is thus dependent upon both the biological productivity and depth of the ocean. Isotope ratio of sediments is largely controlled by the actions of marine organisms. Ferromagnetic minerals are, in contrast, not originated by marine organisms except by one shoal species called Chiton in which magnetite is formed in a part of its teeth (Kobayashi *et al.*, 1963). However, distribution of such magnetite-forming organisms is quite limited and can be neglected in the following consideration.

Nonbiogenic materials in the deep-sea sediments are possibly derived from several sources such as river suspension, turbidity currents, eolian dust, volcanic ash, meteoritic dust and authigenic precipitates. Some of them are transported from the continents, the island arcs, the oceanic volcanoes or the mid-oceanic ridges but the others are formed in their place of occurrence. To judge whether the ferromagnetic constituents are transported fractions or authigenic is of primary importance for the paleomagnetic study of the sediment cores. If they are products of transportation, their natural remanent magnetization is merely the depositional remanent magnetization (DRM). If any chemical or biochemical reaction is involved in the production of ferromagnetics, the natural remanent magnetization of the sediment is suspected to be the chemical remanent magnetization.

In case where most of the ferromagnetics are transported and preserved without any chemical reactions, another important geophysical inference seems possible concerning the relationship between the sediments and their source areas on the basis of the characteristics of the ferromagnetic phase. Ferromagnetic minerals may act as a source indicator in such cases.

Samples

Thirty five deep-sea sediment cores collected by the R. V. Hakuho-Maru in the western and central Pacific Ocean and adjacent seas are examined in the present study. Sampling positions, water depth and core length are summarized in Table 1. Most of them are 4 to 12 m long but a few samples of sediments taken from the bottom surface by dredge haul are also included. From each core 1 to 4 samples of sediment are taken from different levels of the core.

Ferromagnetic minerals are extracted from the sediment samples diluted with water. Size of the extracted minerals ranges between 10μ and 50μ. By this method it is difficult to separate finer ferromagnetics, if any. However, as the saturation magnetization of the residual phase is smaller than original by more than one order of magnitude, it may be said the extracted minerals are responsible for the natural remanent magnetization of the sediment. The following experimental procedures were carried out on this extracted phase.

Table 1. Sampling positions, water depths and lengths of cores examined in the present study

Station No.	Latitude	Longitude	Water Depth (m)	Core Length (cm)
KH67-5-13	09°52′N	149°59′E	5520	*s*[a]
-17	00°00′N	150°05′E	5235	63
-36	11°31′N	177°05′W	5780	*s*
-48	12°17′N	174°16′W	5600	55
-55	15°08′N	170°03′W	5650	58
-57	15°48′N	168°12′W	5220	157
KH68-3- 7	39°20′N	178°01′E	5440	242
-11	44°27′N	171°59′E	5925	565
-15	38°26′N	165°59′E	5492	970
KH68-4- 5	26°51′N	170°01′W	4565	238
-20	02°28′S	170°00′W	5500	992
-22	10°57′S	169°59′W	5110	316
-25	19°59′S	170°02′W	5280	716
-29	25°54′S	170°20 W	5485	918
-31	32°09′S	169°56′W	5550	706
-39	50°07′S	169°59′W	5150	495
-41	54°14′S	169°38′W	5100	322
-49	69°28′S	169°53′W	4200	973
-55	53°14′S	155°12′E	4050	390
KH69-2- 4	37°12′N	144°59′E	5770	1046
-20	43°47′N	138°32′E	3520	1191
-23	41°21′N	134°26′E	3575	1047
-25	40°53′N	132°40′E	3390	1060
KH70-2- 5	38°26′N	170°06′W	5140	1060
- 7	33°11′N	169°54′W	5840	1190
-18	44°02′N	146°00′W	4900	1090
KH72-2- 2	31°46′N	143°59′E	5834	670
- 4	32°31′N	141°31′E	—	*s*
- 6	31°29′N	135°37′E	2930	*s*
-56	21°34′N	132°42′E	5360	745
-58	22°53′N	129°13′E	5340	755
-60	27°49′N	123°49′E	95	*s*
-64	26°54′N	124°15′E	100	*s*
-65	25°29′N	124°49′E	2090	394

[a] Remark: *s* indicates mixed surface sediments collected by dredge haul or similar method.

It is found by microscopic examination that some glassy rock-forming minerals usually coexist with the opaque ferromagnetic phase. The X-ray analyses are therefore conducted after pulverizing the specimens by mortar and pestle and further purifying the ferromagnetic phase.

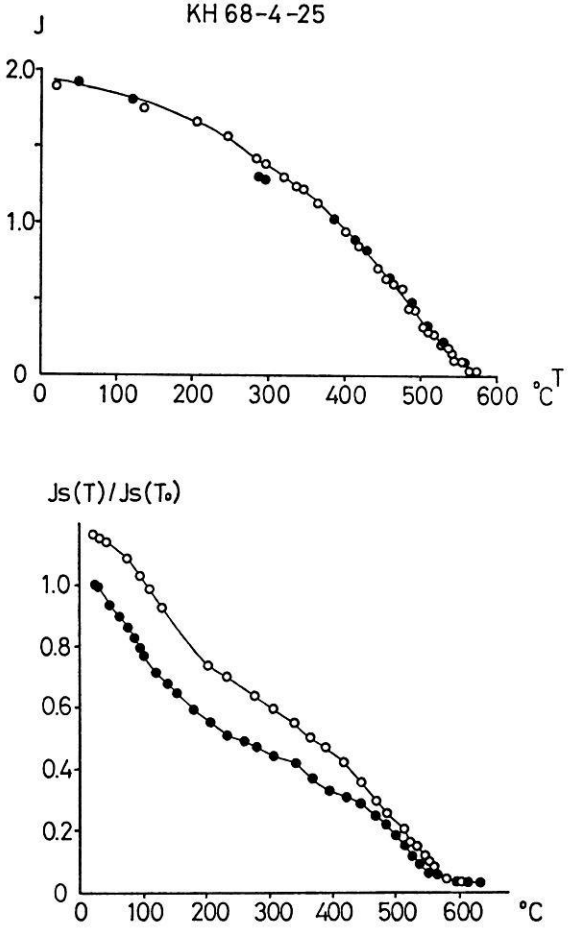

Fig. 1a and b. Thermal changes in saturation magnetization of ferromagnetic phase in sediments in a field of 2400 oe and in vacuum of 10^{-5} torr. Hollow and solid circles indicate heating and cooling, respectively. — a (above) KH68-4-25 — b (below) KH67-5-57

Results of Experiment

1. Thermomagnetic Analysis

Thermal changes of saturation magnetization between 650 °C and ordinary temperatures are measured by means of a magnetic balance in vacuum of 10^{-5} torr. The Curie temperatures of most of the Pacific specimens range from 540 °C to 590 °C (similar to that of stoichiometric

magnetite, 575 °C) and are nearly reversible during a cycle of heating and cooling as shown in Fig. 1(a). In Fig. 1(b) is shown a thermomagnetic curve of a slightly different type with the sediment KH67—5—57 collected on the southern flank of the Wake-Necker Ridge. It has two distinct Curie temperatures at 160 °C and 550 °C. The X-ray diffraction analysis indicates that this phase having the lower Curie temperature is slightly oxidized titaniferous magnetite (cf. Table 3).

The thermal behavior of specimens taken from deeper levels of the cores of the Japan Basin is quite different from that of the other Pacific specimens. The Curie temperature of the original specimens is 370 °C to 390 °C, but at high temperatures the saturation magnetization changes irreversibly and its behavior very much depends upon the atmosphere. This thermal property is often seen with iron sulfides. More detailed descriptions of the Japan Basin cores and their implications have been published elsewhere (Kobayashi and Nomura, 1972). Similar ferromagnetic sulfides have not yet been found in the cores from other areas of the Pacific, although non-ferromagnetic framboidal pyrite is sometimes seen in blue clays and diatom ooze.

2. Crystallographic Analysis by X-Ray Diffraction

The crystal structure of the ferromagnetic minerals is analyzed using an X-ray diffractometer with an Fe target. It is shown that the principal phase has a cubic spinel structure. With this phase the lattice constant a is determined by the angles of the diffracted beams from (422), (333) and (440) lattice planes. The lattice constant of the specimens having the Curie temperature of 540 °C to 590 °C ranges from 8.36 Å to 8.40 Å which corresponds to that of nearly stoichiometric magnetite Fe_3O_4 or slightly oxidized Ti-poor titanomagnetite. The specimens having two Curie temperatures have two cubic phases ($a = 8.36$ Å and 8.42 Å). It is concluded that a phase with $a = 8.42$ Å shows the low Curie temperature (160 °C $\sim$ 230 °C).

The X-ray diffraction patterns indicate that several specimens from the central Pacific contain a phase with the rhombohedral structure which is identified to be nearly stoichiometric ilmenite $FeTiO_3$. Although this phase is not ferromagnetic, it usually occurs as an exsolved lamellae in the ferromagnetic magnetite and cannot be separated due to its fine grain size.

A pseudohexagonal pyrrhotite is identified with specimens from depths of 770—780 cm of the Japan Basin core KH69—2—23. Below these depths pyrite having a cubic spinel structure with $a = 5.42$ Å predominates. It is not known whether this 'pyrite' is ferromagnetic or ferromagnetic pyrrhotite is associated with pyrite but undetected by X-ray analysis, possibly due to its fine grain size and low degree of crystallization.

3. Observation under the Reflection Microscope

The extracted ferromagnetics are molded in epoxy and a surface is polished to examine under the reflection microscope. The ferromagnetic minerals contained in the deep Pacific sediments have an angular shape, while those in sediments of the Japan Basin and the continental shelf are round and smooth. This contrast in shape seems to indicate that the latter are products of erosion and transportation from a continental source.

Round magnetite grains in deep levels of the Japan Basin cores are much sulfurized along the grain surfaces and in cracks. They are usually associated with independent framboidal pyrite grains.

Very fine exsolution lamellae of ilmenite are observed in magnetite grains of some central Pacific sediments and the presence of ilmenite is confirmed by the X-ray diffraction. Such a lamellae structure reduces the effective grain size of the ferromagnetic phase which provides a high magnetic coercive force sufficient for paleomagnetic use of the sediment cores.

4. X-Ray Fluorescence Analysis

Bulk chemical composition of the carefully separated ferromagnetic phase is determined by X-ray fluorescence analysis in respect to the content of Fe. Table 2 gives the mole per cent of each element, Ti, Mn, Cr, Co, Ni, V to the molar content of Fe element. As the content of trace elements other than Ti is negligibly small, the molar ratio of Ti to Fe alone is shown in Table 3. By this method of analysis the total content of Ti is measured when the ilmenite exsolution occurs because such a fine mixture can not at all be separated by the present procedure of separation.

Table 2. Chemical composition of the ferromagnetic minerals determined by the X-ray fluorescence analysis (mole per cent relative to the amount of Fe element)

Core	Sampling level (cm)	Ti	Mn	Cr	V	Co	Ni
KH68-4-25	65-240	10.2	0.64	0.33	1.33	0.92	0.60
KH70-2-18	395-435	10.3	0.66	0.35	0.57	0.45	0.82

It is quite remarkable that the bulk Ti/Fe ratio of the ferromagnetic minerals having ilmenite exsolution (e.g. KH68—4—5, —20, —22) is 20 to 30 % and nearly the same as the Ti/Fe ratio of the specimens showing the low Curie temperature (KH67—5—57, —55). This seems to indicate that both specimens are originated from the same type of magmatic condition but have different histories of temperature and oxygen fugacity after

Table 3. Ferromagnetic minerals in the deep-sea sediments

Station No.	Locality	Sampling Level (cm)	Ti content (Ti/Fe mole %)	Lattice (Å)	Mineral associated	Curie temp. (°C)	Type
KH67-5-13	central equatorial Pacific	0	26.1	8.356	Il	565	III
-17		0-63	9.6	8.379		560	II
-36		0	9.7	8.384		560	II
-48		0-30	—	—		580	II
-55		30-60	18.8	8.413		230 540	III
-57		50-100	24.7	8.416 8.355		160 550	III
KH68-3- 7	northwestern Pacific	25-55	9.7	8.388		580	II
-11		25-75	10.8	8.387		565	II
-15		0-110	9.3	8.384		565	II
KH68-4-5a	central equatorial Pacific	0-50	30.0	8.363	Il	570	III
- 5b		180-230	27.8	8.355	Il	545	III
-20		0-110	26.0	—	Il	560	III
-22		0-60	23.6	8.383	Il	545	III
-25a		0-60	7.4	8.394		550	II
-25b		65-240	11.0	8.387		—	II
-29a		70-135	12.1	8.397		550	II
-29b		800-918	11.8	8.402		545	II
-31		0-520	10.5	8.390		545	II
-39		460-495	21.8	—		585	III
-41	Antarctic Sea, Tasman Sea	40-100	—	—		580	II
-49		20-170	9.1	—		575	II
-55		0-168	11.2	—		555	II
KH69-2- 4a	NW Pacific	495-503	11.3	8.398		540	II
- 4b		850-1040	8.5	8.395		—	II
-20	Japan Basin	0-70	12.1	8.397		570	II
-23a		0-15	4.7	8.368		565	I
-23b		385-395	5.5	8.388		575	I
-23c		985-1025	1.4	8.396 hexagonal	— Prh	— —	I I
-25		440-475	9.9	8.396 5.423	 Py	575 —	I
KH70-2- 5	northeast Pacific	15-395	11.2	—		—	II
- 7		280-395	10.9	8.367		—	II
-18		60-140	10.3	8.393		—	II
KH72-2- 2	NW Pacific	515-600	10.3	8.399		—	II
- 4		0	9.2	8.419		—	II
- 6	Shikoku Basin	0	8.0	8.406		—	II
-56	Philippine Basin	740-745	10.0	8.365		—	II
-58		230-620	7.6	8.390		—	II
-60	E. China Sea	0	5.2	8.396		—	I
-64		0	5.9	8.393		—	I
-65		180-220	8.3	8.392		—	II

Il: ilmenite, Prh: pyrrhotite, Py: pyrite

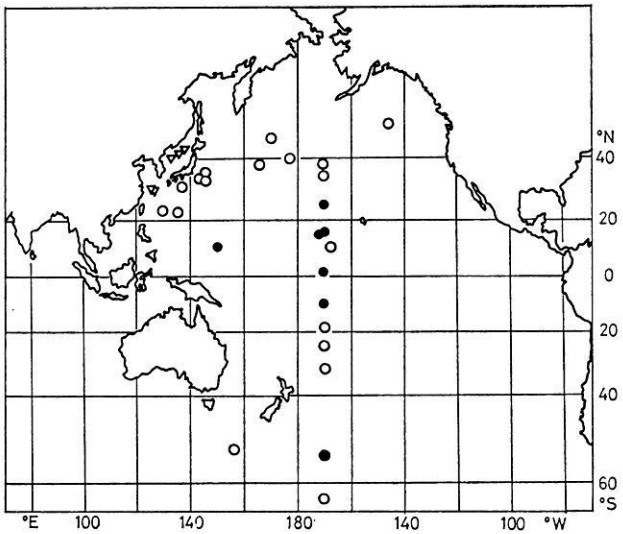

Fig. 2. Geographical distribution of three types of ferromagnetics in the deep-sea sediments. — ▽: type I (Ti/Fe < 6 mole %) — ○: type II (Ti/Fe = 10 ~ 12 mole %) — ●: type III (Ti/Fe = 20 ~ 25 mole %)

solidification. Magnetite with ilmenite exsolution is a product of oxidation at a high temperature, while magnetite having the dual Curie temperatures is formed by a partial oxidation at a low temperature.

Interpretations of Results

As seen in Table 3 which summarizes the results of the present experiment, the ferromagnetic minerals contained in the oceanic sediments can be classified into three groups according to the mole fraction of Ti to Fe: I. Ti-poor magnetite or iron sulfides (Ti/Fe < 6%), II. titaniferous magnetite with Ti/Fe = 10 ~ 12 %, III. titaniferous magnetite with Ti/Fe = 20 ~ 25 % (with or without ilmenite lamellae). Geographic distribution of the three types is shown in a map of Fig. 2.

Except for the cores from the Japan Basin no appreciable vertical variation in Ti content and other characteristics of the ferromagnetics with depths is seen. This result indicates that the sedimentary environment in the Pacific ocean is unchanged throughout the geological periods of the past several million years during which the cores of 10 m in length are deposited.

Buddington and Lindsley (1964) shows that there exists a systematic relationship between the bulk composition of titaniferous magnetite and type of volcanic, hypabyssal, and plutonic rocks. For example, more than

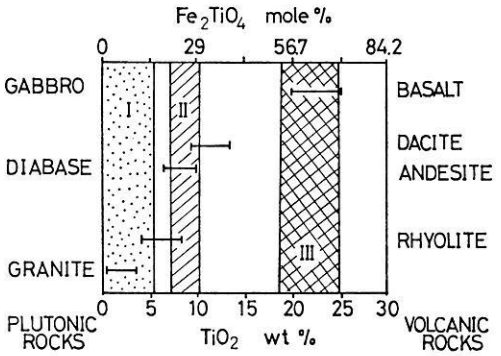

Fig. 3. Relation between rock types and titanium content in iron oxides (modified from Buddington and Lindsley (1964) with titanium content of three types of ferromagnetics, I, II and III

seventy per cent of the analyses of titaniferous magnetite in basalt shows that the weight per cent of TiO_2 ranges from 20 to 25 %, while the weight per cent of TiO_2 in hornblende andesite and granite is 7 to 10 % and 0 to 3 % respectively. Fig. 3. represents the range of composition of titaniferous magnetite in several rocks thus given. The range of composition of the ferromagnetic phase contained in three types of oceanic sediments is also shown. It is clear that the type I ferromagnetic mineral is similar to that in granite, the type II corresponds to that in andesite or rhyolite and the type III is that in basalt.

The occurrence of type I is limited to the continental margins and marginal seas. It seems to indicate that the type I magnetite is a product of erosion and transportation from continental granite. Only the iron sulfides in the Japan Basin are authigenic but none of the others has evidence of secondary alteration. The type III is, on the other hand, found in the mid-Pacific area around the Hawaiian ridge and adjacent oceanic islands. Its occurrence and compositional correlation with basaltic rocks may possibly indicate that its source is oceanic volcanoes. However, the thermomagnetic characteristics are different from those of the seamount rocks and greater fractions of type III minerals have an evidence of high-temperature oxidation but no trace of erosion. It is thus concluded that type III is originated from the pyroclastic falls from active oceanic volcanoes and their secondary deposits along the archipelagic apron. No specimens were taken from the East Pacific Rise but a sample KH68—4—39 near the flank of the Pacific-Antarctic Ridge appears to belong to type III as well.

The type II ferromagnetic minerals are most widely distributed and are found in most of the pelagic sediments. They can be correlated with

andesitic magma and so their origin is possibly the explosive volcanic eruptions of the islands arcs. These often scatter large amounts of fine ash over the ocean. Coarser volcanic shards are distributed only on the east side near the source volcano by the action of the eastward wind. Finer particles with iron oxides are thrown up to great heights in the atmosphere and are scattered over wide areas of the ocean. Such fine fractions do not form distinct layers but occur in any depths of the sediments with roughly constant rates.

The sediments treated in the present study have great variety in color, grain size and composition. However, the occurrence of three types of ferromagnetics is not primarily correlated with kinds of sediments. It may be inferred that the source of the ferromagnetic phase is in some cases independent of other components such as biogenic tests and authigenic clays.

In most parts of the deep basins of the Pacific in which the reddish brown clays predominate, oxidizing conditions prevail. In slightly shallower areas (near the crest of the ridges and seamounts) and in the zones of high biological productivity (around the equatorial upwelling current system and the subpolar regions) the condition at the bottom of the ocean is more reducing and the bluish clays or oozes occurs. The present study shows that all of the three types of titaniferous magnetite are stable or at least metastable and are free from dissolution and recrystallization. The Ti-rich magnetite with low Curie temperature is oxidized and partly altered to titanomaghemite under this condition but the reaction is far from the complete decomposition and dissolution into water. This result indicates that the natural remanent magnetization of these deep-sea sediments is the depositional remanent magnetization (DRM) acquired when the ferromagnetic minerals are eventually fixed in the sediments at one time during or sometime after the deposition.

Spherical ferromagnetic materials which are presumably cosmic or meteoritic spherules are found in the reddish brown sediments from the mid-Pacific area (Crozier, 1960). They are identified to be stoichiometric magnetite with a vacant hole inside (Kitazawa and Kobayashi, 1968). Nickel-iron alloy forming the inner core of the spherule which is often found in the cosmic spherules does not exist in our samples and it is concluded that the phase is dissolved into sea water because the metallic alloy is much more soluble than the oxides. This may be an evidence of the chemical stability of magnetite in the bottom sediments under oxidizing and moderately reducing conditions. It should be noted, however, that relative amounts of such ferromagnetic spherules are very small compared with the terrestrial magnetite (actually only several milligrams of spherules are collected in 1 kilogram of the sediments!) and that the resultant contribution of the cosmic spherules to the paleomagnetic properties of the deep-sea sediments seems to be negligibly small.

The drastic distinction of ferromagnetic constituents between the upper several meters and the lower levels of the cores from the Japan Basin is quite exceptional among the present samples. As already reported by the same authors (Kobayashi and Nomura, 1972), values of pH and redoxpotential measured soon after the cores were raised to the deck of the ship shows that the deeper levels of the cores are very reducing. In such a highly reducing environment magnetite seems to be unstable and to be sulfurized to iron sulfides. Co-existence of magnetite and pyrrhotite is seen only in a highly reducing condition. The reducing condition is caused by the huge supply of organic matter from the land as well as from the surface of the sea. However, the bottom of the present Sea of Japan is very oxidizing due to the action of the oxygen-rich cold water pouring from the northern seas. Therefore, this record of transition in the bottom environment shows that the Sea of Japan was very stagnant probably due to enclosure by land when the sea level was about 120 m lower than the present during the glacial period.

Conclusion and Acknowledgement

From the present study of ferromagnetic minerals in the deep-sea sediments the following may be concluded;

1. Titaniferous magnetite is stable in the environment of the Pacific deep-sea sediment. No evidence of dissolution and complete recrystallization of magnetite is found. Therefore, the natural remanent magnetization of the deep-sea sediments is the depositional remanent magnetization (DRM). This statement is particularly correct with a type of titaniferous magnetite formed by the high temperature oxidation.

2. Titaniferous magnetite in the deep-sea sediments is classified into three types: I (Ti-poor), II (Ti-intermediate), III (Ti-rich). The type I is related to the continental granite, type II to the eruptive activities of the andesitic volcanoes in the island arcs and type III to the mid-Pacific island volcanoes like Hawaii.

3. No changes in the characters of ferromagnetics are found in the 10 m cores except those of the Japan Basin. It indicates that the sedimentary environment and in particular geographic relationship with the source areas have been unchanged in the Pacific basin for several million years. If longer cores collected by the Deep-Sea Drilling Project are examined by the same method, drift of the ocean floor relative to the continents and island arcs may be detected. Study of the paleogeographical relation of ferromagnetics with the oceanic volcanoes would hopefully be very interesting because the location of the ancient activities of the oceanic volcanloes is important in respect to the problem of the hot-spots and mantle plumes. The present result may possibly provide the basic data for such an attempt.

4. Drastic change of ferromagnetic minerals in the cores of the Japan Basin indicates that magnetite is sulfurized into pyrrhotite and pyrite under a strongly reducing condition, as already reported.

The authors are very grateful to the scientific members, officers and crew of the R. V. Hakuho-Maru with which the present cores were collected.

References

Buddington, A.F., Lindsley, D.H.: Iron-titanium oxide minerals and synthetic equivalents. J. Petr. *5*, 310–357, 1964

Crozier, W.D.: Black magnetic spherules in sediments. J. Geophys. Res. *65*, 2971–2977, 1960

Kitazawa, K., Kobayashi, K.: Magnetic and crystallographic investigations of small spherules found in deep-sea sediments. Annual Prog. Rep. Paleogeophys. Res. in Japan 1–8, 1968

Kobayashi, K., Nomura, M.: Iron sulfides in the sediment cores from the Sea of Japan and their geophysical implications. Earth Planet. Sci. Lett. *16*, 200–208, 1972

Kobayashi, K., Tashbook, L.F., Nagata, T.: Magnetism of biochemical magnetite in Polyplacophora (Chitons). Trans. Am. Geophys. Un. *44*, 862, 1963

Kazuo Kobayashi
Masafumi Nomura
Ocean Research Institute
University of Tokyo
Tokyo, Japan

J. Geophys. 40, 513–536, 1974

Oceanic Basalt Magnetic Properties and the Vine and Matthews Hypothesis*

W. Lowrie

Lamont-Doherty Geological Observatory Palisades, New York, USA

Received March 12, 1974

Abstract. Königsberger ratios of DSDP basalts were rather low (mean value around 7) but were usually high enough to justify interpreting oceanic anomalies with a remanent magnetization model. Natural remanent magnetizations were considerably lower than in dredged basalts but were strong enough to account for amplitudes of oceanic magnetic anomalies. Both stable and unstable remanent types were encountered. The observed stable inclinations showed a large scatter when compared to expected inclinations, largely due to non-cancellation of secular variation. All the basalts were categorized in deuteric oxidation Class I by opaque petrology observations. Extensive maghemitization, inferred from thermomagnetic analyses, may explain the low NRM intensities. Unstable specimens easily acquired large viscous remanent magnetizations, in some cases as large as the NRM. The basalt magnetic properties were in general accord with the expectations of the Vine and Matthews hypothesis.

Key words: DSDP Basalt — Paleomagnetism — Magnetic Properties — Viscous Remanent Magnetization — Rock Magnetism.

Introduction

The Vine and Matthews hypothesis (1963) requires certain magnetic characteristics of the basalts which form Layer 2 of the oceanic crust. Prior to the formulation of this hypothesis only a relatively limited amount of information about oceanic basalt magnetic properties was available from dredged samples and the Mohole project (Matthews, 1961; Cox and Doell, 1962; Ade-Hall, 1964). Since then information has been obtained from many more unoriented dredge haul samples (Vogt and Ostenso, 1966; Opdyke and Hekinian, 1967; Luyendyk and Melson, 1967; Carmichael, 1970; Park and Irving, 1970; Irving, Robertson and Aumento, 1970; de Boer, Schilling and Krause, 1970; Schaeffer and Schwartz, 1970; Watkins and Paster, 1971; Fox and Opdyke, 1973) and also from a number of Deep Sea Drilling Project (DSDP) samples (Lowrie and Opdyke, 1972; Lowrie and Opdyke, 1973; Lowrie and Hayes in press; Lowrie, Løvlie and Opdyke,

---

* Lamont-Doherty Contribution No. 2109.

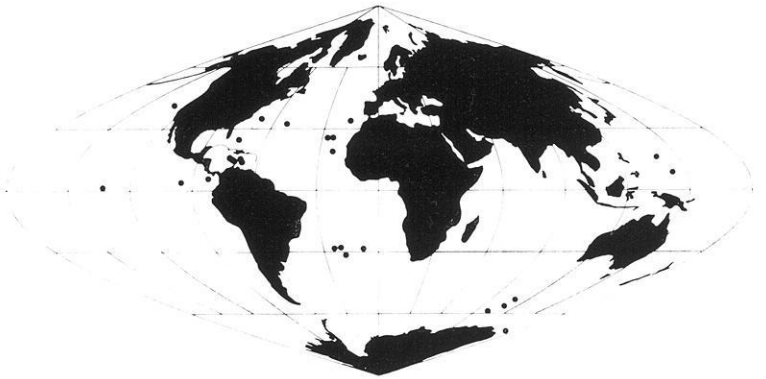

Fig. 1. Locations of the 26 DSDP sites of this study

1973(a), 1973(b)) and other drilled samples (Brooke, Irving and Park, 1970; Ade-Hall, Aumento, Brooke, McKeown, Ryall and Gerstein, 1973). The DSDP basalt collection has certain advantages over the dredged samples; the samples are semi-oriented, in that the vertical direction is known relative to each sample, which permits the inclination of remanent magnetization to be measured. Also, deep sea drilling has been carried out in many deep ocean basins, whereas dredged samples have been obtained only from restricted regions, such as seamounts, fracture zones and ridge crests. The fairly extensive DSDP and dredged collections now allow comparison of the observed magnetic properties with the requirements of the Vine and Matthews hypothesis.

The primary basalt characteristics required for validity of the hypothesis are: (a) the basalt magnetization should be dominated by the remanent component, that is the Königsberger ratio (Q_n) should be much greater than 1.0, (b) the remanent intensity (J_r) should be strong enough to account for the amplitude of the observed anomalies, and (c) the polarity of the remanence should correspond to the sign of the anomaly in which the sample was taken. These in turn require that the remanence should be stable enough to preserve the original magnetization direction over geologic periods of time and through subsequent polarity changes of the geomagnetic field. The magnetic inclinations should also agree with those expected after appropriate plate reconstructions have been made. This leads to the subsidiary but important requirement that significant secondary magnetization components which might alter the original remanent magnetization should not be present.

DSDP basalts from a representatively large number of sites have now been studied. The magnetic properties of basalts from 26 DSDP sites are described here. The site locations (Fig. 1, Table 1) are fairly well distributed

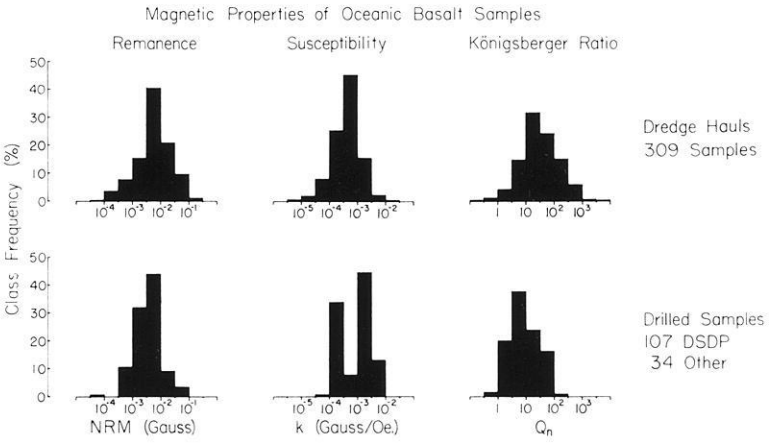

Fig. 2. Histograms of natural remanent magnetization intensity, susceptibility and Königsberger ratio in dredged and drilled oceanic basalt samples

among the world's oceans. There are notable gaps in the Indian Ocean and Central and South Pacific Oceans. However the latitudinal distribution of the 26 sites is good.

The distribution of samples among the sites is not entirely adequate (Table 1). Several samples were obtained from most sites, but some sites are represented by only a single sample. Three or four partially oriented small specimens were obtained and their magnetic properties averaged to give representative values for each sample.

Remanent Magnetic Properties

Histograms of the natural remanent magnetization (NRM), the susceptibility (k) and the Königsberger ratio (Q_n) of 309 dredged samples and 141 drilled samples (107 from DSDP sites) are shown in Fig. 2. For both collections the NRM intensities cover a wide range of almost three orders of magnitude. The (geometric) mean NRM intensity of the dredged basalts is almost double that of the DSDP basalts (Table 2). Although NRM intensity may occasionally vary by an order of magnitude within a given site, most of the variation expressed in the histograms is between-site variation. The mean susceptibility of the dredged basalts is less than half that of the DSDP basalts. Within-site variation is generally not as large as for the NRM intensity. Again, however, there is considerable between-site variation.

The differences in these parameters between the two collections are probably real and reflect differences in the sampling distributions. The distribution of dredge haul sites is naturally biassed to regions where basement

Table 1. DSDP site locations, ages, number of samples and specimens, and basalt descriptions from Initial Reports

Site	Location		Age (my)	Number of Samples	Number of Specimens	Flow or Sill	Basalt Description
10	32.6°N	52.3°W	Miocene	6	20	Sill	Fresh, ophitic, vesicular
14	28.3°S	21.0°W	Eocene (39)	3	9	Sill	Weathered, cryptocrystalline to fresh, fine-grained
15	30.9°S	18.0°W	Miocene (21)	1	3	Flow	Fresh, aphanitic
18	28.0°S	8.0°W	Oligocene (25)	2	7	Flow	Weathered, aphanitic
19	28.5°S	23.7°W	Eocene (53)	4	14	Flow	Weathered, aphanitic, vesicular
36	41.0°N	130.1°W	Miocene (8–13)	3	7	Flow	Fresh, glassy
54	15.6°N	140.3°E	Miocene	3	6	Flow	Hydrothermally altered, variolitic
57	8.7°N	143.5°E	Oligocene	7	15	Flow	Fresh, doleritic
77	0.5°N	133.2°W	Oligocene (36)	1	8	Sill	Fresh, fine-grained, vesicular
83	4.0°N	95.7°W	Miocene (11)	1	3	Sill	Fresh, fine-grained
84	5.8°N	82.9°W	Miocene (7–9)	1	9	Sill	Fresh, fine-grained

100	24.7°N	73.8°W	Oxfordian (150)	9	9	Flow	Fresh, fine-grained
105	34.9°N	69.2°W	Oxfordian	14	14	Flow	Altered, fine-grained
136	34.2°N	16.3°W	Aptian (108)	4	6	Flow	Altered, subophitic to intergranular diabase
137	25.9°N	27.1°W	Albian (101)	3	4	Flow	Altered, brecciated with glassy groundmass
138	25.9°N	25.6°W	Cenomanian (105–110)	6	8	Sill	Altered at top, coarse-grained
141	19.4°N	24.0°W	Miocene	5	8	—	Altered (serpentinized)
146	15.1°N	69.4°W	Turonian (87–91)	12	12	Flow	Fresh, doleritic
150	14.5°N	69.4°W	Coniacian (84–87)	3	3	Sill	Fresh, doleritic
151	15.0°N	73.4°W	Santonian (80–84)	2	2	Flow	Fresh, fine-grained, vesicular
152	15.9°N	74.6°W	Campanian (72–80)	3	3	Flow	Weathered, vesicular
153	14.0°N	72.4°W	Turonian (87–91)	3	3	Sill	Fresh, fine-grained, amygdaloidal
265	53.5°S	109.9°E	Miocene (12–15)	2	8	Flow	
266	56.4°S	110.1°E	Oligocene	2	5	Flow	
267	59.3°S	104.5°E	Eocene	1	2	Sill	
274	69.0°S	173.4°E	Eocene	4	17	Flow	

Table 2. Geometric mean values, by samples and by sites, of the natural remanent magnetization (NRM) intensities, susceptibilities (k) and Königsberger ratios (Q_n) in 309 dredged basalt samples and 107 DSDP basalt samples

	Number	Geometric Mean Values		
		Natural Remanent Magnetization (10^{-3} G)	Susceptibility (10^{-3} G/oe)	Königsberger Ratio
Sample Means				
DSDP	107	2.73	1.06	6.06
Dredge-hauls	309	5.37	0.408	29.0
Site Means				
DSDP	26	2.06	0.632	7.92
Dredge-hauls	110	5.76	0.318	39.9

rocks crop out. The DSDP collection does not suffer from this restriction; coverage is more extensive areally over the ocean basins and samples often are obtained at depths from the sediment-basalt interface to several meters below it. The dredge collection probably represents younger and fresher crustal rock, and may also have finer grain sizes than the DSDP collection. This would account for the higher remanence and lower susceptibility of the dredge-hauled material.

The DSDP susceptibility distribution was bimodal. The lower mode resulted principally from unusually low susceptibilities measured in DSDP basalts from the South Atlantic Ocean (Lowrie, Løvlie and Opdyke, 1973(a)) which also had much lower than average NRM intensities.

The Königsberger ratios of the DSDP basalts were much lower than in the dredged samples (Fig. 2); the mean value for dredged basalts was five times larger than for DSDP basalts (Table 2). Nevertheless the DSDP mean value of 6—8 was sufficiently high that in most cases the remanence was the dominant magnetization component, and induced magnetization effects could be neglected However, the existence of a large number of oceanic basalt samples with Q_n close to, or less than, unity indicates the need to consider the perturbing effects of induced magnetizations on anomaly profiles in some regions.

The data show that either the common choice of Layer 2A magnetization of 0.01—0.02 Gauss in anomaly modelling (*e.g.* Herron, 1972) is too high or the magnetic properties of the oceanic basalts dredged and drilled to date represent only the surface skin of Layer 2 and are unrepresentative

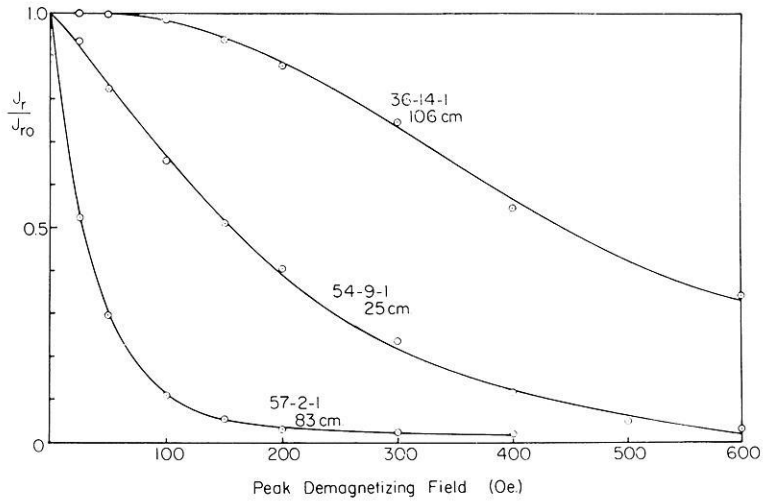

Fig. 3. Variation of remanent intensity during alternating field demagnetization of typical DSDP basalt specimens

of the whole layer. The thickness of the strongly magnetized part of Layer 2 is usually taken to be 500 m (Talwani, Windisch and Langseth, 1971), but if the results of this study are in fact representative, Layer 2A must have at least double this thickness. Resolution of this point must await the analysis of material from the deeper holes planned for future deep sea drilling.

Stability of Magnetization

Storage tests of only a few weeks showed that most, but not all, of the DSDP basalts had stable magnetizations. Detailed alternating field (AF) demagnetization was carried out on every specimen to establish its stable direction of magnetization.

AF Stability of Remanent Intensities

AF demagnetization curves for some representative specimens are shown in Fig. 3. Most specimen demagnetization curves were similar to those of the site 36 or site 54 specimens, but some revealed the presence of large components of low coercivity magnetization as in the case of the site 57 specimen. There was not much variation in magnetic hardness between specimens from the same site. Median destructive fields in the range 200–400 oe. were representative of the largest number of sites (Fig. 4). However, at many sites the median destructive field was much lower, often less than 100 oe.

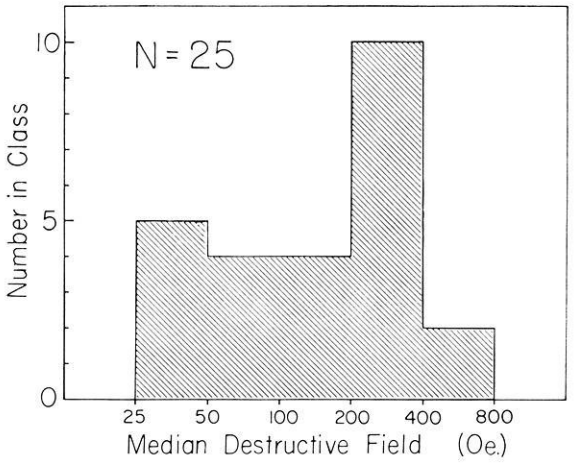

Fig. 4. Geometric mean values of median destructive field at 25 DSDP sites

AF Stability of Remanent Directions

Vector diagrams show the effects of AF demagnetization on the horizontal and vertical components of magnetization in specimens with stable and unstable remanences (Fig. 5). As the peak alternating field is progressively increased there is little variation in either declination or inclination in the specimen from site 77. The stable negative inclination of this site is well defined. The unstable magnetization of the site 57 specimen shows large directional changes as the initial soft component is removed. The stable inclination for this site was only defined for fields between 100 and 250 oe; after treatment in 300 oe. or higher the magnetization became so unstable that it changed even during the time required to make a measurement. It was often not possible to measure quite strongly but unstably magnetized specimens with a 105 Hz spinner magnetometer due to rapid growth or decay of the signals, yet the same unstable magnetizations could be measured satisfactorily with a 5 Hz spinner magnetometer. The large soft component of magnetization apparently could be influenced easily by the stresses involved in spinning them at 105 Hz, which amount to around 444 g at a radius of 1 cm from the rotation axis.

It was possible to define without difficulty a stable direction for specimens whose median destructive fields were greater than 200 oe. For less stable specimens the direction taken was the average of the fairly closely grouped directions in the 100—200 oe. AF demagnetization range. A mean inclination for each site was found by averaging the sample inclinations, which in turn represented the averages of individual specimen inclinations. Each mean was corrected to compensate for the absence of declinations (Briden and Ward, 1966).

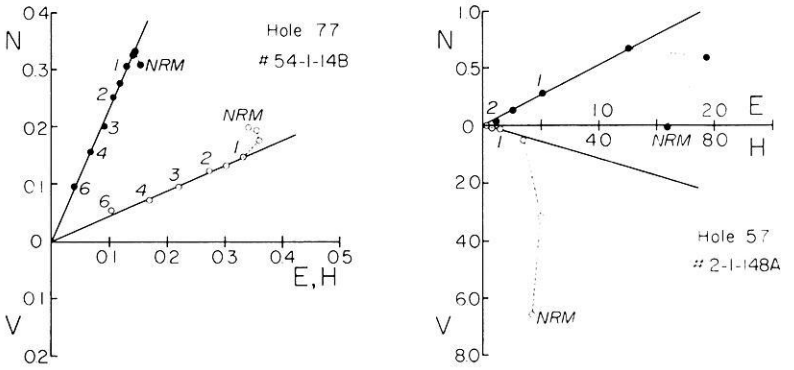

Fig. 5. Vector diagrams representing AF demagnetization of stable and unstable remanences in DSDP basalts

Site Mean Remanent Inclinations

At many sites one or more samples had opposite polarity to the others from the site. This was caused by orientation error resulting from the difficulty of unambiguously orienting the core samples on board ship. It presented a serious problem at sites where only one or two samples were obtained. The polarities observed in the basalts agreed with the anomalies at each site where they were known. For further analysis of the site inclinations, all reversed site mean inclinations were converted to their normal equivalents.

The expected inclinations at the sites were deduced from the following sources. For Legs 2, 3, 11 and 14 in the Atlantic Ocean the global plate reconstructions of Phillips and Forsyth (1972), which incorporate paleomagnetic data from Africa, Europe and North and South America, were used to determine the site paleolatitude at the time of its formation. From this the axial dipole field (ADF) inclination at the site was computed. The ADF inclinations of Leg 15 specimens (Lowrie and Opdyke, 1973) were computed from the Phillips and Forsyth model and also from Cretaceous paleomagnetic data of Creer (1970), Watkins and Cambray (1970), and MacDonald and Opdyke (1972).

Good estimates of the expected inclinations for sites from Legs 5, 6 and 9 in the Pacific Ocean are not possible because of the scarcity of relevant high quality terrestrial paleomagnetic data for the ages involved (Oligocene to Miocene). Tertiary North Pacific pole positions were used for sites 36, 57, and 77; N. American Miocene pole positions for sites 83 and 84, and Taiwan and Ryuku poles for site 54 in the Philippine Sea (McElhinny, 1973).

Paleomagnetic virtual pole positions from the Antarctic continent (McElhinny, 1973) do not differ appreciably from the present pole of

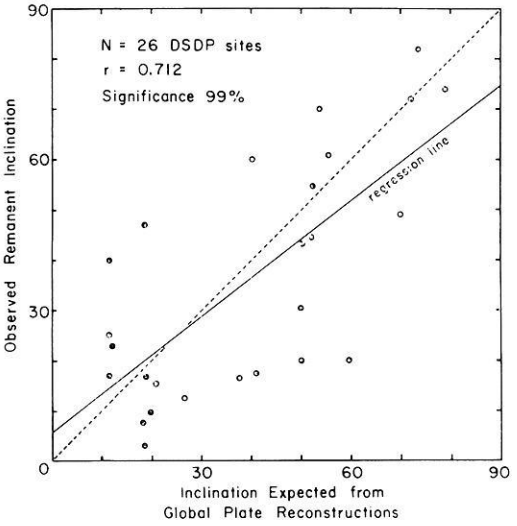

Fig. 6. Comparison of observed site mean remanent inclinations with their expected values

rotation. The formation of the South Indian Ocean is assumed to have taken place by migration of Australia away from a fixed Antarctic plate (Weissel and Hayes, 1972). Expected mean inclinations for Leg 28 sites are therefore assumed to be the ADF inclinations at the sites.

A plot of the site mean remanent inclinations observed in the basalts from the 26 sites of this study against the values expected from the above calculations shows a large amount of scatter (Fig. 6). The correlation (coefficient $r=0.715$) is moderately strong and is significant. It is also superior to correlations of the observed inclinations with the present ADF site inclinations ($r=0.625$) and the 1965.0 IRF ($r=0.525$). In spite of the observed scatter there is statistical agreement between the observed site mean inclinations of DSDP basalts and the inclinations expected from global plate considerations.

The deviation between observed and expected inclinations at any given site varied from 0° at site 266 to as much as 40° at site 36; the mean (absolute) deviation was 14°. Sixteen remanent inclinations were shallower than expected, nine were steeper while one was in exact agreement. The regression line consequently has a lower slope than the line of perfect agreement (Fig. 6). The deviation may result from errors associated with both the expected and observed inclinations. For example, the computations of expected inclination are inexact, involving several stages of approximation. Either the expected inclination is computed directly from the

average of a small quantity of relevant paleomagnetic data, or it results from best-fit paleolatitudes determined by determining average VGP locations and combining these with plate rotations about suitable rotation axes.

There are several possible sources of error in the observed remanent inclinations. Sampling errors in this type of study are greater than in a normal paleomagnetic study largely as a result of inexact determination of the true vertical direction for each sample of core. Other factors which might disturb the observed remanence values are post-magnetization tilting of crustal blocks and the effects of secondary magnetizations, which will be discussed further below.

It is probable, however, that the discrepancies can largely be accounted for by secular variation effects. Due to the rapid cooling undergone by oceanic basalts, many of which have chilled outer crusts, their remanent magnetizations will be acquired in the direction of the ambient geomagnetic field, without averaging to zero the effects of secular variation as might be the case in more slowly cooling igneous bodies. Creer (1962) has shown that within-site dispersions as large as the inclination deviations observed here can result from secular variation of the dipole and non-dipole fields.

Magnetic Mineralogy

Opaque Petrology

Polished sections of several specimens were made for reflected light study using oil immersion lenses giving magnifications up to 1100 diameters.

Opaque minerals were identified by their colors, anisotropy and birefringence. Observations made on Atlantic and Pacific Ocean specimens (Lowrie, Løvlie and Opdyke, 1973(a), 1973(b)) are summarized in Table 3.

The opaque minerals consisted of homogeneous titanomagnetites (or titanomaghemites) with lesser amounts of ilmenite and sulphides (such as pyrrhotite). The titanomagnetite grains were generally finer than 10μ. Some specimens contained coarser grains which on close optical examination showed whitened areas along cracks and on their rims indicative of maghemitization. Most specimen grain sizes were finer than 10μ, and contained a large number of visible grains finer than 1μ in size. It is distinctly likely that an even finer submicroscopic fraction, below the resolution of optical techniques, exists in these specimens. Electron microscope studies have shown large populations of discrete titanomagnetite grains much finer than 0.1μ in diameter in oceanic basalts from the mid-Atlantic ridge (Evans and Wayman, 1972).

Table 3. Opaque petrology descriptions of basalts from Atlantic Ocean and North Pacific Ocean DSDP sites (from Lowrie, Løvlie and Opdyke, 1973(a), 1973(b)).

Site	Description of grains			Volume % Ore Minerals	Degree of Maghemitization
	Titanomagnetites	Ilmenites	Other ore Minerals		
10	Euhedral, 1μ—5μ; skeletal, ($10\mu \times 30\mu$) Large grains non-uniformly magnetized	Euhedral and skeletal, $\sim (3\mu \times 50\mu)$	Some fine sulfides ($<2\mu$) Some chromite	$1^1/_2$—$2^1/_2$%	Moderate (10% by volume)
14	Very fine, 1μ—3μ homogeneous grains	None identified	Some sulfides, some chromite	$2^1/_2$—3%	None observed
15	Skeletal, 2μ—6μ Largest grains non-uniformly magnetized	A few euhedral grains $\sim (3\mu \times 25\mu)$	Sulfides (<5% of total ore minerals)	3%	Slight; on largest grains
18	Some large euhedral grains, most very fine ($<1\mu$)	A few skeletal grains, $\sim (10\mu \times 10\mu)$	A few sulfides	1%	Slight; on largest grains
19	A few large skeletal grains ($\sim 10\mu$), non-uniformly magnetized 60%—95% are $<5\mu$	None identified	None identified	1%	None observed
36	Fine, skeletal, $<5\mu$; uniformly magnetized	Some euhedral grains; rods $\sim (5\mu \times 20\mu)$	Some sulfides, ($<1\mu$)	1—2%	None observed
54	Skeletal, ($<5\mu$) and skeletal, 10μ—60μ	A few rods with hematite rims	Some sulfides	2%	None observed
57	Large, skeletal; 50% are $<10\mu$; 50% are 10μ—200μ	Large rods, often with magnetite	Pyrrhotite, $<1\mu$ to 10μ (10% of total ore)	3—6%	None observed
77	Anhedral, $<5\mu$; some euhedral and anhedral grains, 10μ—40μ	Rods, ($1\mu \times 10\mu$) to ($5\mu \times 40\mu$)	Relics of chromite	3—6%	Slight; on largest grains
83	Anhedral and skeletal $<10\mu$ and 40μ—60μ	Needles, $<5\mu$ thick	Sulfides ($<10\mu$)	2—5%	On largest grains
84	Fine skeletal and anhedral grains, $<5\mu$ Color suggests no alteration	None identified	Sulfides, $<10\mu$ to 20μ (10% of total ore). Chromite relics	1—5%	None observed

The rate at which low-temperature oxidation of the original magnetic mineralogy takes place depends upon the specific surface area and the presence of lattice imperfections (Colombo, Fagherazzi, Gazzarini, Lanzavecchia, and Sironi, 1968). Consequently, the finest grains in an assemblage will be affected by low-temperature oxidation more seriously than coarser grains, and opaque petrological observations made on relatively coarse grains may be inapplicable to finer grains, particularly those below the limit of optical resolution. It is probable that optical techniques are inadequate to describe the degree of maghemitization of fine-grained oceanic basalts. Bulk thermomagnetic analysis provides a suitable alternative technique.

Thermomagnetic Analysis

By rapidly heating basalt specimens in a vacuum to temperatures in excess of 600 °C it has been shown possible to distinguish titanomagnetite from titanomaghemite as the dominant ferrimagnetic mineral (Ozima and Ozima, 1971). When thermomagnetic analysis is carried out in air the same unambiguous interpretation is not possible, but it is possible by using properties of the parent and daughter products of the analysis to identify titanomaghemite (Lowrie, Løvlie and Opdyke, 1973(b)).

The thermomagnetic curve in air of oceanic basalt containing either titanomagnetite or titanomaghemite is irreversible (Ozima and Ozima, 1971). A typical example is shown in Fig. 7(a). The initial magnetization (J_i), produced in a strong field of 3000 oe. or more, decreases on heating rapidly past its initial Curie temperature, which is usually in the range 100—400 °C. When the specimen is heated beyond this stage the original mineral separates into a Ti-rich phase (hemo-ilmenite) and a Ti-poor phase close in composition to magnetite. On cooling from high temperature the stronger magnetization of this magnetite appears at a high Curie temperature, and increases to its room temperature value (J_f). This is greater than the initial value, provided the specimen is not maintained too long at or above 600 °C. This can cause oxidation of the magnetite product, and results in J_f being less than J_i.

Strong-field thermomagnetic curves were measured in air with three sets of Curie balance; a horizontal motion type (University of Bergen), and automatically recording, vertical motion types corrected for specimen weight loss (University of Pittsburgh, and Lamont-Doherty Geological Observatory). Magnetizations were uncalibrated; temperature measurement accuracy was 5 °C.

For titanomagnetites ($xFe_2TiO_4 \cdot (1—x)Fe_3O_4$) the composition parameter, x, which defines the ulvospinel proportion in the titanomagnetite, determines the initial Curie temperature. After phase separation the mag-

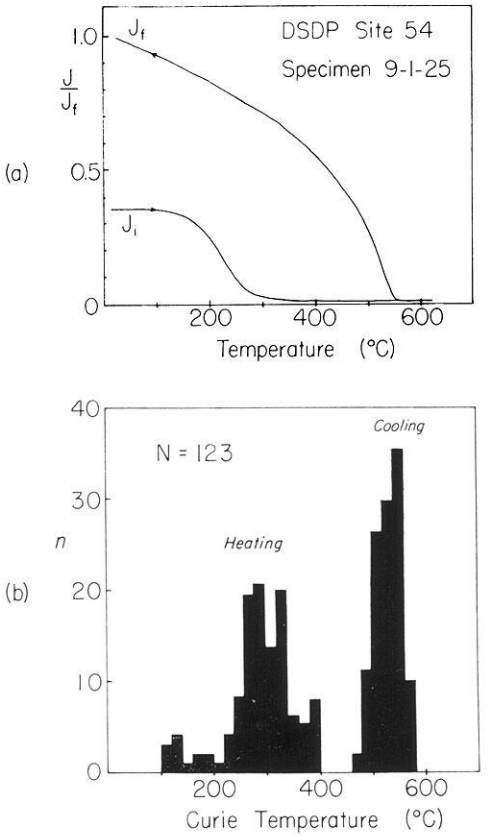

Fig. 7 a. Typical thermomagnetic curve in a DSDP basalt. b Curie temperatures of the initial and final magnetic minerals from thermomagnetic analyses of 123 DSDP basalt specimens

netite end-member should have an x-value of around 0.05 (Kawai, Kume and Sasajima: in Nagata, 1962). The mean of the higher Curie temperatures measured in 123 thermomagnetic analyses of DSDP basalts (Fig. 7(b)) was 530 °C, corresponding to a mean $x = 0.085$ (Nagata, 1962). The initial Curie temperatures of these specimens were mainly between 220 °C and 400 °C, with a small group lower than 200 °C corresponding to specimens from site 57.

The room-temperature strong field magnetization, J_f, of the near-magnetite product mineral may be computed according to its known dependence on x (Nagata, 1962). The magnetization of the initial titanomagnetite, J_i, may then be expressed in terms of the final mineral by using the measured ratio (J_i/J_f) from the thermomagnetic curves. The titano-

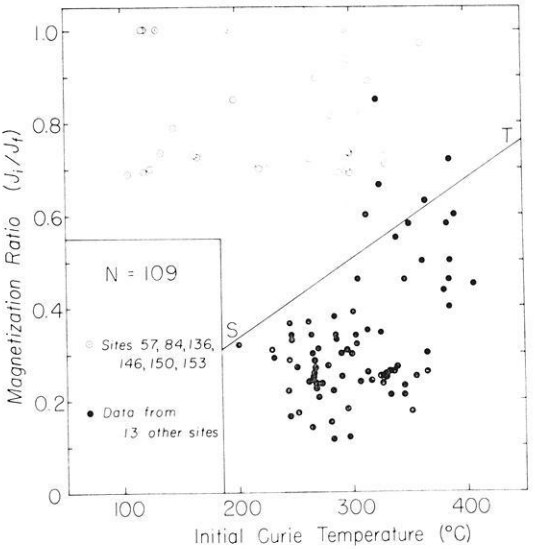

Fig. 8. Ratios of initial to final magnetizations and the initial Curie temperatures in thermomagnetic analyses of 109 DSDP basalt specimens

magnetite magnetization J_i and its initial Curie temperature are related by the compositional parameter x. It is therefore possible to determine the exact relationship between (J_i/J_f) and initial Curie temperature for a stoichiometric titanomagnetite. For the range of x observed in oceanic basalts this is the straight line S—T in Fig. 8. The magnetization ratios, J_i/J_f, observed in 109 DSDP specimens (50 samples; 19 sites) are plotted against the initial Curie temperature of the specimen. Thermomagnetic analyses in which the magnetite product was apparently oxidized have been excluded from these considerations.

There are several reasons why the points in Fig. 8 do not lie on the line S—T. Firstly, the volume of the product magnetite is likely to be less than that of the initial titanomagnetite, as a Ti-rich phase also exsolves. Because of this volume change the observed magnetization ratio should be greater than the ratio of the spontaneous magnetizations; stoichiometric titanomagnetites should be represented by points above the line S—T. Secondly, partial high temperature oxidation of the magnetite formed will reduce J_f, and will give a point above the line. This will also happen if incomplete phase separation takes place. Each of these effects displaces a point above the line S—T in Fig. 8.

If the initial titanomagnetite is non-stoichiometric, the point will fall below the line. Maghemitization causes elevation of the Curie temperature and reduction of the spontaneous magnetization (Ade-Hall, Palmer and

Hubbard, 1971; Readman and O'Reilly, 1972). Each of these displaces a point below the line S—T. However, if the magnetite product is oxidized at high temperature, J_i/J_f will be increased and the point may fall in the upper field. It is, therefore, not possible to discuss without ambiguity the original condition of the titanomagnetites from sites 57, 84, 136, 146, 150 and 153 (Fig. 8) all of which are represented by points in the upper field.

It is quite apparent from these data, however, that oceanic basalts from a large majority of the 19 DSDP sites studied are maghemitized. Points from 13 sites fall almost entirely in the lower field, with only a small number near or above the separating line. If volumetric change could be taken into account, the position of line S—T would be even higher on the figure.

It may be concluded from these thermomagnetic studies that maghemitization, whether resulting from ocean-floor weathering (Marshall and Cox, 1972) or regional hydrothermal alteration (Ade-Hall, Palmer and Hubbard, 1971), may have altered considerably the original magnetic properties of the basalts. It is unlikely, even if chemical remanent magnetization (CRM) is associated with the oxidation, that the original directions will have been appreciably altered (Marshall and Cox, 1972), although this may possibly contribute to the observed discrepancies between observed and expected inclinations (Fig. 6). The reduction in remanent intensity which accompanies the maghemitization (Johnson and Merrill, 1973) has been proposed as an explanation for the observed decrease of magnetic anomaly amplitude with distance from the axis of a mid-ocean ridge (Irving, 1970). The proposal is supported by the results of this study.

Viscous Remanent Magnetization

Acquisition of VRM

Although most DSDP basalt specimens were found to be quite stable, specimens from several sites showed significant changes in direction during storage tests in the geomagnetic field, and had median destructive fields lower than 100 oe. The large soft components in these specimens made them very susceptible to the acquisition of viscous remanent magnetization (VRM).

VRM was given to many specimens with median destructive fields lower than 150 oe. The specimens were first demagnetized, their remanences were measured, and they were placed in a uniform constant field for up to 3 months. At repeated intervals the remanent magnetization was measured with a spinner magnetometer, each observation time (less than 5 minutes) being much shorter than the time of acquisition, t. The increase in magnetization over the $t=0$ value represented the acquired VRM. Typical VRM acquisition curves are shown in Fig. 9.

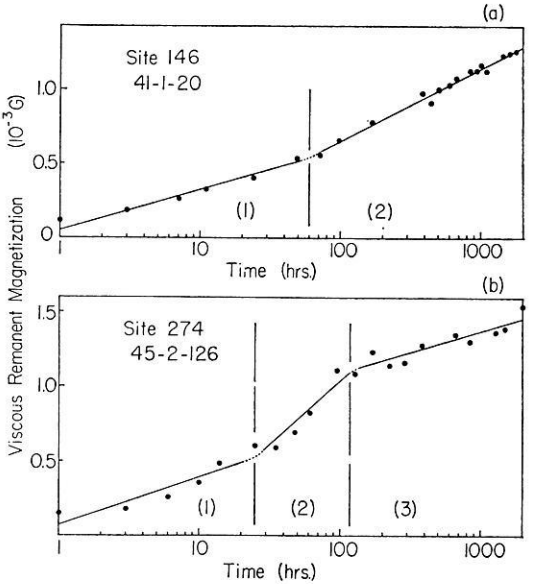

Fig. 9. a Two-stage and b three-stage acquisition of viscous remanent magnetization

The acquired VRM at time t can be expressed

$$\mathrm{VRM}(t) = S(t) \log t$$

where $S(t)$ is the magnetic viscosity coefficient.

Two general types of acquisition curve have been observed in DSDP basalts (Fig. 9). The first, and most commonly observed, consists of two stages in each of which the magnetic viscosity coefficient is a constant. The second type shows three-stage development of VRM. The magnetic viscosity coefficients in the first and third stages (S_1 and S_3, respectively) are considerably smaller than in the second stage (S_2; Table 4). It is possible that the two-stage type might develop into a three-stage type if the observations were continued beyond the three month duration of each of these experiments.

Origin of the VRM

Logarithmic development of VRM may result from either a multidomain process or one involving fine particles whose size places them close to the boundary between superparamagnetic and single domain behavior at room temperature. This fine-grain VRM would necessarily involve a narrow range of particle sizes with appropriate magnetic relaxation times.

Table 4. Acquisition of viscous remanent magnetization in DSDP basalts. Site 57 specimens acquired VRM in 0.53 oe. field; all other acquisitions were in 1.0 oe. field. VRM_{1000} is the VRM acquired in 1000 hours; S_1, S_2 and S_3 are the measured magnetic viscosity coefficients in three stages of the acquisition (see text). NRM intensity, susceptibility and median destructive field (m.d.f.) represent the initial remanent properties of the specimens

Site	Specimen	Natural Remanent Magnetization (10^{-3} G)	Susceptibility (10^{-3} G/oe)	Median Destructive Field (oe)	S_1 (10^{-3} G)	S_2 (10^{-3} G)	S_3 (10^{-3} G)	VRM_{1000} (10^{-3} G)	$\frac{VRM_{1000}}{NRM}$ (%)
57	2–1– 83	4.20	1.93	28	0.19	0.32	—	0.83	20
	2–1–113	2.43	2.35	47	0.14	0.39	—	0.92	38
	2–1–148A	6.85	2.05	29	0.15	0.32	—	0.79	12
	2–1–148C	3.15	1.96	102	0.19	0.28	—	0.75	24
	2–2– 48	6.85	1.58	35	0.13	0.30	—	0.73	11
	2–2– 60	3.32	1.42	49	0.09	0.35	—	0.79	24
	2–2–149	2.81	2.25	29	0.15	0.39	—	0.93	33
	3–1– 12	2.57	1.71	34	0.17	0.35	—	0.87	34
100	11–1– 20	16.04	3.76	74	0.43	0.72	0.50	1.83	11
	11–1–100	23.69	3.16	94	—	0.51	—	1.51	6
	11–1–125	6.18	3.59	61	0.54	0.95	0.62	2.49	40
105	42–2– 5	3.53	1.46	156	0.16	0.51	0.11	0.68	19
	42–2– 38	1.07	2.84	84	0.36	0.66	0.19	1.34	124
	42–2– 71	3.09	2.40	120	0.25	0.63	0.23	1.18	38
	42–2–105	3.21	2.17	129	0.21	0.71	0.24	0.98	31
	42–2–121	1.43	2.59	79	0.39	1.13	0.36	1.55	108
	42–2–147	3.27	1.87	144	0.26	0.59	0.16	0.91	28
136	9–1– 4	15.20	3.47	15	0.16	0.44	—	1.07	7
	9–1– 14	8.06	2.86	48	0.14	0.49	—	0.99	123
	9–1– 34	8.86	3.53	41	0.20	0.84	—	1.84	21

137	17–1– 65	2.43	0.81	89	0.04	0.05	—	0.14	6
138	7–1– 68	3.60	3.07	92	0.08	0.13	—	0.38	11
	7–1– 79	3.17	2.71	105	0.04	0.12	—	0.26	8
	7–1–120	0.49	0.68	66	0.02	0.04	—	0.10	21
	7–1–145	2.14	2.69	34	0.12	0.22	—	0.56	26
141	10–1– 97	4.14	0.92	141	0.02	0.06	—	0.15	4
	10–1– 99	3.17	1.02	139	0.04	0.08	—	0.18	6
	10–1–110	1.63	1.09	113	0.05	0.10	—	0.20	12
146	41–1– 20	2.65	2.35	41	0.28	0.49	—	1.13	43
	41–2– 2	1.21	2.91	36	0.27	0.37	—	1.13	93
	42–2– 70	2.81	2.38	56	0.42	0.71	—	1.75	62
	42–3–148	2.78	2.48	35	0.42	0.76	—	1.72	62
	43–2–123	5.93	2.37	34	0.27	0.54	—	1.39	23
	43–3– 73	3.79	2.53	42	0.47	0.71	—	1.75	46
	43–4–130	4.98	2.47	39	0.49	0.67	—	1.76	35
150	11–2– 65	3.92	1.83	50	0.23	0.66	—	1.39	36
	12–1–132	6.64	1.98	65	0.32	0.66	—	1.40	21
	12–2–125	4.69	2.06	64	0.37	0.66	—	1.46	31
151	14–1–118	5.84	1.59	110	0.08	0.14	—	0.56	10
	15–1–148	1.96	1.36	117	0.08	0.15	—	0.39	20
152	23–1–112	2.38	3.54	102	0.17	0.34	—	0.75	31
	24–1– 68	1.68	3.33	127	0.13	0.33	—	0.58	35
	24–2– 75	8.32	3.46	96	0.12	0.29	—	0.57	7
153	19–1–118	8.81	3.45	41	0.33	0.76	—	1.53	17
	20–1–147	5.88	3.28	52	0.27	0.70	—	1.39	24
	20–2– 82	3.52	3.02	40	0.33	0.72	—	1.55	44
274	44–1– cc	2.74	1.45	81	0.21	0.56	0.18	1.32	48
	44–3– cc	2.22	1.54	61	0.23	0.86	0.18	1.78	84
	45–1– cc	12.33	1.57	98	0.07	0.44	0.08	0.94	8
	45–2– 2	12.19	1.27	115	0.21	0.63	0.26	1.37	11

Because of the relatively large magnetic moments associated with the grains, fine particle VRM should be stronger than multidomain VRM acquired under equivalent conditions (Dunlop, 1973).

The close similarity between the magnetic coefficients S_1 and S_3 suggests that they represent the same process. Stage 1 VRM (and stage 3, when present) may represent multidomain behavior. However, true multidomain behavior in pure magnetite only exists in particles larger than 17 μ in size (Parry, 1965). In titanomagnetites or titanomaghemites the critical grain size is even larger. Most titanomagnetite grains observed in polished sections of these basalts (Table 3) are much finer than this so true multidomain behavior is unlikely. Possibly the VRM is associated with pseudo-single domain particles (Stacey, 1962) which should be common in the range of opaque mineral grain sizes observed in oceanic basalts.

Superposed on this pseudo-single domain or multidomain VRM is the stage 2 process, which is not activated until after a threshold interval of 10—50 hours. This may be associated with fine particles between single domain and superparamagnetic sizes. The superparamagnetic (relaxation time $< 10^2$ sec) to single domain threshold grain size is 0.052 μm in titanomagnetite ($x = 0.4$) and 0.108 μm if it is non-stoichiometric (Readman and O'Reilly, 1972). Development of a superparamagnetic fraction (defined by relaxation times shorter than the unusually large but geologically reasonable limit of 1000 years) has been shown to be possible in oceanic basalts as a result of maghemitization (Butler, 1973) Because of the known fine grain size determined optically for many of these DSDP basalts and the reported presence of discrete submicroscopic titanomagnetites in oceanic basalts (Evans and Wayman, 1972) it seems likely that the stage 2 VRM acquisition is associated with a narrow range of very fine grain sizes close to the room-temperature superparamagnetic-single domain transition threshold, possessing relaxation times of the order of a few days.

Implications of VRM

The seriousness of VRM in the DSDP basalt specimens studied may be seen by comparing the intensity of VRM acquired in 1,000 hours (VRM_{1000}) in a 1 oe. field with the intensity of NRM in the same specimen (Table 4). In a few specimens this VRM_{1000} exceeded the original NRM intensities and in half of the specimens it amounted to over 30 % of the NRM; in 18 % of the specimens the VRM_{1000} was less than 10 % of the NRM intensity. Considerable variation of the fraction (VRM_{1000}/NRM) occurred among specimens from the same site.

These data were obtained only for specimens with median destructive fields below 150 oe. As yet no data have been obtained for specimens from sites with more stable remanent characteristics. However, because of their

higher median destructive fields and the general absence of significant changes during preliminary storage tests, it is unlikely that VRM could amount to more than a few percent of the NRM in such specimens. Also, most of the VRM were acquired from the demagnetized state. It is not expected that the ability to acquire VRM depends upon the state of remanence in such fine grained basalts. However, the acquisition of VRM in different remanent states, and in high m.d.f. specimens, is currently being investigated.

It may be concluded from these studies that, although VRM is probably not a significant component of the NRM of stably magnetized specimens, in low m.d.f. specimens it may amount to a large percentage of the original NRM.

The low m.d.f. sites are located primarily in regions where linear magnetic anomaly patterns are absent or poorly developed (e.g. Carribbean Sea, E. and W. Atlantic margins, Southeast Indian Ocean margin). Remagnetization of the oceanic crust by VRM acquisition would cause deterioration of any original anomaly pattern. This characteristic has been offered as an explanation of magnetic quiet zones (Lowrie, 1973). The mineralogical or textural properties that give rise to this viscous magnetic behavior are thought to result from unusual conditions during initial continental rifting (Irving, 1970).

Conclusions

The natural remanent magnetizations of most DSDP basalts from regions with well developed linear magnetic anomaly patterns were in good accord with the expectations of the Vine and Matthews hypothesis (1963). The remanence was much greater than the magnetization that could be induced in the basalts by the ambient geomagnetic field, although the Königsberger ratios were considerably lower than those measured in dredged basalts. The NRM intensities were large enough to give observed magnetic anomaly amplitudes, but the magnetic anomalies must be attributed to a thicker magnetized layer than the 500 m usually assumed in model studies.

The remanent polarities agreed with the signs of local magnetic anomalies at all sites where such survey information was available. The stable remanent inclination at individual sites commonly was appreciably different from the value expected at the site. However, in spite of the large scatter there was good statistical agreement between observed and expected inclinations when compensation was made for global plate motions. The discrepancies were attributed largely to non-cancellation of secular variation effects.

Optical petrology and thermomagnetic analyses indicated that all of the DSDP basalts studied belonged to class I of the deuteric oxidation scheme of

Wilson and Watkins (1967). Extensive maghemitization appeared to be present in basalts from a majority of the sites investigated. Although the chemical remanent magnetization associated with the maghemitization probably could not account for the inclination discrepancies, it may be the principal reason for the rather low remanences found in the DSDP samples.

Although most samples had good stability against alternating field demagnetization and in storage tests, a significant proportion had large soft components. These acquired viscous remanent magnetization so readily that large fractions of the NRM could be developed in only a few weeks in the laboratory.

Acknowledgements. I wish to thank Dr. M. D. Fuller and Dr. K. Storetvedt for the use of their Curie balances. Many of the thermomagnetic analyses were performed by Mr. R. Løvlie, who also made the opaque petrology observations. Constructive criticisms of the manuscript by Dr. N. D. Opdyke, Dr. R. Larson, Mr. D. V. Kent and Mr. Løvlie are gratefully acknowledged. The research was supported by National Science Foundation grant GA 30569 and by Office of Naval Research grant N00014-67-A-0108-0004.

References

Ade-Hall, J.M.: The magnetic properties of some submarine oceanic lavas. Geophys. J. *9*, 85–92, 1964

Ade-Hall, J.M., Palmer, H.C., Hubbard, T.P.: The magnetic and opaque petrologic response of basalts to regional hydrothermal alteration. Geophys. J. *24*, 137–174, 1971

Ade-Hall, J.M., Aumento, F., Brooke, J., McKeown, D.L., Ryall, P.J.C., Gerstein, R.: The mid-Atlantic ridge near 45°N: XII. Magnetic results from basalt drill cores from the median valley. Can. J. Earth Sci. *10*, 679–696, 1973

Briden, J.C., Ward, M.A.: Analysis of magnetic inclination in borecores. Pure Appl. Geophys. *63*, 133–152, 1966

Brooke, J., Irving, E., Park, J.K.: The mid-Atlantic ridge at 45°N: XIII. Magnetic properties of basalt bore core. Can. J. Earth Sci. *7*, 1515–1527, 1970

Butler, R.F.: Stable single-domain to superparamagnetic transition during low-temperature oxidation of oceanic basalts. J. Geophys. Res. *78*, 6868–6876, 1973

Carmichael, C.M.: The mid-Atlantic ridge near 45°N: VII. Magnetic properties and opaque mineralogy of dredged samples. Can. J. Earth Sci. *7*, 239–256, 1970

Colombo, U., Fagherazzi, G., Gazzarini, F., Lanzavecchia, G., Sironi, G.: Mechanism of low-temperature oxidation of magnetites. Nature *219*, 1036–1037, 1968

Cox, A., Doell, R.R.: Magnetic properties of the basalt in hole EM7, Mohole Project. J. Geophys. Res. *67*, 3997–4004, 1962

Creer, K.M.: The dispersion of the geomagnetic field due to secular variation and its determination for remote times from paleomagnetic data. J. Geophys. Res. *67*, 3461–3476, 1962

Creer, K.M.: A paleomagnetic survey of South American rock formations. Phil. Trans. Roy Soc. London *A267*, 457–558, 1970

de Boer, J., Schilling, J.G. and Krause, D.C.: Reykjanes ridge: implications of magnetic properties of dredged rock. Earth Planet. Sci. Lett. *9*, 55–60, 1970

Dunlop, D.J.: Theory of the magnetic viscosity of lunar rocks. Rev. Geophys. Space Phys. *11*, 855–901, 1973

Evans, M.E., Wayman, M.L.: The mid-Atlantic ridge near 45°N: XIX. An electron microscope investigation of the magnetic minerals in basalt samples Can. J. Earth Sci. *9*, 671–678, 1972

Fox, P.J., Opdyke, N.D.: Geology of the oceanic crust: Magnetic properties of oceanic rocks. J. Geophys. Res. *78*, 5139–5154, 1973

Herron, E.M.: Sea-floor spreading and the Cenozoic history of the East Central Pacific. Geol. Soc. Am. Bull. *83*, 1671–1692, 1972

Irving, E.: The mid-Atlantic ridge at 45°N: XIV. Oxidation and magnetic properties of basalt; review and discussion. Can. J. Earth Sci. *7*, 1528–1538, 1970

Irving, E., Robertson, W.A., Aumento, F.: The mid-Atlantic ridge near 45°N: VI. Remanent intensity, susceptibility and iron content. Can. J. Earth Sci. *7*, 226–238, 1970

Johnson, H.P., Merrill, R.T.: Low-temperature oxidation of a titanomagnetite and the implications for paleomagnetism. J. Geophys. Res. *78*, 4938–4949, 1973

Lowrie, W.: Viscous remanent magnetization in oceanic basalts, Nature *243*, 27–29, 1973

Lowrie, W., Hayes, D. E.: Magnetic properties of oceanic basalt samples. Initial Reports of the Deep Sea Drilling Project, vol. *28*, U.S. Government Printing Office, Wash-ington, D. C., in press

Lowrie, W., Opdyke, N.D.: Paleomagnetism of igneous samples. Initial Reports of the Deep Sea Drilling Project, vol. *14*, pp. 777–784, U.S. Government Printing Office, Washington, D.C., 1972

Lowrie, W., Opdyke, N.D.: Paleomagnetism of igneous and sedimentary samples, Initial Reports of the Deep Sea Drilling Project. vol. *15*, pp. 1017–1022 U.S. Government Printing Office, Washington, D.C., 1973

Lowrie, W., Løvlie, R., Opdyke, N.D.: The magnetic properties of Deep Sea Drilling Project basalts from the Atlantic Ocean. Earth Planet. Sci. Lett. *17*, 338–349, 1973(a)

Lowrie, W., Løvlie, R., Opdyke, N.D.: Magnetic properties of Deep Sea Drilling Project basalts from the North Pacific Ocean. J. Geophys. Res. *78*, 7647–7660, 1973(b)

Luyendyk, B.P., Melson, W.G.: Magnetic properties and petrology of rocks near the crest of the mid-Atlantic ridge. Nature *215*, 147–149, 1967

MacDonald, W.D., Opdyke, N.D.: Tectonic rotations suggested by paleomagnetic results from Northern Colombia, South America. J. Geophys. Res. *77*, 5720–5730, 1972

McElhinny, M.W.: Paleomagnetism and Plate Tectonics. 358 pp. Cambridge University Press, 1973

Marshall, M., Cox, A.: Magnetic changes in pillow basalt due to sea-floor weathering. J. Geophys. Res. *77*, 6459–6469, 1972

Matthews, D.H.: Lavas from an abyssal hill on the floor of the N. Atlantic ocean. Nature *190*, 158–159, 1961

Nagata. T.: Magnetic properties of ferrimagnetic minerals of Fe-Ti-O system, Proc. Benedum Symposium, pp. 69–86, Univ. Pittsburgh Press, 1962

Opdyke, N.D., Hekinian, R.: Magnetic properties of some igneous rocks from the mid-Atlantic ridge. J. Geophys. Res. *72*, 2257–2260, 1967

Ozima, M., Ozima, M.: Characteristic thermomagnetic curve in submarine basalts. J. Geophys. Res. *76*, 2051–2056, 1971

Park, J. K., Irving, E.: The mid-Atlantic ridge near 45°N: XII. Coercivity, secondary magnetization, polarity, and thermal stability of dredged samples. Can. J. Earth Sci. *7*, 1499–1514, 1970

Parry, L. G.: Magnetic properties of dispersed magnetite powders. Phil. Mag. *11*, 303–312, 1965

Phillips, J. D., Forsyth, D.: Plate tectonics, paleomagnetism and the opening of the Atlantic. Geol. Soc. Am. Bull. *83*, 1579–1600, 1972

Readman, P. W., O'Reilly, W.: Magnetic properties of oxidized (cation-deficient) titanomagnetites (Fe, Ti, □)$_3$ O$_4$. J. Geomagn. Geoelectr. *24*, 69–90, 1972

Schaeffer, R. M., Schwarz, E. J.: The mid-Atlantic ridge near 45°N: IX. Thermomagnetics of dredged samples of igneous rocks. Can. J. Earth Sci. *7*, 268–273, 1970

Stacey, F. D.: A generalized theory of thermoremanence, covering the transition from single domain to multi-domain magnetic grains. Phil. Mag. *7*, 1887–1900, 1962

Talwani, M., Windisch, C., Langseth, M. G., Jr: Reykjanes ridge crest: A detailed geophysical study. J. Geophys. Res. *76*, 473–517, 1971

Vine, F. J., Matthews, D. H.: Magnetic anomalies over oceanic ridges. Nature *199*, 947–949, 1963

Vogt, P. R., Ostenso, N. A.: Magnetic survey over the mid-Atlantic ridge between 42°N and 46°N. J. Geophys. Res. *71*, 4389–4411, 1966

Watkins, N. D., Cambray, F. W.: Paleomagnetism of Cretaceous dikes from Jamaica. Geophys. J. *212*, 163–179, 1970

Watkins, N. D., Paster, T. P.: The magnetic properties of igneous rocks from the ocean floor. Phil. Trans. Roy. Soc. London *A 268*, 507–550, 1971

Weissel, J. K., Hayes, D. E.: Magnetic anomalies in the southeast Indian Ocean, Antarctic Oceanology II, The Australian-New Zealand Sector, Antarctic Res. Ser. Vol. *19*, (editor D. E. Hayes), pp. 165–196, AGU Washington, D.C., 1972

Wilson, R. L., Watkins, N. D.: Correlation of petrology and natural magnetic polarity in Columbia plateau basalts. Geophys. J. *12*, 405–424, 1967

W. Lowrie
Lamont-Doherty Geological Observatory
of Columbia University
Palisades, New York 10964, USA

J. Geophys. 40, 537–548, 1974

Magnetic Properties and Mineralogy of Exposed Oceanic Crust on Macquarie Island

S. K. Banerjee, R. F. Butler*, and J. H. Stout

Department of Geology and Geophysics, University of Minnesota

Received April 20, 1974

Abstract. Comparison of magnetic properties of young dredged pillow lavas with pillow lava and doleritic dyke samples from Macquarie Island shows several interesting contrasts. The NRM intensities of Macquarie Island pillow lavas range from 0.8 to 6.3×10^{-3} gauss in contrast to the 10^{-2} gauss intensities observed in young dredged pillow basalts. AF demagnetization curves also indicate a low stability of NRM in the Macquarie Island pillow lavas. Thermomagnetic analysis confirms that the diminished NRM intensity and AF stability of these late Tertiary pillow basalts is the result of low temperature oxidation. Doleritic dyke samples show NRM intensities only slightly lower than the Macquarie Island pillows. AF demagnetization indicates that the NRM of the doleritic dykes is much more stable than that of the pillow basalts. Thermomagnetic analysis, optical microscopy, and microprobe data indicate that fine-grained magnetites within host feldspar crystals are the important magnetic minerals in the dolerites. The primary metamorphism of these dykes on emplacement has not affected the host feldspar or the magnetite grains. These observations suggest that the contribution of pillow lavas to marine magnetic anomalies will decrease with age whereas the contribution from underlying dyke swarms will remain essentially constant.

Key words: Remanent Magnetization — AF-Stability — Zoned Plagioclase — Magnetic Needles — Pillow Lavas — Doleritic Dykes — Macquarie Island — Ophiolites — Ocean Crust — Magnetic Anomalies.

1. Introduction

Global plate tectonic models strongly depend on data from marine magnetic anomalies. However, even though the Vine-Matthews hypothesis can explain adequately the origin of marine magnetic anomalies (Vine and Matthews, 1963), it is generally accepted that the Vine-Matthews model is only a first approximation. Hence, considerable work is being done to characterize more fully the source rocks which produce marine magnetic anomalies in order that we can correctly interpret their less well-understood characteristics. Several specific observations which are yet to be fully ex-

* Present address: Department of Geosciences, The University of Arizona, Tucson, Arizona 85721, USA.

plained are: (a) the large central anomalies observed in some spreading centers, (b) the so-called quiet zones of unusually small anomaly amplitudes and (c) the total absence of anomalies from certain parts of the world's oceans.

There are three approaches to the problem of identifying the relative contributions of the different rock-types in the oceanic crust to the observed marine magnetic anomalies: (1) the study of dredge-hauls from the crest of actively spreading ridges, (2) the study of short cores of basalts recovered from the JOIDES deep sea drilling program and (3) the study of sub-aerially exposed ancient oceanic crusts or ophiolites. The first approach has been utilized by Carmichael (1970), Irving (1970), Marshall and Cox (1971, 1972). Their work has resulted in characterizing the magnetic and petrologic properties of young (less than 10 million years old) pillow lavas which comprise the upper layer of young oceanic crust. The intensities of natural remanent magnetization (NRM) and Koenigsberger ratios indicate that a relatively thin (<1 km thick) layer of pillow basalts could account for the amplitude of marine magnetic anomalies if the NRM intensities do not decrease with depth or age. However, it was also clearly shown by the above workers that the fine-grained titanomagnetite minerals, which are the magnetic carriers in the fresh pillow lavas, are extremely susceptible to low temperature (<200 °C) oxidation under marine conditions. Thus it is not at all clear whether pillow lavas older than a few tens of million years could still be the predominant contributors to the anomalies.

The study of JOIDES basalts by Lowrie (1973) has shown that the upper basalt layer of ancient oceanic crust is much less strongly magnetized than are young dredged basalts. Also the JOIDES basalts frequently show the the property of acquiring large unstable viscous remanent magnetizations (VRM). This property would not be expected for the source-rocks of stable marine magnetic anomalies. These undesirable properties of JOIDES basalts along with the limited depth penetration inherent in the drilling technique make it reasonable to question whether the JOIDES program alone will result in an adequate model of the oceanic crust to be used in explaining the marine magnetic anomalies.

A third approach, as exemplified by the present work, is to search for present day sub-aerial occurrences of ancient oceanic crust, also known as ophiolite complexes. Such an approach was pioneered by Vine and Moores (1972) when they studied the NRM and Koenigsberger ratios of various rock types from the ophiolite sequence exposed at the Troodos massif in Cyprus. Our work on the ophiolites from Macquarie Island in the Southern Ocean (54°15′S, 159°E) presents a more detailed rock magnetic and petrologic investigation with the same ultimate purpose. We have chosen this island over other known ophiolite occurrences (e.g., Papua, California or Newfoundland) because of the relatively young age ($\sim$29 million years)

and the relatively mild tectonic disturbance suffered by the island during its uplift and eventual exposure (Varne and Rubenach, 1972). Both of the above facts suggest that the rock-types exposed at Macquarie Island are representative of Tertiary oceanic crustal material.

Field geological, petrological and geochemical investigations of Macquarie Island by Varne *et al.* (1969) and by Varne and Rubenach (1972) show a blockfaulted ophiolite sequence of pillow lavas, basaltic and doleritic dyke swarms, gabbroic intrusives and mafic and ultramafic rocks, similar to the observations of Moores (1969) in Greece and of Gass and Sweming (1973) in Cyprus.

The average chemical composition and trace element abundances of representative samples from Macquarie Island agree with those of forty samples dredged from the mid-Atlantic ridge. Marine magnetic anomalies to the west of the island are associated with the Australia-Antarctica ridge and in fact, anomaly 7 (age: approximately 29 million years) approaches the island from the west. This east-west trend of the marine magnetic anomalies parallels the dominant east-west strike of the dyke swarms in the central portion of the island. Paleontological evidence agrees with the above age of the island and also points to the island having once been submerged to a depth of 2000—4000 m. We believe, therefore, that Macquarie Island does indeed belong to the Indian plate and that the oceanic crust represented by the island was originally formed at the actively spreading Australia-Antarctic ridge. Subsequent interaction of the Pacific and Indian plates along the Macquarie Ridge complex has resulted in the sub-aerial exposure of the island.

2. *Magnetic Properties*

To date we have studied mostly hand samples and a preliminary report on the magnetic properties has been published elsewhere (Butler and Banerjee, 1973). A field-trip to Macquarie Island in December, 1973 has resulted in a large collection of oriented samples of the different lithologies. These are under study at the time of this writing. Here we shall concentrate on two rock-types only, pillow lavas and dyke-swarm rocks (predominantly dolerites). The contrasting magnetic properties of these two rock-types will be highlighted and in the next section, some unusual petrological observations in the dykes will be correlated with the magnetic properties.

The pillow samples ranged from 0.8 to 6.3×10^{-3} gauss (emu cm^{-3}) in their NRM values. These NRM intensities are almost two orders of magnitude lower than the strongly magnetized fresh pillows dredged from the mid-Atlantic ridge at 45°N (Irving, 1970). A second characteristic difference between these pillows and the dredged samples is shown in their alternating field (AF) demagnetization curves. (Fig. 1 shows the AF-

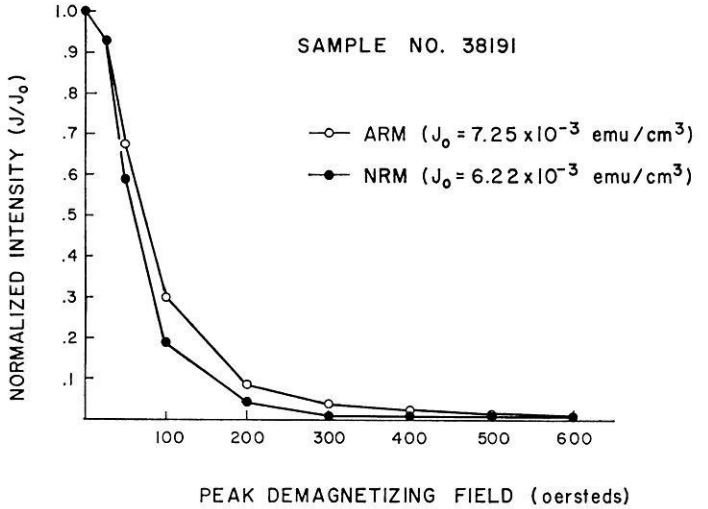

Fig. 1. AF demagnetization of pillow lava sample. Median destructive force of NRM was only 60 oersted

demagnetization curves of the NRM and ARM (anhysteretic remanent magnetization) of sample no. 38191 from Macquarie Island. The median destructive field of the NRM is seen to be only 60 oersted in contrast to a few hundred oersted for the NRM of the dredged samples. Thus, these 29 million year-old pillow lavas are both much weaker in their NRM intensity and also much less stable than their younger counterparts. An explanation for this has already been provided in the various chemical and physical models for the alteration of pillow lavas at the sea-floor (Irving, 1970; Butler, 1973; Banerjee, 1971). The most important of the alteration effects must be low temperature oxidation or titanomaghemitization, which produces metastable cation-deficient titanomaghemite phases. On reheating in the laboratory, irrespective of the ambient oxygen fugacity, such oxidized pillows become thermally unstable and exsolve into a titanium-rich ilmenohematite phase and an iron-rich titanomagnetite phase. In Fig. 2 we observe the magnetic evidence of such an exsolution process. Sample 38193, a pillow lava sample shows an increase in saturation magnetization as a function of annealing time (10 minutes) at 350 °C and 450 °C in a vacuum of 10^{-6} torr. The irreversible increase in magnetization is directly attributable to the formation of an iron-rich titanomagnetite phase with a Curie point near 500 °C at the expense of the original cation-deficient titanomaghemite phase which had a Curie point of about 350 °C.

Fig. 3. shows an AF demagnetization curve of a representative dyke sample (No. 112). For this sample the median destructive field of the NRM and

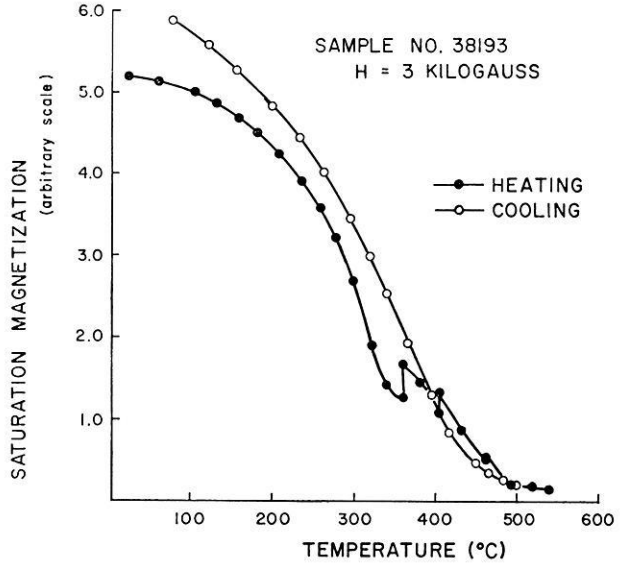

Fig. 2. Saturation magnetization versus temperature for pillow lava sample. Heating was done in vacuum of 10^{-6} torr and 3 koe magnetizing field. The vertical lines in the heating curve at 360° and 405°C show the effects of holding the sample at this temperature for 10 min. An initial Curie temperature of 350°C on heating was followed by a higher Curie point (~500°C) and an increase in room temperature saturation magnetization

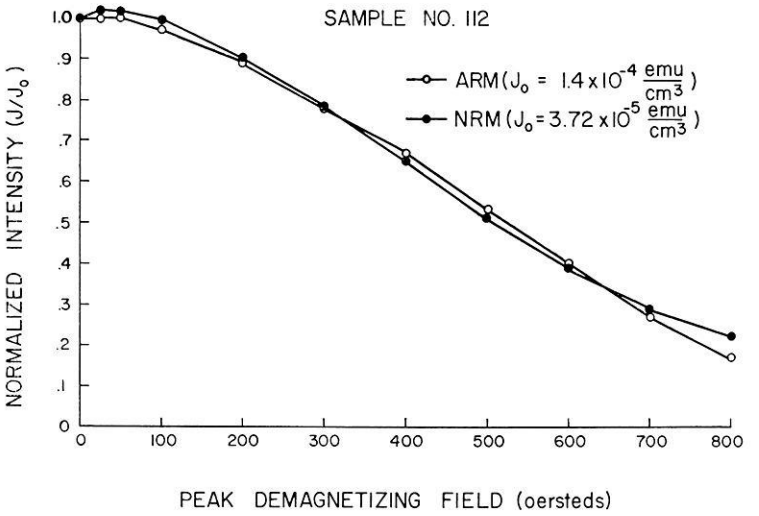

Fig. 3. AF demagnetization curve of doleritic dyke sample. Median destructive force of NRM was ~525 oersted

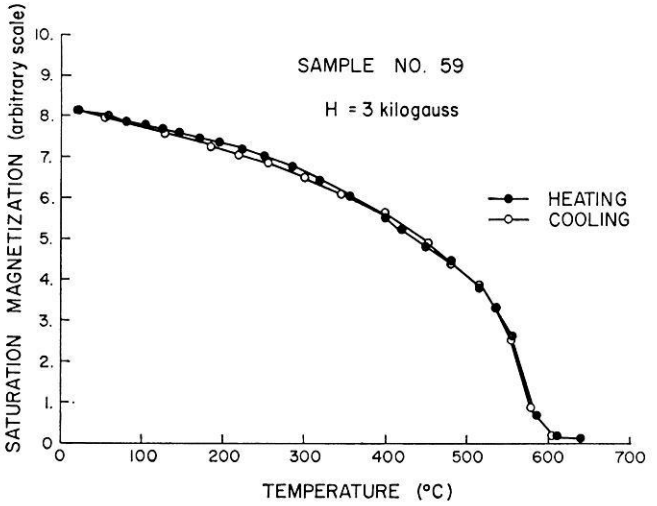

Fig. 4. Saturation magnetization versus temperature for doleritic dyke sample. Heating was done in vacuum of 10^{-6} torr and magnetic field of 3 koe. Coincident heating and cooling curves and Curie point of 580°C were observed

ARM of the dyke sample is 525 oersted, almost a factor of 9 greater than the corresponding figure for the pillow lava sample discussed previously. The intenstiy of NRM of this dyke was 0.4×10^{-4} gauss. However, NRM intensities up to 2×10^{-3} gauss were observed in other dyke samples. Thus, the basaltic and doleritic dyke layer of the oceanic crust may be an important contributor to marine magnetic anomalies. The similarity between the NRM and ARM demagnetization curves for both the dyke sample and the pillow sample attest to the primary nature of the NRM. The strong AF-stability of the NRM of the dyke samples makes them excellent carriers for stable magnetic anomalies on a geological time-scale. This is in marked contrast to the poor behavior seen in the oxidized pillow lavas. An explanation for the high stability is seen in the thermomagnetic curve shown in Fig. 4 for another dyke sample (no. 59). The heating and cooling curves are identical showing a Curie point (580 °C) corresponding to pure magnetite. It would appear from the magnetic data, therefore, that the carriers of NRM in the dyke samples are fine-grained magnetite and are less subject to wholesale chemical alteration than the titanomagnetites of the pillow lavas. This tentative conclusion is confirmed by reflected light microscope and electron-microprobe data discussed in the next section.

3. Optical and Microprobe Data

Petrographic and electron microprobe examination of 4 samples from dyke swarms has revealed a wide range of metamorphism. Sample no. 59

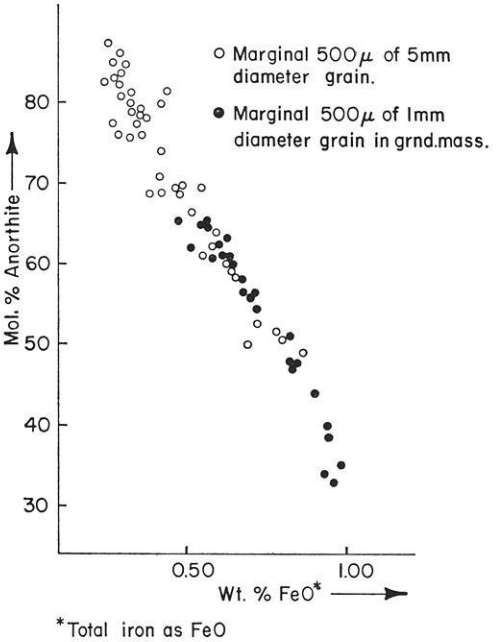

Fig. 5. Anorthite content versus weight percent FeO in plagioclase feldspar from dyke swarm sample no. 63. Intensities of CaK_α and FeK_α radiation were monitored simultaneously at each 5μ diameter spot chosen for analysis. Analyses were done on a M.A.C. instrument using 20 kv accelerating potential, .03 micro Amperes sample current and 24-second counting interval

(mentioned above; Curie point of 580 °C) is relatively fresh and unaltered except for minor amounts of interstitial chlorite and green calcic amphibole. The primary igneous assemblage is calcic plagioclase, augite, ilmenite and trace amounts of chalcopyrite. Megacrysts of calcic plagioclase up to 5 mm in diameter are strongly zoned from An_{80-85} (core) to An_{50}(rim). Interstitial plagioclase is finer grained, euhedral, and less calcic. The latter is zoned from An_{65} (core) to An_{35} (rim) and is associated with augite, ilmenite and chlorite. Both feldspar occurrences show pronounced zoning of Fe as shown in Fig. 5. Megacrysts are progressively enriched to 0.8 wt. % FeO in their margins whereas the smaller, less calcic interstitial grains are enriched up to 1.0 wt % FeO. Normal oscillatory zoning occurs in the megacrysts and is indicative of relatively slow cooling from liquidus temperatures.

In contrast, dyke swarm sample no. 118 (Curie point = 580 °C) is an incompletely recrystallized metadolerite. The original doleritic texture is totally preserved. Relict augite occurs in the cores of fine-grained, greenish

calcic amphibole and provides unambiguous evidence for the original igneous assemblage of augite, calcic plagioclase and ilmenite. But inspite of the virtually complete recrystallization of ferro-magnesian silicates, the original igneous plagioclase is retained and apparently has not equilibrated with the metamorphic assemblage. Plagioclase from sample no. 118 is compositionally zoned from An_{65} (cores) to An_{38} (rims) and from 0.60 wt. % FeO (cores) to 0.90 wt. % FeO (rims). These feldspars occur as euhedral laths and normal oscillatory zoning is common. These, too, are believed to have a primary igneous origin.

In all of the dyke swarm samples studied, the feldspars contain variable amounts of oriented opaque needles which are generally less than a micron in length and have a length-width ratio of about 8:1. It is not possible to use microprobe analysis to show that these ultrafine grains are indeed magnetite, but their presence is undoubtedly reflected in the FeO concentrations shown in Fig. 5. However, from the work of Hargraves and Young (1969) and Evans and Wayman (1970) it has now been abundantly established that such opaque needles in feldspars are most likely to be single-domain magnetite. These particles represent one of the most effective carriers of NRM. Our observation of high AF-stability (Fig. 3) and Curie point typical of magnetite (Fig. 4) enables us to make this preliminary correlation. We are now extending our magnetic measurements to the individual feldspar crystals in order to show magnetic evidence of the presence of single-domain magnetite.

Accepting tentatively, however, that the feldspars contain the magnetic carriers, it is instructive to determine whether the varying degrees of metamorphism seen in the different dyke rocks can be related to their magnetic properties. No correlation between degree of iron-magnesium silicate alteration and intensity of NRM and Curie point values could be seen. Sample no. 63 (Fig. 6a) is the least-altered of the dyke-swarm samples and has the smallest intensity of NRM. The primary augite in sample no. 118 (Fig. 6b) is completely recrystallized to calcic amphibole and has an intermediate value of NRM intensity and a Curie point, again, of 580°C. These observations point to the feldspars being, for all practical purposes, a closed system to the prevailing primary metamorphism suffered by the dykes on emplacement. This conclusion is substantiated by a comparison of the preciously mentioned An-zoning (and a parallel iron-zoning) in feldspars with the variable chemistry of the minerals which they contact. Fig. 7 shows the now familiar zoning of calcium from core to rim seen by microprobe analysis in two feldspar grains from dyke-swarm samples no. 63 (fresh) and no. 118 (metamorphosed). The zoning is apparently independent of the nature of the minerals in contact with the feldspar grains and is also independent of the differing alterations seen in the iron-magnesium silicates in the respective samples.

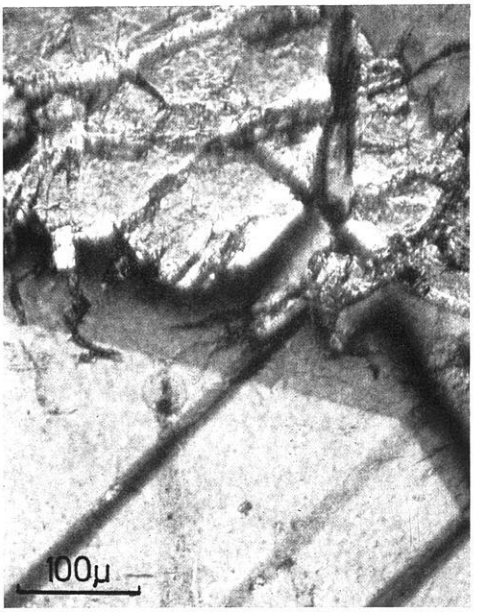

no. 63 a

no. 118 b

Fig. 6a. Photomicrograph (transmitted light, crossed polarizers) of a fresh sample (no. 63) from dyke-swarm showing primary igneous zonation in plagioclase (bottom) and primary augite (top); b Photomicrograph (transmitted light) of an incompletely metamorphosed sample (no. 118) from dyke swarm showing euhedral, compositionally zoned laths of primary plagioclase in a ground-mass of calcic amphibole (dark) and minor chlorite

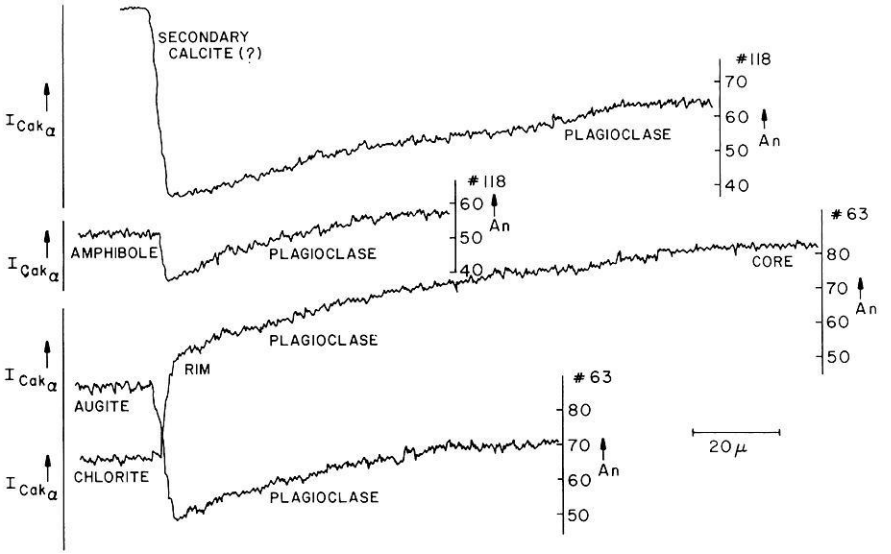

Fig. 7. Continuous electron microprobe scans of I_{CaK_α} across 4 compositionally zoned feldspar grains in dyke swarm samples no. 118 (metamorphosed) and no. 63 (fresh). Compositions of the plagioclase-augite pair (no. 63, bottom) represent liquidus equilibration. Primary igneous zonation is retained in feldspars contacting chlorite (≠63) and amphibole (≠118)

These observations are unusual for continental rocks but they are rather common in metadolerites and metagabbros dredged from the mid-ocean ridges. Practically identical mineralogic and textural relationships are described by Cann (1971) for metadolerites and metagabbros in dredge hauls from the Palmer Ridge and by Miyashiro *et al.* (1971) from the mid-Atlantic ridge near 24° and 30°N. This, of course, confirms even further the essentially oceanic nature of Macquarie Island.

4. Conclusion

Magnetic and petrologic investigations of rocks from Macquarie Island indicate that magnetic anomalies over Tertiary age oceanic crust may have a significant contribution from the NRM of doleritic dykes. The NRM intensities of dyke samples from Macquarie Island are low compared to young dredged pillow lavas but are only slightly less than the NRM intensities observed in Macquarie Island pillow lavas. This suggests that the NRM intensities of pillow lavas are diminished by low temperature oxidation and/or low grade metamorphism. The existence of titanomaghemite produced by low temperature oxidation was confirmed by thermomagnetic analysis. High AF demagnetization stability, optical microscopy, and

microprobe data from dyke samples indicate that the magnetic carriers are fine-grained magnetites in host feldspar. These magnetites have not undergone alteration during the primary metamorphism suffered by the dykes on emplacement. The model of the oceanic crust suggested by our investigation of Macquarie Island rocks is one in which the contribution to marine magnetic anomalies from the basaltic and doleritic dyke layer remains constant while the contribution from the overlying pillow layer decreases with age.

Acknowledgement. We wish to thank Dr. R. Varne for supplying the Macquarie Island hand samples. This research was funded by National Science Foundation grants GA 35249 and GA 36092 and by the Graduate School of the University of Minnesota.

References

Banerjee, S.K.: Decay of marine magnetic anomalies by ferrous ion diffusion. Nature Phys. Sci. *229*, 181–183, 1971

Butler, R.F.: Stable single-domain to superparamagnetic transition during low-temperature oxidation of oceanic basalts. J. Geophys. Res. *78*, 6868–6876, 1973

Butler, R.F., Banerjee, S.K.: Magnetic properties of exposed oceanic crust on Macquarie Island. Nature Phys. Sci. *244*, 115–118, 1973

Cann, J.R.: Petrology of basement rocks from Palmer ridge, N.E. Atlantic. Phil. Trans. Roy. Soc. London, Ser. A *268*, 605–617, 1971

Carmichael, C.M.: The mid-Atlantic ridge near 45°N. Vii. Magnetic properties and opaque mineralogy of dredged samples. Can. J. Earth Sci. *7*, S. 239–256, 1970

Evans, M.E., Wayman, M.L.: An investigation of small magnetic particles by means of electron microscopy. Earth Planet. Sci. Lett. *9*, 365–370, 1970

Gass, I.G., Smewing, J.D.: Intrusion, extrusion, and metamorphism at contructive margins: Evidence from the Troodos Massif, Cyprus. Nature *242*, 26–29, 1973

Hargraves, R.B., Young, W.M.: Source of stable remanent magnetism in Lambertville diabase. Am. J. Sci. *267*, 1161–1177, 1969

Irving, E.: The mid-Atlantic ridge at 45°N. XIV. Oxidation and magnetic properties of basalt; review and discussion. Can. J. Earth Sci. *7*, 1528–1538, 1970

Lowrie, W.: Viscous remanent magnetization in oceanic basalts. Nature *243*, 27–29, 1973

Marshall, M., Cox, A.: Magnetism of pillow basalts and their petrology. Bull. Geol. Soc. Am. *82*, 537–552, 1971

Marshall, M., Cox, A.: Magnetic changes in pillow basalt during sea floor weathering. J. Geophys. Res. *77*, 6459–6469, 1972.

Miyashiro, A., Shido, F., Ewing, M.: Metamorphism in the mid-Atlantic ridge near 24° and 30°N. Phil. Trans. Roy. Soc. London, Ser. A *268*, 589–603, 1971

Moores, E.M.: Petrology and structure of the Vourinos ophiolite complex of Northern Greece. Geol. Soc. Am. Spec. Paper No. 118, 1969

Varne, R., Gee, R.D., Quilty, P.G.J.: Macquarie Island and the cause of oceanic linear magnetic anomalies. Science *166*, 230–233, 1969.

Varne, R., Rubenach, M.J.: Geology of Macquarie Island and its relationship to oceanic crust. Ant. Res. Ser. *19*, 251–266, 1972

Vine, F. J., Matthews, D. H.: Magnetic anomalies over oceanic ridges. Nature *199* 947–949, 1963

Vine, F. J., Moores, E. M.: A model of the gross structure, petrology and magnetic properties of oceanic crust. Geol. Soc. Amer. Mem. *132*, 195–205, 1972

Prof. S. K. Banerjee
Department of Geology and Geophysics
University of Minnesota
108 Pillsburg Hall
Minneapolis, Minnesota 55455, USA

J. Geophys. 40, 549–564, 1974

4. Correlation with Petrography

Magnetic Characteristics of Some Precambrian Basement Rocks

E. G. Lidiak

Department of Earth and Planetary Sciences, University of Pittsburgh

Received March 12, 1974

Abstract. The relation between aeromagnetic anomalies and Precambrian rocks in the Bighorn Mountains of Wyoming and in the Minnesota River Valley of Minnesota reveal a good correlation between total magnetic intensity and the induced and natural remanent magnetization. The predominantly silicic plutonic rocks of the Bighorns are not distinguishable from one another on the basis of susceptibility or remanent intensities. In addition, except for a rough correspondence with structural trends, the mapped geology bears no close resemblance to the aeromagnetic anomalies. However, contouring of the susceptibility data and to a lesser extent of the remanence data produces a distinct magnetic trend and a series of highs and lows that approximate the aeromagnetic anomaly pattern. These results indicate that even in areas of similar rock type with adequate sampling it is possible to correlate the geology with the aeromagnetic anomalies.

In the Minnesota River Valley a complex of upper amphibolite to granulite facies gneisses coincides with a prominent series of aeromagnetic highs. Preliminary magnetic data suggest that these highs are mainly attributable to the granulitic gneisses, and that the partitioning of Fe and Ti between coexisting oxide and silicate phases during metamorphic reactions may be important in enhancing the magnetic intensity.

The change in magnetic intensity across a series of metamorphic isograds in northern Michigan was also investigated. The magnetic intensity increases from the chlorite zone to the biotite zone, decreases in the garnet zone, and then increases markedly in the staurolite and sillimanite zones. The intensity of metamorphism thus appears to be an additional factor that affects magnetization and needs to be studied further.

Key words: Aeromagnetic Anomalies — Continental Basement — Magnetism — Precambrian — Metamorphism.

Introduction

Aeromagnetic maps are becoming increasingly available for many parts of the continental United States. These maps are being used with considerable success to help interpret the regional lithologic and structural relations of the basement and other crystalline rocks. To gain an even better understanding of the relations between the geology and the aeromagnetic patterns, trends, and intensities, more detailed knowledge of the magnetic properties of continental basement rocks is necessary. It is the purpose of this paper to

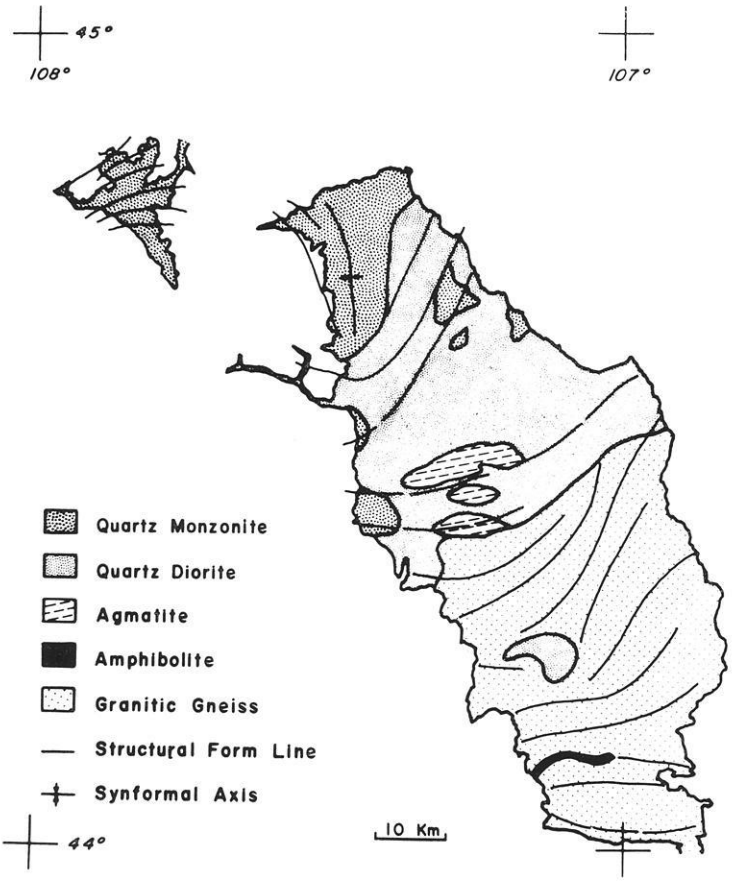

Fig. 1. Regional geological and structural map of the Bighorn Mountains, Wyoming (generalized from Heimlich, 1969, 1971)

present preliminary results on the magnetic characteristics of some Precambrian basement rocks from the Bighorn Mountains of Wyoming and the Minnesota River Valley of Minnesota, areas that are typical of part of the North American craton. In addition, the thermally metamorphosed rocks of northern Michigan were studied to investigate the relation between the intensity of magnetization and the grade of metamorphism.

Bighorn Mountains, Wyoming

The Bighorn Mountains comprise a large crustal block that was uplifted initially during the Laramide orogeny. Continued uplift and erosion has exposed a core of Precambrian rocks surrounded by Paleozoic and Mesozoic strata. The Precambrian rocks occupy an area of approximately 2900 sq.

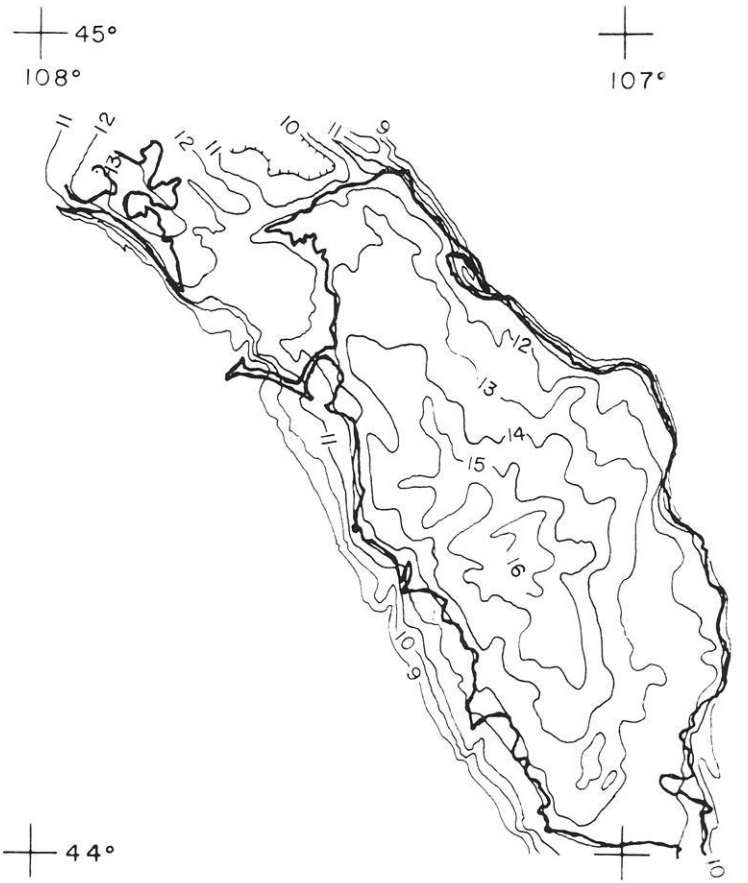

Fig. 2. Structure contour map of the Bighorn Mountains, Wyoming (generalized from Hodgson, 1965). Contours are in thousands of feet. Contours drawn on top of the Cretaceous Cloverly Formation

km and consist mainly of quartz monzonite, quartz diorite, agmatite, amphibolite, and various kinds of granitic gneiss (Heimlich, 1969). The distribution of the major rock types and their main structural trends are shown on Figure 1. The major rock types are in general gradational to one another and probably evolved to their present state during regional metamorphism that reached the staurolite zone of the amphibolite facies (Heimlich and Banks, 1968; Heimlich, 1969, 1971; Heimlich and Armstrong, 1972). This complex of plutonic rocks are cut by a series of diabase dikes (Condie *et al.*, 1969a, 1969b) which are not shown on Fig. 1 because of scale. Some of these rocks have been subjected to retrograde metamorphism, principally along shear zones (Heimlich and Uthe, 1973).

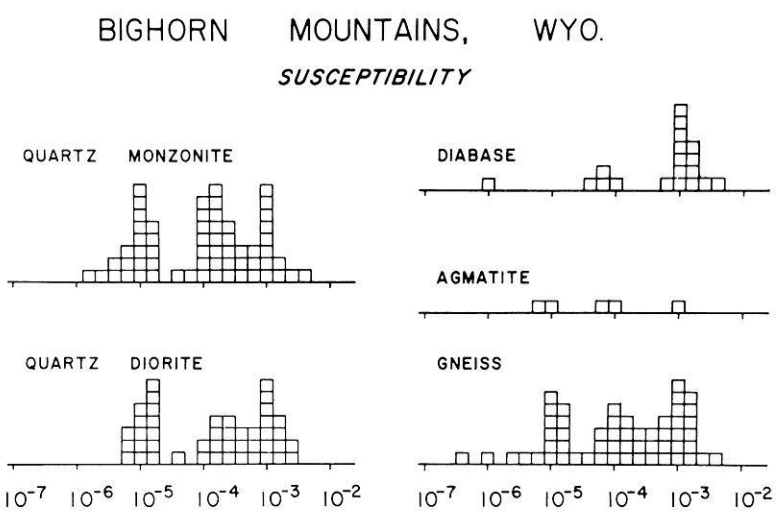

Fig. 3. Histograms of susceptibility for the Precambrian rocks of the Bighorn Mountains, Wyoming. Each square represents one sample

This complex of silicic plutonic rocks is in part representative of some large Precambrian terranes in the midcontinent of the United States, for example, the basement rocks of Nebraska (Lidiak, 1972). Aeromagnetic maps have been used in such areas of widely-spaced sample control to help map the basement lithology and structure. It is therefore useful to determine whether the magnetic properties of more closely-spaced samples correlate with aeromagnetic anomalies and whether they reflect the lithologic and structural trends.

An aeromagnetic map has been made for this region but it presently is restricted and not available for publication. However, a structural contour map of the uplift, shown on Fig. 2, provides a rough approximation of the aeromagnetic map and can be used for comparative purposes. The main feature of the map is a pronounced northwest-trending series of highs. The main highs occur near (1) lat. 44°20′N., long. 107°10′W., and (2) lat. 44°35′N., long. 107°28′W., (3) lat. 44°47′N., long. 107°50′W., and (4) lat. 44°47′N., long. 107°25′W., the latter being a subsidiary high. Lows are present in the vicinity of (1) lat. 44°00′N., long. 107°15′W., (2) lat 44°35′N , long. 107°00′W., and (3) lat. 44°50′N., long. 107°40′W.

It is clear from a comparison of Figs. 1 and 2 that the mapped lithology, which is based mainly on variations in silicate mineralogy, bears no close relationship to the aeromagnetic anomalies. The structural trend does, however, show some general correspondence. The major synformal axis in the northern part of the uplift is subparallel to the main magnetic trend,

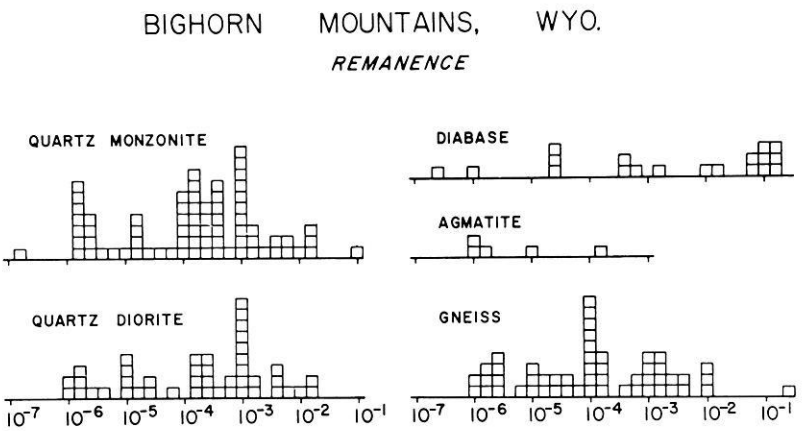

Fig. 4. Histograms of natural remanent intensity for the Precambrian rocks of the Bighorn Mountain, Wyoming. Each square represents one sample

and the main metamorphic fold lines (which represent the trend of the dominant foliation) are approximately at right angles to the magnetic trend.

To investigate the relationships further, the suspectibility and remanence of nearly 200 samples of the main rock types were measured. The results are shown in histogram form on Figs. 3 and 4, respectively. Two comments about this data appear worthy of note: (1) the quartz monzonites, quartz diorites, and granitic gneisses show wide variation in susceptibility and remanent intensity, with many values higher than ordinarily attributed to such silicic rocks; and (2) the diabases yield in part higher values than the other rock types, but the more silicic rock groups cannot be distinguished from one another on the basis of susceptibility and remanence. The overlapping intensities may account for the apparent lack of correlation between the mapped geology and the aeromagnetic anomalies. However, such relations do not preclude a correlation, but indicate that the intensity of magnetization gives only a rough approximation of silicate rock type.

Preliminary microscopic examination of about 50 polished rock specimens suggests that the high susceptibility and remanent values occur in rocks that have higher concentrations of magnetite. The magnetite commonly contains thin lamellae of hematite. Minor discrete ilmenite grains may also be present. The lower magnetic intensities appear to be the result of either sparse magnetite content, oxidation or hydration of magnetite, or of ilmenite being the sole Fe-Ti oxide phase in the rock.

In making the magnetic measurements a grouping of magnetic intensity by locality was recognized. Accordingly, it was decided to contour the susceptibility and remanent intensities to determine the regional pattern and trend. Contour maps were constructed utilizing a computer printout. It

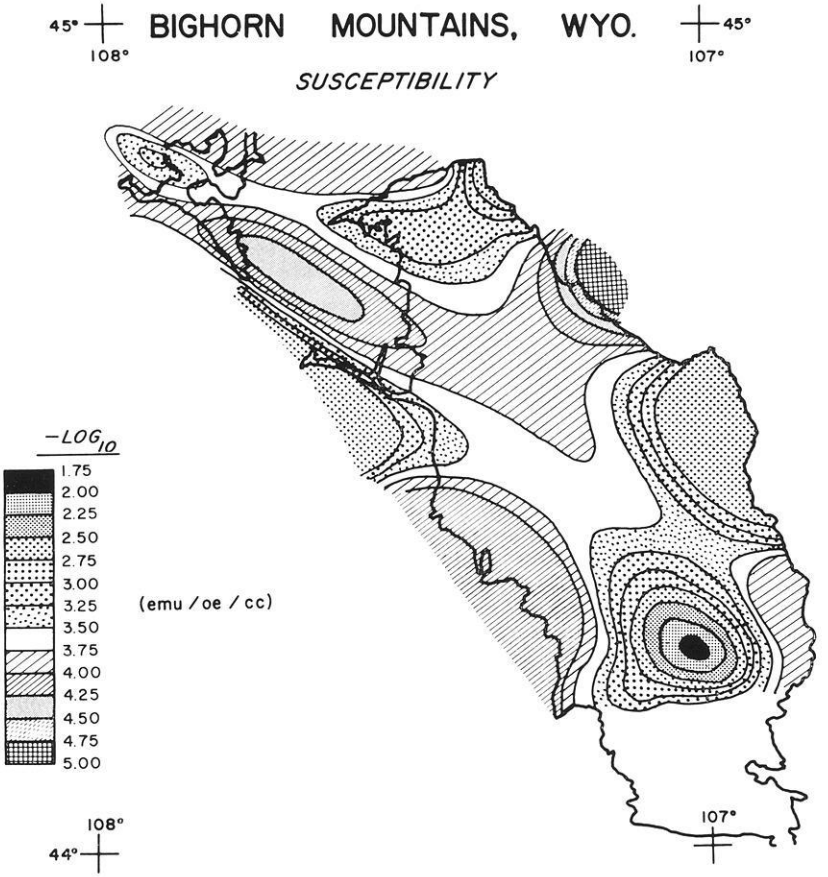

Fig. 5. Contour map of the susceptibility variations in the Precambrian rocks of the Bighorn Mountain, Wyoming

should be emphasized that the resulting maps are not standard contour maps inasmuch as some of the contours and the values between contour lines represent an extrapolation of the data points rather than an interpolation.

The contoured susceptibility data is shown on Fig. 5. A strong northwest trend of the anomalies, closely similar to the aeromagnetic trend, is present. Three of the aeromagnetic highs (1,2,3) previously noted are somewhat displaced relative to the three main susceptibility highs, but all lie along the main northwest trend. The subsidiary aeromagnetic high (4) coincides with the broad susceptibility high near lat. 44°45′N., long. 107°25′W. Similarly, aeromagnetic low (3) corresponds to the broad susceptibility low in the northermost part of the contoured area. Aero-

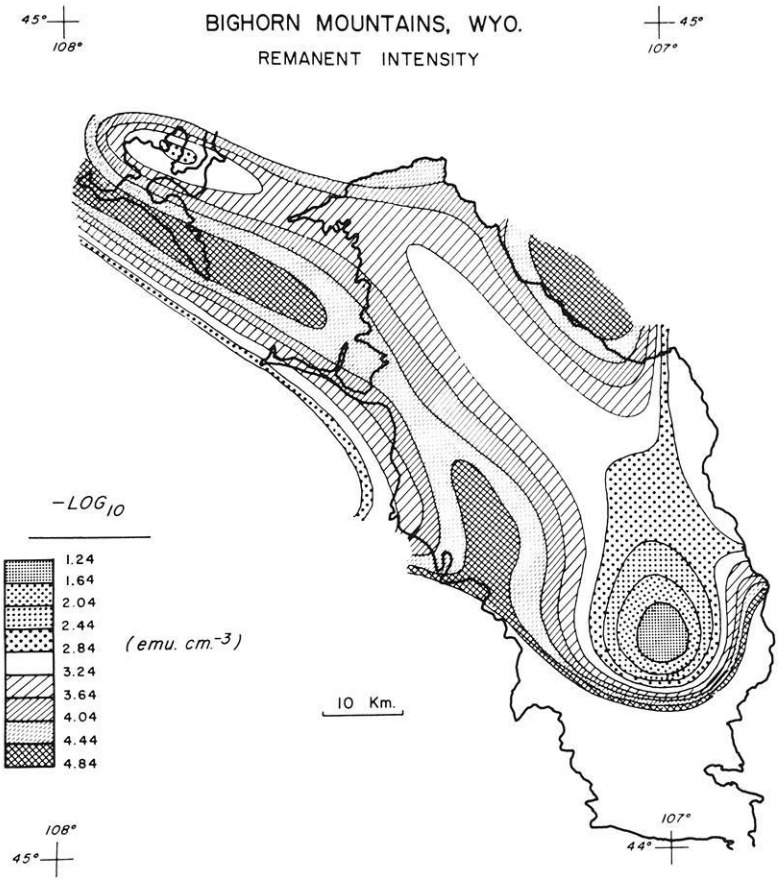

Fig. 6. Contour map of the natural remanent intensity variations in the Precambrian rocks of the Bighorn Mountains, Wyoming

magnetic low (2) lies along the steep susceptibility gradient near lat. 44°35′N., long. 107°00′W.; aeromagnetic low (1) is south of the contoured area. In general, it can be stated that the regional susceptibility pattern corresponds well to the variation in total magnetic intensity.

The remanent intensity was also contoured and the results are shown in Fig. 6. A prominent northwest trend is similarly apparent in this map. The remanence highs and lows do not, however, correspond to the aeromagnetic highs and lows as closely as do the susceptibility anomalies. Aeromagnetic highs (1 and 3) occur, respectively, along the western and along the southwestern gradient of the two main remanence highs. Aeromagnetic lows (2 and 3) also occur along remanence gradients. One of the aeromagnetic highs, (2), occupies the saddle between the two elongate lows

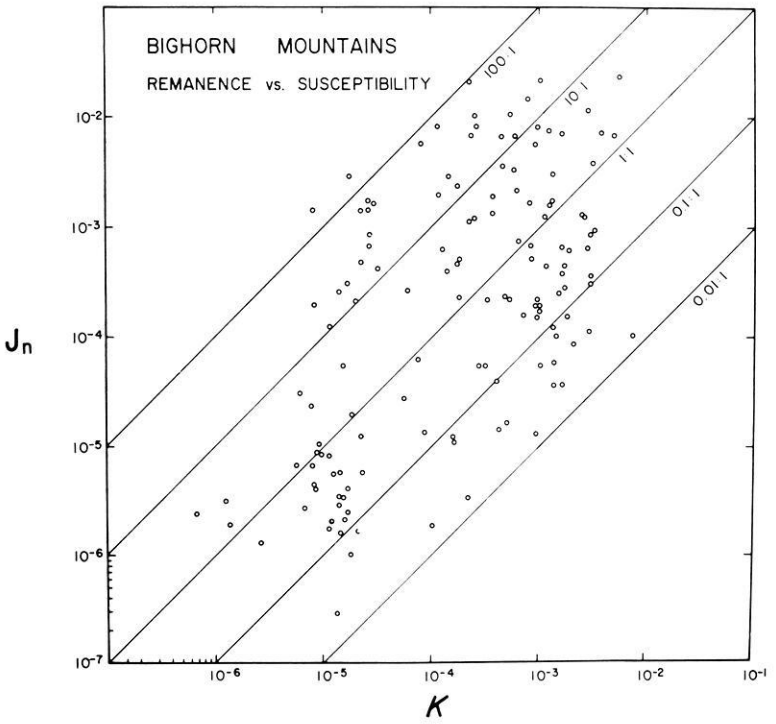

Fig. 7. Variation of the Königsberger ratio (Q') in the Precambrian rocks of the Bighorn Mountains, Wyoming

along the southwestern part of Fig. 6. Only aeromagnetic high (4) coincides with a remanence high; it lies along the northwest-trending high in the center of the map. It is thus apparent that the remanent intensity pattern only roughly approximates the total magnetic intensity. This lack of a close correlation may be due in part to the fact that the remanence was contoured as a scalar quantity rather than as a vector. The effect of the remanent direction on the regional anomaly pattern needs to be considered further.

It appears from the foregoing discussion that the main contribution to the total magnetic intensity derives from the susceptibility. That the remanence also contributes to the total intensity is evident from a consideration of a modified Königsberger ratio ($Q' = J_{NRM}/K$) of the individual rocks. These are shown in Fig. 7. The plotted ratios have both a positive slope and a wide variation, with ratios ranging from about 100 : 1 to about 0.01 : 1.

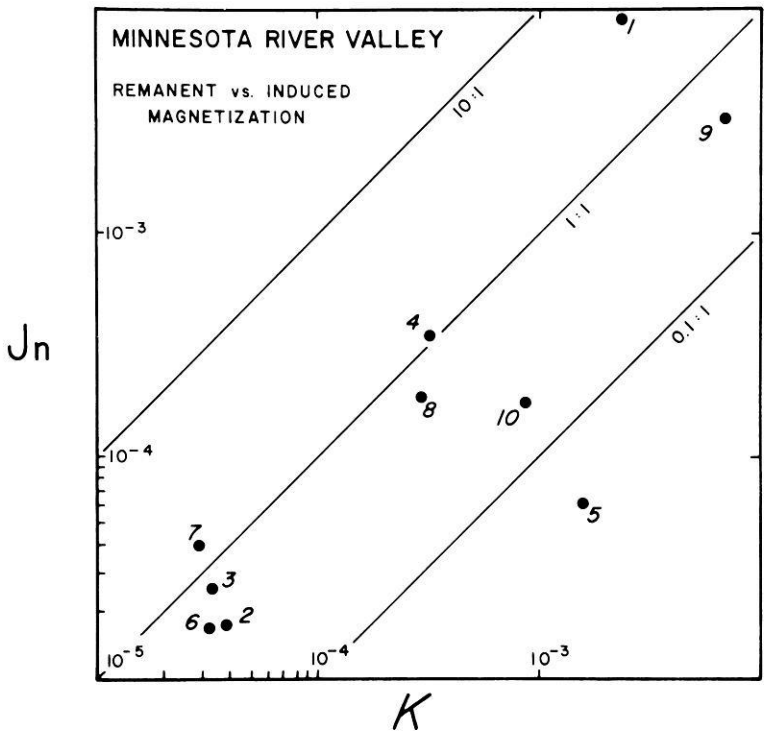

Fig. 8. Variation of the Königsberger ratio (Q') in the Precambrian rocks of the Minnesota River Valley. Granulite facies gneiss (1, 7, 8, 10), amphibolite facies gneiss (2, 3, 4, 6), granite (5), diabase (9)

Minnesota River Valley

Another sequence of basement rocks that may have wide distribution southwest of the Canadian Shield are the early Precambrian granitic gneisses and younger intrusive rocks that are exposed in the Minnesota River Valley of southwestern Minnesota. The main rock types are a series of migmatitic gneisses that have been intruded by granite plutons, and in turn, by diabase dikes and other small intrusions (Lund, 1956; Goldich *et al.*, 1961; Himmelberg, 1968; Grant, 1972). Some of the gneisses are 3550 m. y. old, and they have been metamorphosed, deformed, and intruded by granite 2650 m. y. ago (Goldich *et al.*, 1970). These events have left the gneisses with a metamorphic grade in the upper amphibolite or granulite facies, and with a predominant east to east-northeast-trending foliation and a steep dip (Himmelberg and Phinney, 1967; Grant, 1972). The younger diabase dikes have a similar orientation. Some of these rocks were subjected to low grade metamorphism about 1850 m. y. ago.

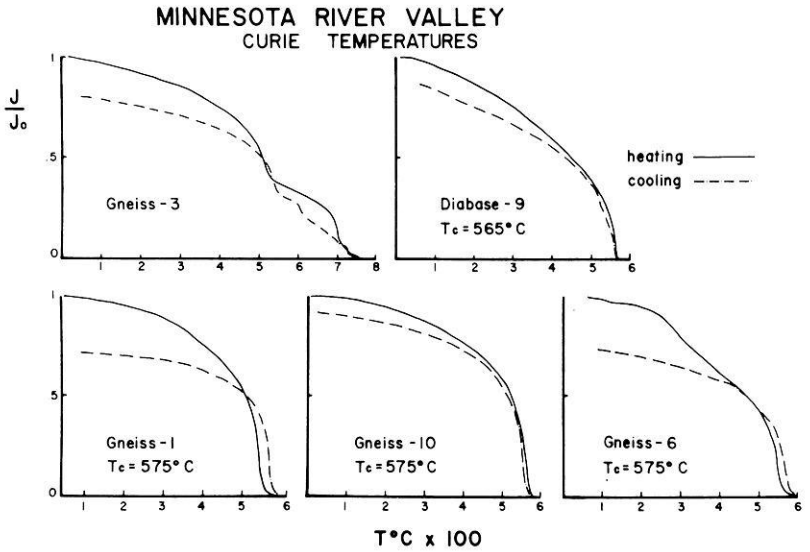

Fig. 9. Curie temperatures from Precambrian rocks of the Minnesota River Valley. Sample numbers are the same as in Fig. 8

The rocks are exposed only in the valley of the Minnesota River, but magnetic and gravity anomalies suggest that the rocks have a much greater extent in the subsurface. For example, a prominent series of magnetic highs extends for a distance of about 400 km from south-central Minnesota (Zietz and Kirby, 1970) through the Minnesota River Valley to east-central South Dakota (Lidiak, 1971). In view of the antiquity of the gneisses and their significance to early Precambrian geology of the North American craton, it is important to establish whether the magnetic highs can indeed be attributed to the high grade gneisses or whether other causes must be sought.

With this object in mind, the magnetic properties of ten rocks from the Minnesota River Valley were studied. Four of the samples (1, 7, 8, 10) belong to the granulite facies, four (2, 3, 4, 6) to the upper amphibolite facies, one (5) is a granite, and one (9) is a diabase. The susceptibility and remanence of these rocks were determined and the results are shown on Fig. 8 in the form of a modified Königsberger ratio (Q'). Three of the four granulites have moderate to high susceptibility and remanence; the amphibolite grade rocks have low to moderate intensities. These results, although not compelling statistically, are compatible with the suggestion that the granulites, and probably also the diabases, may be responsible for the high magnetic anomalies.

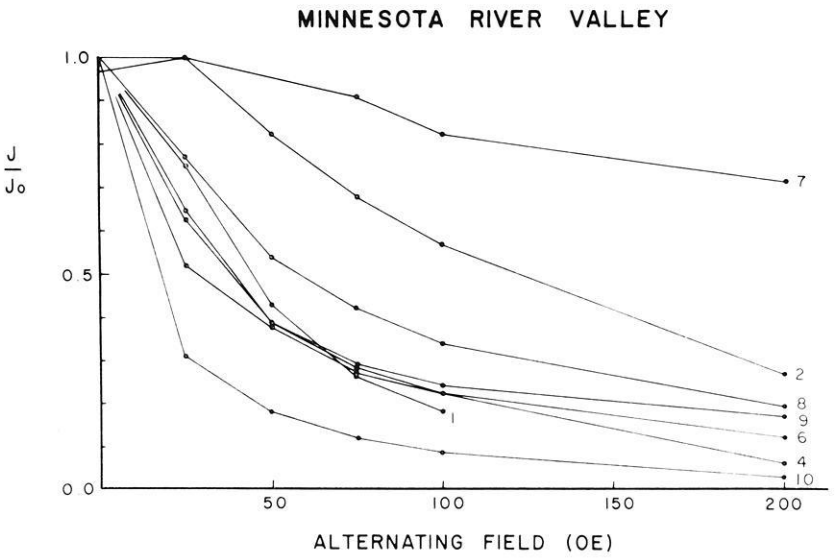

Fig. 10. Alternating-field demagnetization curves of Precambrian rocks from the Minnesota River Valley. Sample numbers are the same as in Fig. 8

Reflected and transmitted light studies of the ten samples reveal differences in opaque mineralogy and mineral associations that help to account for the variation in magnetic intensity. Magnetite is the main oxide phase; ilmenite occurs only as a minor accessory. The magnetite is essentially homogeneous but may contain sparse blebs or thin lamellae of hematite. Some of the magnetite is also peripherally altered to hematite, which, in turn, may be rimmed by maghemite. Rocks showing the greatest amount of oxidation are samples 2, 3, and 7, all having low magnetic intensity.

In addition to oxidation, another factor that may help to account for variations in intensity is the composition of the magnetite. Magnetite occurs both as discrete grains and in association with biotite, orthopyroxene, or hornblende. The latter mode of occurrence is particularly applicable to the granulites where most of the magnetite is partly intergrown with titanbiotite or orthopyroxene. Fig. 9 shows that the magnetite in the granulites has a Curie temperature of essentially pure Fe_3O_4. An additional factor in the magnetic intensity of the granulites may thus be metamorphic reactions in which Ti is preferentially partitioned in the silicate rather than in the oxide phase.

The grain size of the magnetites in these rocks is variable but mainly in the range from 0.01 mm to 0.5 mm in diameter. The grains are thus of the multi-domain type. Demagnetization curves (Fig. 10) show that the

remanent intensity of the magnetite in six of eight samples is decreased by more than one-half in an alternating field of less than 100 oersteds.

Northern Michigan

The apparent relation between magnetic intensity and grade of metamorphism in the Minnesota River Valley prompted a further investigation into the extent to which metamorphism may affect magnetic intensity. The well-known thermal domes of metamorphism in the upper peninsula of Michigan described by James (1955) were studied to determine the effect over a wider range of metamorphism. The eastern part of this region was selected because (1) a series of mineral isogards ranging from the low-grade chlorite zone through the high-grade sillimanite zone are developed in a variety of rock types, (2) rock exposures are adequate, (3) the metamorphism is mainly of the thermal type, and (4) aeromagnetic maps are available for the region.

The Precambrian rocks in the upper peninsula have been described by Van Hise and Leith (1911), Leith *et al.* (1935), and James (1955, 1958). Detailed geologic maps for the parts of the area studied have been published by Bayley (1959), Bayley *et al.* (1966), Dutton (1971), Gair and Weir (1956), James *et al.* (1961, 1968), and by Weir (1967). The rocks consist of a lower sequence of greenstones, granitic gneisses, and amphibolites that are overlain unconformably by a series of metamorphosed iron formations, metasedimentary graywackes and shales, and metavolcanic strata, and by a younger sequence of essentially unmetamorphosed sandstones, conglomerates, and extrusive volcanic rocks. The aforementioned zones of metamorphism were imprinted prior to the deposition of the youngest sequence near the end of or after the last major peroid of metamorphism and igneous intrusion in the region. The metamorphic zones are delineated by the chlorite, biotite, garnet, staurolite, and sillimanite isogards or their equivalents that are developed around four nodes or thermal domes. The metamorphic pattern shows no close relation to the regional structure or exposed granitic bodies and has been ascribed to metamorphism by subjacent igneous intrusion (James, 1955).

Case and Gair (1965) have shown that there is a close correlation between the aeromagnetic anomaly pattern and the known or inferred geology. The trend of the iron formations in particular is clearly outlined, but other units can be delineated as well. Similar results were obtained by Meshref and Hinze (1970) in a large area immediately to the west. These investigations show the value of aeromagnetic data in determining the regional structure and lithology in Precambrian terranes.

In order to determine whether the grade of metamorphism has an effect on the magnetization of the various lithologic units, the mineral

MAGNETIC INTENSITY (Gammas)

METAMORPHIC ISOGRADS, NO. MICHIGAN

		CHLORITE	BIOTITE	GARNET	STAUROLITE	SILLIMANITE
IRON FORMATIONS	MAX.	6,950	12,130	2,760	10,470	11,650
	MIN.	1,100	2,820	2,000	2,830	3,750
META-SEDIMENTS	MAX.	1,800	2,060	1,500	4,500	4,550
	MIN.	1,050	1,350	1,400	1,320	2,320
GREENSTONE	MAX.	1,440	2,000	1,720	—	—
	MIN.	850	1,160	1,000	—	—

Fig. 11. Relation between magnetic intensity (in gammas) and grade of metamorphism in northern Michigan. Intensity is relative to an arbitrary datum

isograd pattern was superimposed on the regional aeromagnetic map of Case and Gair (1965). The maximum and minimum magnetic anomaly intensities for the different grades of metamorphism in the greenstones, metasedimentary graywackes and shales, and iron formation were then determined. An attempt was made in compiling this data to select only regional maxima and minima that are not affected by magnetic edge effects. The averaged data are summarized on Fig. 11. These results show that for all three rock types the total magnetic intensity increases from the chlorite to the biotite zone, decreases in general in the garnet zone, and then increases in the staurolite and sillimanite zones. A metamorphic effect is thus indicated. The specific cause for the changes in intensity has not been investigated in detail but probably reflects various metamorphic reactions that produced the series of isogards.

The effect of metamorphic grade on intensity of susceptibility and remanent magnetization was also studied on 21 samples of the metasedimentary graywacke and shale sequence. The results (Fig. 12) show some scatter but do indicate that both the susceptibility and the remanence are mainly higher in the staurolite and sillimanite zones. A lower remanence is also indicated in the garnet zone. The intensities in the chlorite and biotite zones, however, are essentially the same. These results, particularly from the higher isograds, are in general agreement with the variations in total magnetic intensity. Further study is clearly indicated, however, before the effects of metamorphism on magnetization can be ascertained.

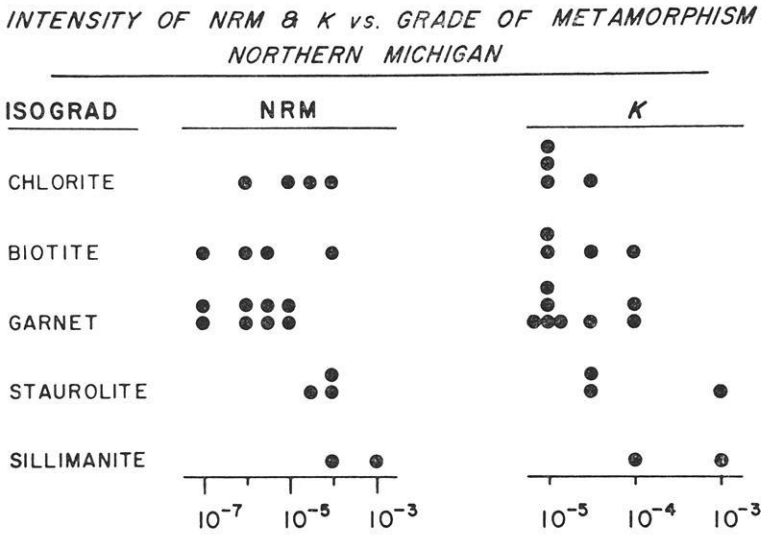

Fig. 12. Relation between intensity of remanent and induced magnetization and the grade of metamorphism in metasedimentary rocks from northern Michigan

Conclusions

This study has shown that exposed Precambrian crystalline rocks can be correlated very well with regional aeromagnetic maps not only in terranes that contain widely diverse magnetic rock types but also in regions where basement lithology is similar. In the rocks studied in this report susceptibility and remanent magnetization are both important components of the total magnetic intensity. Both parameters need to be considered in evaluating aeromagnetic data and in making quantitative interpretations.

The concentration of magnetic minerals is probably the main parameter that controls the intensity of magnetization among rock bodies. Preliminary results on the metamorphic rocks reported on in this paper indicate that grade of metamorphism is also a factor that affects magnetic intensity. As most if not all Precambrian crystalline rocks are metamorphosed to some degree, this effect needs to be considered in evaluating aeromagnetic anomalies. The variation in magnetic intensity with grade of metamorphism has application not only to exposed rocks but also to rocks buried at depth in the crust, particularly in areas of high heat flow where a series of metamorphic isograds may be developed.

Acknowledgments. Samples from the Bighorn Mountains were made available through the courtesy of Jan Smith. The help of Henry Pollak and S. G. Khoury in contouring Figs. 5 and 6 is greatly appreciated.

References

Bayley, R.W.: Geology of the Lake Mary quadrangle, Iron County, Michigan. U.S. Geol. Surv. Bull. *1077*, 112 p., 1959

Bayley, R.W., Dutton, C.E., Lamey, C.A.: Geology of the Menominee iron-bearing district, Dickinson County, Michigan, and Florence and Marinette Counties, Wisconsin. U.S. Geol. Surv. Prof. Paper *513*, 96 p., 1966

Case, J.E., Gair, J.E : Aeromagnetic map of parts of Marquette, Dickinson, Baraga, Alger and Schoolcraft Counties, Michigan, and its geologic interpretation. U.S. Geol. Surv. Geophys. Inv. Map GP-467, 1965

Condie, K.C., Barsky, C.K., Mueller, P.A.: Geochemistry of Precambrian diabase dikes from Wyoming. Geochim. Cosmochim. Acta *33*, 1371–1388, 1969a

Condie, K.C., Leech, A.P., Baadsgaard, H.: Potassium-argon ages of Precambrian mafic dikes in Wyoming. Geol. Soc. Am. Bull. *80*, 899–906, 1969b

Dutton, C.E.: Geology of the Florence area, Wisconsin and Michigan. U.S. Geol. Surv. Prof. Paper *633*, 54 p., 1971

Gair, J.E., Weir, K.L.: Geology of the Kiernan quadrangle, Michigan. U.S. Geol. Surv. Bull. *1044*, 88 p., 1956

Goldich, S.S., Nier, A O., Baadsgaard, H., Hoffman, J.F., Krueger, H.W.: The Precambrian geology and geochronology of Minnesota. Minnesota Geol. Surv. Bull. *41*, 193 p., 1961

Goldich, S.S., Hedge, C.E., Stern, T.W.: Age of the Morton and Montevideo gneisses and related rocks, southwestern Minnesota. Geol. Soc. Am. Bull *81*, 3671–3696, 1970

Grant, J.A.: Precambrian geology of the Minnesota River Valley between Morton and Montevideo, Part 1 — Geology and Structure. Minnesota Geol. Surv. Guidebook 5, 1–16, 1972

Heimlich, R.A.: Reconnaissance petrology of Precambrian rocks in the Bighorn Mountains, Wyoming. Contr. Geology *8*, 47–61, 1969

Heimlich, R.A.: Chemical data for major Precambrian rock types, Bighorn Mountains, Wyoming. Contr. Geology *10*, 131–140, 1971

Heimlich, R.A., Armstrong, R.L.: Variance of Precambrian K-Ar biotite dates, Bighorn Mountains, Wyoming. Earth Planet. Sci. Lett. *14*, 75–78, 1972

Heimlich, R.A., Banks, P.O.: Radiometric age determinations, Bighorn Mountains, Wyoming. Am. J. Sci. *266*, 180–192, 1968

Heimlich, R.A , Uthe, R.E.: Retrograde metamorphism of amphibole, Bighorn Mountains, Wyoming. Geol. Soc. Am. Abstracts with Programs *5*, 176, 1973

Himmelberg. G.R.: Geology of Precambrian rocks, Granite Falls-Montevideo area, southwestern Minnesota. Minnesota Geol. Surv. Spec. Pub. Ser. *5*, 33 p., 1968

Himmelberg, G.R., Phinney, W.C.: Granulite facies metamorphism, Granite Falls-Montevideo area, Minnesota. J. Petrol. *8*, 325–348, 1967

Hodson, R.A.: Genetic and geometric relations between structures in basement and overlying sedimentary rocks, with examples from Colorado Plateau and Wyoming. Am. Assoc. Petrol. Geol. *49*, 935–949, 1965

James, H.L.: Zones of regional metamorphism in the Precambrian of northern Michigan. Geol. Soc. Am. Bull. *66*, 1455–1488, 1955

James, H.L.: Stratigraphy of pre-Keweenawan rocks in parts of northern Michigan. U. S. Geol. Surv. Prof. Paper 314-C, *27–44*, 1958

James, H.L., Clark, L.D., Lamey, C.A., Pettijohn, F.J.: Geology of central Dickinson County, Michigan. U. S. Geol. Surv. Prof. Paper 310, 176 p., 1961

James, H. L., Dutton, C. E., Pettijohn, F. J., Weir, K. L.: Geology and ore deposits of the Iron River—Crystal Falls district, Iron County, Michigan. U. S. Geol. Surv. Prof. Paper 570, 134 p., 1968

Leith, C. K., Lund, R. J., Leith, A.: Precambrian rocks of the Lake Superior region. U. S. Geol. Surv. Prof. Paper 184. 34 p., 1935

Lidiak, E. G.: Buried Precambrian rocks of South Dakota. Geol. Soc. Am. Bull. *82*, 1411–1420, 1971

Lidiak, E. G.: Precambrian rocks in the subsurface of Nebraska. Nebraska Geol. Surv. Bull. *26*, 41 p., 1972

Lund, E. H.: Igneous and metamorphic rocks of the Minnesota River Valley. Geol. Soc. Am. Bull. *67*, 1475–1490, 1956

Meshref, W. M., Hinze, W. J.: Geologic interpretation of aeromagnetic data in western upper peninsula of Michigan. Michigan Geol. Surv. Rept. Inv. *12*, 25 p., 1970

Van Hise, C. R., Leith, C. K.: The geology of the Lake Superior region. U. S. Geol. Surv. Mon. *52*, 641 p., 1911

Weir, K. L.: Geology of the Kelso Junction quadrangle, Iron County, Michigan. U. S. Geol. Surv. Bull. *1226*, 47 p., 1967

Zietz, I., Kirby, J. R.: Aeromagnetic map of Minnesota. U. S. Geol. Surv. Geophys. Inv. Map GP-725, 1970

Edward G. Lidiak
Department of Earth and Planetary Sciences
University of Pittsburgh
Pittsburgh, Pennsylvania 15260, USA

J. Geophys. 40, 565–569, 1974

Cohenite Diagnosis in South Urals Ultrabasites

T. M. Koshkina, M. V. Lagutina, and V. A. Shapiro

Institute of Geoph. Ural. Sci. Centre, USSR Academy of Science

Received March 12, 1974

Abstract. Dense black serpentinous dunites with a characteristic sooty appearance were investigated. Microscopic examination shows that the rock consists mainly of serpentine with rare olivine grains, disseminated sulphides, mostly pyrrhotite with magnetite plates. Along the cracks in the rock or in the serpentine veins a black finely dispersed substance develops. The carbon content in the rocks according to seven samples varies from 0.08 to 0.40 per cent. On acid treatment the rocks are discoloured which indicates the mainly sulphide composition of the sooty substance. After hydrofluoric acid treatment only chromite is found in the insoluble residue which indicates the presence of carbon in soluble, i.e. carbide form. In order to verify this suggestion a thermomagnetic analysis of the samples was carried out since all the carbides of iron are ferromagnetic. Magnetic susceptibility varied from 310.10^{-6} up to 3570.10^{-6} e.m.u. According to natural remanent magnetization I_n and Q_n — coefficient groups of rocks are determined: I_n = 54—310.10^{-6} e.m.u., Q_n 1 and I_n = 16300—81000.10^{-6} e.m.u., Q_n = 20—64. Thermal demagnetization of I_{rs} dunites for 11 samples resulted in I_{rs} (T) curves that are characteristic of a three-phase system with the Curie temperatures varying in the ranges of 200–230°C, 300–400°C, 550–570°C due to the presence of cohenite — Fe_3C, pyrrhotite with different sulphur content and magnetite, respectively.

The samples investigated confirm the presence of the soluble form of carbon-cohenite in ultrabasics which is the main carbon carrier in those rocks.

Key words: Serpentinous Dunites — Cohenite — Magnetic Properties — Thermal Demagnetization — Curie Temperature.

Thermomagnetic analysis of ultrabasic rocks has been employed for the first time in order to detect the soluble form of carbon, cohenite Fe_3C, present in rocks in a finely dispersed condition. Cohenite is called 'cementite' in metallurgy.

Investigations were carried out at the Urals Scientific Centre of the USSR Academy of Sciences, in the Institute of Geophysics' Geomagnetism and Magnetometry laboratory, under supervision of prof. N. A. Ivanov, and also at the Petrography laboratory of the Geology Institute under the supervision of prof. D. S. Steinberg.

The research on cohenite was carried out using serpentinous dunites taken from the Southern part of the Kempersy massif situated in the Ural-

Taus anticline. The rock samples were taken from boreholes situated in the South-Western arched uplift of the massif, where the deposits of chromite are located. Our data are related to the Almazno-Zhemchuznoe and Molodyozhnoe deposits.

The dense black serpentinous dunites, with a characteristic sooty appearance, occur in these deposits near chromite bodies. Their thickness varies from one to some dozen metres. The dunites are characterized by immense sulphide impregnation. Microscopic examination showed that the rock consists mainly of serpentine with rare olivine grains. The degree of serpentinization of these rocks (alpha-chrysotile) is from 80% to 95%.

The development of a black finely dispersed substance along the cracks in the rock or in the serpentine veins attracts one's attention. Microscopic examination of the ore minerals in reflected light showed that they are represented mainly by sulphides, pyrrhotite predominating, rare grains of pyrrhotite — petlandite being marked. More rarely, chalcopyrites can be met as proudcts of disintegration in pyrrhotite. Magnetite plates in pyrrhotite form an exsolution structure. Chromite has sometimes magnetite rims. The method of magnetic powdergraphy is used to mark ferromagnetic and antiferromagnetic varieties among pyrrhotites.

The carbon content in the rocks, according to seven samples, varies from 0,08 to 0.40 per cent. On acid treatment the rocks are discoloured, which indicates the mainly sulphide composition of the sooty substance. After hydrofluoric acid treatment only chromite is found in the insoluble residue, which indicates the presence of carbon in soluble, i.e. carbide form (Steinberg, 1972).

Since carbides were not found with the help of a microscope, because they are finely dispersed (by analogy with brucite), and since the carbide of iron is ferromagnetic, thermomagnetic analysis was employed in order to find the carbide in the rock. According to Bosort (1956), Vol (1962), and Kosolapova (1968), cohenite's Curie point is 210—220°C, and the Curie point of carbide (Fe_2C) — is 265°. Cementite's saturation magnetization is approximately 1000 gauss according to Yanus (1946).

The remanent magnetization and magnetic susceptibility measurements were made using a ballistic device constructed by N. A. Ivanov and V. M. Menkov (1956), with a full scale sensitivity of $E = 400.10^{-6}$ e.m.u. of magnetic moment. Rock sample heating in steps of 30 to 50° was carried out in a tubular nonmagnetic furnace. In order to get the remanent magnetization of saturation the rock samples were magnetized in an electromagnet in fields up to 8000 Oe.

The magnetic properties of the rock samples are given in the table. Magnetic susceptibility varies from 310.10^{-6} up to 3570.10^{-6} e.m.u. According to natural remanent magnetization two groups have been found: $J_n = 54$—310.10^{-6} emu and $J_n = 16300.10^{-6}$ emu. Two groups are also

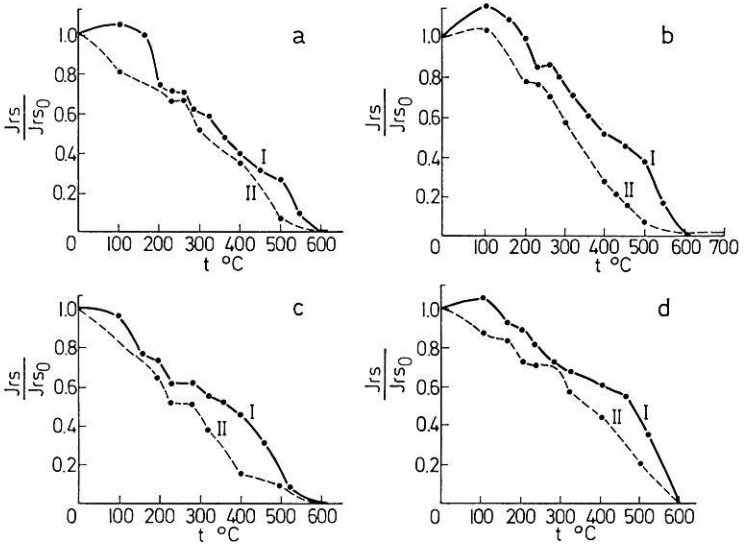

Fig. 1 Thermal demagnetization Irs of the dunite samples: a A-1; b A-3; c A-8; d M-11; Sample Nos are given in corresponding Table *I* first heating; *II* repeated heating

The curves suggest three ranges of Curie points: 200°—230°, most clearly marked in a-I, b and c, 300°—400° and 550°—570° corresponding to the presence of cohenite, pyrrhotite and magnetite respectively

evident in the Q-ratio the first with $Q < 1$, the second with $Q = 20$ to 64.

Thermal demagnetization of the saturation remanence resulted in curves suggesting a three-phase system with Curie temperatures varying in the ranges of 200—230°, 300—400°, 550—570° (Fig. 1). The 200 to 230° phase is probably due to the presence of cohenite. The 300—400° phase may be due to pyrrhotite with varying sulphur content. The 550—570° phase corresponds to magnetite. In three samples, A-3, 4 and 5, (Fig. 1, b), a phase with Curie point in the range of 250—265°C was observed, apparently represented by carbide of iron Fe_2C. This phase is observed only in those samples which do not contain a cohenite phase. In the samples A-3 and A-2 (Fig. 1, b), the phase with Curie point 460° is noted, but it remains to be seen optically.

Repeated heatings caused no big curve changes, but the kinks shifted to higher temperatures. The saturation remanence amplitude increased after the second cycle of heating. Such an increase of remanence after heating, may be explained by the presence of ferromagnetic pyrrhotites. Brodskaya *et al.* (1970) noted remanence increases in ferromagnetic pyrrhotites of 1,5 to 3,5 times after heating. The cohenite quantity was not determined but theo-

Table 1. The results of investigations

Samples Nos	The Content of free carbon (in %)	The Calculated quantity of cohenite (%)	Magnetic data						Observed Curie points				
			In. 10^6 e.m.u.	$\varkappa$. 10^6 e.m.u.	Q	Irs. 10^6 e.m.u.			Cohenite 200—220°C	Fe_2C 250 265°C	Pyrrhotite 300—400°C	460°C	Magnetite 550—570°C
						Before heating	After the first heating	After the second heating					
A—1	0,29	4,8	210	590	0,71	194000	730000	785000	215	—	320	—	570
A—2	0,29	4,8	16300	1610	20	150000	695000	800000	230	—	320	460	570
A—3	0,29	4,8	74500	3570	41,5	151000	740000	780000	—	250	—	460	570
A—4	0,29		81000	2520	64	299250	980000		—	265	330		560
A—5	0,29		19400	1070	36	265000	930000		—	250	320		570
A—6	0,08	1,3	310	1100	0,56	236000	640000	722000	205	—	300	—	560
A—7	0,08	1,3	230	1710	0,27	190000	470000	486000	210	—	350—400	—	570
A—8	0,23	3,8	64	465	0,27	83000	86500	66100	210	—	320—400	—	560
A—9	0,18	3,0	85	905	0,19	220000	142000	98900	210	—	—		550
M—10	0,40	6,6	183	2640	0,14	640000	800000	735000	220	—	300	—	560
M—11	0,16	2,6	54	310	0,35	207000	590000	493000	210	—	340	—	560

retically it can be calculated from the content of free carbon. These data are given in the Table 1.

Thermomagnetic research has therefore confirmed the presence of the soluble form of carbon-cohenite, which is the main carrier of carbon in the ultrabasic rock of the Kempersy massif. It may be that cohenite will become a useful magnetic mineral for rock magnetists and palaeomagnetists.

References

Bosort, R.: Ferromagnetism, Inostrannaya Literatura, Moscow 1956

Brodskaya, S.Yu., Vetoshkin, N.D., Zherdenko, O.I.: Magnetism Gornih Porod i Paleomagnetism. Proceedings of the VIII Conference, Kiev 1970

Ivanov, N.A., Menkov, V.I.: Geophysicheskoe Priborostroenye, ed. 22. Leningrad 1965

Kosolapova, T.S.: Carbides, Metallurgia, Moscow 1968

Steinberg, D.S., Lagutina, M.V.: 1972 Proceedings of Geological and Geochemical Int. of the Urals Scientific Center, USSR Academy of Science, Sverdlovsk 1973

Vol, A.E.: Structure and Properties of Double Metal System, v.2. Moscow: Physmatgyz 1962

Yanus, R.I.: Magnetic Defectoscopy, Gostehizdat. Moscow—Leningrad 1946

T. M. Koshkina
Institute of Geophysics
Ural Sci. Centre
USSR Academy of Science
USSR 620169, Sverdlovsk K-66
Pervomaiskaya 91